

รายงานวิจัยฉบับสมบูรณ์

โครงการ ผลกระทบของภาวะความเป็นกรดกับ การเจริญเติบโตของเซลกระดูก

โดย พ.ญ. สินี ดิษฐบรรจง

สิงหาคม 2548

สัญญาเลขที่ RSA4580037

รายงานวิจัยฉบับสมบูรณ์

โครงการ ผลกระทบของภาวะความเป็นกรดกับ การเจริญเติบโตของเซลกระดูก

พ.ญ.สินี ดิษฐบรรจง หน่วยโรคไต ภาควิชาอายุรศาสตร์ คณะแพทยศาสตร์รพ.รามาธิบดี

สนับสนุนโดยสำนักงานกองทุนสนับสนุนการวิจัย (ความเห็นในรายงานนี้เป็นของผู้วิจัย สกว.ไม่จำเป็นต้องเห็นด้วยเสมอไป)

กิตติกรรมประกาศ

คณะผู้วิจัยขอขอบคุณ ศ.นพ.รัชตะ รัชตะนาวิน คณบดีคณะแพทยศาสตร์รพ.รามาธิบดี ที่ช่วยชี้แนะ ให้การสนับสนุน และให้โอกาสในการทำวิจัย สำนักงานกองทุนสนับสนุนการวิจัย สำหรับเงินทุน นางปิยะนุช ระเด่นอาหมัด ผู้ช่วยวิจัยที่ขยันและมีความละเอียดรอบคอบ สำนัก งานวิจัย และเจ้าหน้าที่ในหน่วยงานต่างๆ ของคณะแพทยศาสตร์รพ.รามาธิบดี ที่อำนวยความ สะดวกในการใช้เครื่องมือในการทำวิจัย

สารบัญ

1.	Abstract	5
2.	บทคัดย่อ	6
3.	Introduction	7
4.	Objective	11
5.	Summary of results	11
6.	Conclusion	12
7.	Materials and Methods	13
8.	Results	19
9.	Discussion	32
10	.Bibliography	37
11	.Suggestions for future research projects	41
12	. Output	42
13	. ภาคผนวก	43

Abstract

Project Code: RSA4580037

Project Title: Effect of metabolic acidosis on osteoblast differentiation

Investigator: Sinee Disthabanchong, M.D.

Division of Nephrology, Department of Medicine, Ramathibodi Hospital,

Mahidol University, Bangkok 10400, Thailand

E-mail Address: tesdb@mahidol.ac.th

Project Period: Aug 2002 – Jul 2005

Distal renal tubular acidosis (dRTA) is characterized by impairment of distal tubular acid secretion resulting in persistent metabolic acidosis. Recent examination of bone histology of dRTA patients showed markedly decreased bone formation with impaired bone matrix mineralization that is not entirely explained by an alteration in the mineral balance. Data from in vitro studies suggests a direct inhibitory effect of metabolic acidosis on osteoblast function. We investigated the effects of chronic metabolic acidosis on osteoblast differentiation from mesenchymal precursor cells (MSCs). Human MSCs were isolated from bone marrow aspiration specimen. Osteoblast differentiation was induced in the presence of dexamethasone in culture. Concentrated HCl was added to lower the medium pH. The expression of various osteoblastic genes was determined by quantitative real-time RT-PCR. Our isolated MSCs displayed characteristic spindle-shaped morphology. Flow cytometry revealed characteristic MSC surface marker profile. The mRNA expression of early osteoblast transcription factor, cbfa-1, and the major bone matrix protein, type I collagen, reached its peak at day 5-10 in control culture. Chronic metabolic acidosis was found to enhance the expression of cbfa-1 and type I collagen in a dose dependent manner. In contrast, the mRNA expression of osterix (a transcription factor downstream of cbfa-1) and alkaline phosphatase (an enzyme normally upregulated in intermediately mature osteoblasts) as well as alkaline phosphatase enzyme activity was decreased. The study on the expression of mature osteoblast marker, osteocalcin is currently ongoing. Impaired bone matrix mineralization was demonstrated by a reduction in both calcium deposition and number of bone nodules visualized by von Kossa staining. In conclusion, chronic metabolic acidosis enhanced early osteoblast differentiation while attenuating bone matrix mineralization.

Keywords: acidosis, osteoblast, mesenchymal, renal tubular acidosis

บทคัดย่อ

รหัสโครงการ: RSA4580037

ชื่อโครงการ: ผลกระทบของภาวะความเป็นกรดกับการเจริญเติบโตของเซลกระดูก

ชื่อนักวิจัย: พ.ญ. สินี ดิษฐบรรจง

หน่วยโรคไต ภาควิชาอายุรศาสตร์ คณะแพทยศาสตร์รพ.รามาธิบดี

มหาวิทยาลัยมหิดล

E-mail address: tesdb@mahidol.ac.th

ระยะเวลาโครงการ: สิงหาคม 2545 – กรกฎาคม 2548

ภาวะความเป็นกรดในเลือดเกิดจากการที่ไตขับกรดออกจากร่างกายไม่ได้ ภาวะนี้มักมีความผิดปกติของระดับแคลเซียม ฟอสเฟต วิตามินดี และ ฮอร์โมนพาราไธรอยด์ ในเลือด ส่งผลให้มีการลดลงของการสร้างกระดูกทำให้มีมวลกระดูกลดลง การศึกษาในห้อง ทดลองยังพบว่าภาวะความเป็นกรดสามารถยับยั้งการทำงานของเซลกระดูกได้โดยตรง เนื่อง จากเซลกระดูกเจริญเติบโตมาจาก mesenchymal stem cells (MSCs) คณะผู้วิจัยจึงทำการ ศึกษาผลกระทบของภาวะความเป็นกรดต่อการเจริญเติบโตของเซลกระดูก โดยใช้ MSCs นี้ได้ มาจากไขกระดูกของคนปกติ นำมาเพาะเลี้ยงในห้องทดลอง (cell culture) แล้วกระตุ้นให้เซล เหล่านี้เจริญเติบโตไปเป็นเซลกระดูกโดยการผสม dexamethasone, ß-glycerophosphate และ L-ascorbate phosphate เข้าไปในสารเลี้ยงเซล และอาศัยการเติมกรด hydrochloric ปริมาณ เล็กน้อย เพื่อให้ได้ระดับ pH ประมาณ 7.1-7.4 จากนั้นศึกษาการเปลี่ยนแปลงของระดับ mRNA โดยใช้วิธี quantitative real-time RT-PCR และ โปรตีนที่สกัดจาก MSCs เป็นระยะๆ โดยเริ่มตั้งแต่ระยะแรกที่เริ่มกระตุ้นด้วย dexamethasone จนกระทั่งระยะหลังที่เซลเปลี่ยน แปลงไปเป็นเซลกระดูกที่เจริญเติบโตเต็มที่ นอกจากนี้ยังได้ศึกษา mineralization ของเซลก ระดูกโดยใช้วิธีการย้อมแบบ Von Kossa ผลการทดลองพบว่า MSCs ที่เพาะเลี้ยงได้มีรูปร่าง เรียว (spindle shape) และจากการทำ flow cytometry สามารถยืนยันได้ว่าเซลที่ได้เป็น MSCs จริง ภาวะความเป็นกรดมีผลกระตุ้นให้มีการเพิ่มขึ้นของ cbfa-1 (ซึ่งเป็น transcription factor ที่จำเพาะและจำเป็นต่อการเจริญเติบโตของ osteoblast) และ type I collagen mRNA (90% ของ bone matrix protein ที่สร้างจาก osteoblast) ใน young osteoblasts เมื่อเปรียบเทียบกับ เซลที่เพาะเลี้ยงใน pH 7.4 ในขณะที่ osterix (downstream transcription factor ของ cbfa-1) และ alkaline phosphatase ซึ่งปรากฏในเซลกระดูกที่เจริญเติบโตในระดับกลาง มีปริมาณลดลง ขณะนี้คณะผู้วิจัยกำลังทำการศึกษาปริมาณของ osteocalcin mRNA ซึ่งพบในเซลกระดูกที่ เจริญเติบโตเต็มที่อยู่ เมื่อย้อมเซลกระดูกเหล่านี้ด้วยวิธี Von Kossa พบว่าเซลที่เลี้ยงในสภาวะ ที่เป็นกรดมีปริมาณ bone matrix mineralization ลดลง สรุปได้ว่าภาวะความเป็นกรดสามารถ แต่ยับยั้งการเกิด กระตุ้นการเจริญเติบโตของเซลกระดูกในระยะเริ่มต้น mineralization

คำหลัก: acidosis, osteoblast, mesenchymal, renal tubular acidosis

Introduction

Distal renal tubular acidosis (dRTA) is a clinical syndrome characterized by impaired renal excretion of ammonium and titrable acid resulting in persistent metabolic acidosis. The presence of chronic metabolic acidosis results in various metabolic consequences, including hypokalemia, hypercalciuria, hypophosphatemia and abnormal bone metabolism ¹⁻³. Recent bone histologic studies of dRTA patients from our laboratory revealed findings of osteopenia and suppressed bone formation when compared to healthy controls ⁴ (Table 1). Correction of metabolic acidosis with alkaline therapy improved the abnormality ⁵ (Table 2). The modest decrease in osteoblastic surface at baseline, which only improved slightly after alkaline treatment, could not explain the striking improvement in bone formation, suggesting the possibility of additional influence of metabolic acidosis on osteoblast function and/or bone matrix mineralization.

Table 1 Bone histomorphometry of dRTA patients compared to normal controls

Histomorphometric Parameters	dRTA	Normal	
Osteoblast Surface	0.78 ±1.03	2.6 ± 1.1	
(Ob.S/BS %)	U.76 ±1.03	2.0 ± 1.1	
Osteoclast Surface	0.05 + 0.02	0.42 + 0.22	
(Oc.S/BS %)	0.05 ± 0.03	0.13 ± 0.23	
Bone Formation Rate	0.00 + 0.00*	0.07 . 0.045	
(BFR/BS $\mu \text{m}^3/\mu \text{m}^2/\text{day}$)	0.02 ± 0.02*	0.07 ± 0.045	

^{*} P < 0.05 compared to normal controls. Adapted from Domronkitchaiporn et al 4 .

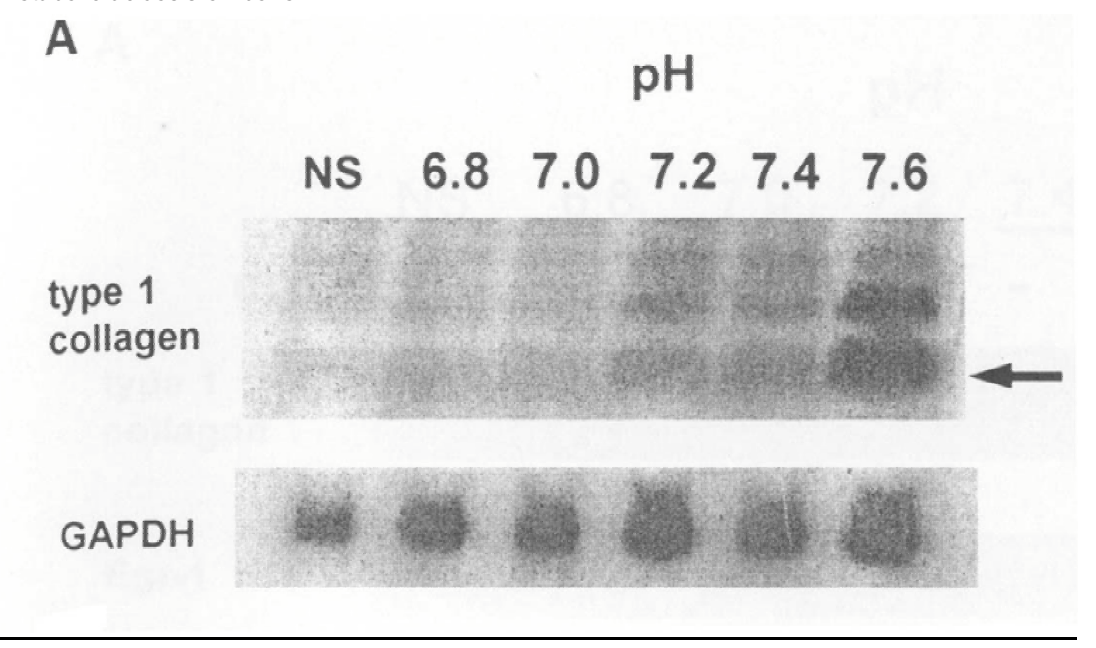
Table 2 Bone histomorphometry of dRTA patients before and after alkaline therapy

Histomorphometric Parameters	Pre alkaline	Post alkaline	
Osteoblast Surface	1 10 + 0 00	1 70 + 0 21	
(Ob.S/BS %)	1.19 ± 0.88	1.79 ± 0.21	
Osteoclast Surface	0.04 + 0.04	0.05 + 0.06	
(Oc.S/BS %)	0.04 ± 0.04	0.05 ± 0.06	
Bone Formation Rate	0.00 . 0.00	0.00 . 0.00*	
(BFR/BS $\mu\text{m}^3/\mu\text{m}^2/\text{day}$)	0.02 ± 0.02	0.06 ± 0.03*	

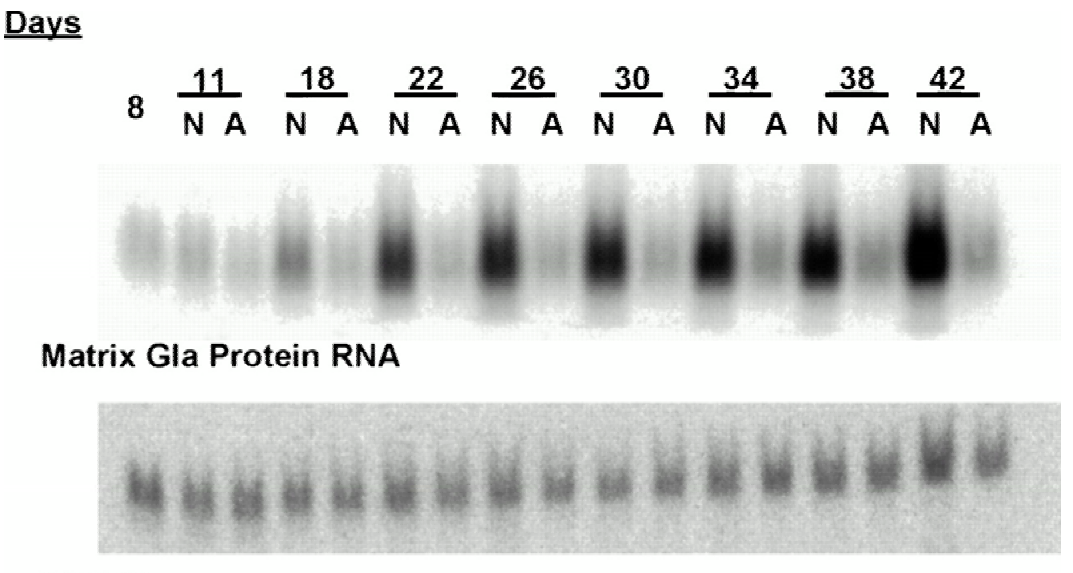
^{*} *P* < 0.05 compared to pre-alkaline. Adapted from Domronkitchaiporn et al ⁵.

Previously, Bushinsky et al investigated the effect of metabolic acidosis on bone and discovered that metabolic acidosis resulted in skeletal demineralization through physicochemical dissolution of the bone as excess protons were buffered by bone carbonate ^{6, 7}. Later on, the effect of metabolic acidosis on bone cells was examined. Using an in vitro model of bone organ culture derived from neonatal mouse calvariae, Krieger et al observed that short-term incubation of calvariae in acidic medium suppressed type I collagen synthesis and lowered alkaline phosphatase enzyme activity ⁸. In a later study, the same group examined the effect of acute metabolic acidosis on

primary bone cells. Incubation of calvariae-derived osteoblasts in acidic medium for 30 minutes resulted in marked decrease in erg-1 and type I collagen gene expression ⁹ (figure 1). Furthermore, chronic metabolic acidosis diminished the expression of matrix Gla protein (figure 2) and osteopontin mRNA (figure 3) of primary osteoblasts derived from the same source and impaired bone matrix mineralization ¹⁰. This evidence supports the existence of both cellular and non-cellular effect of metabolic acidosis on bone.

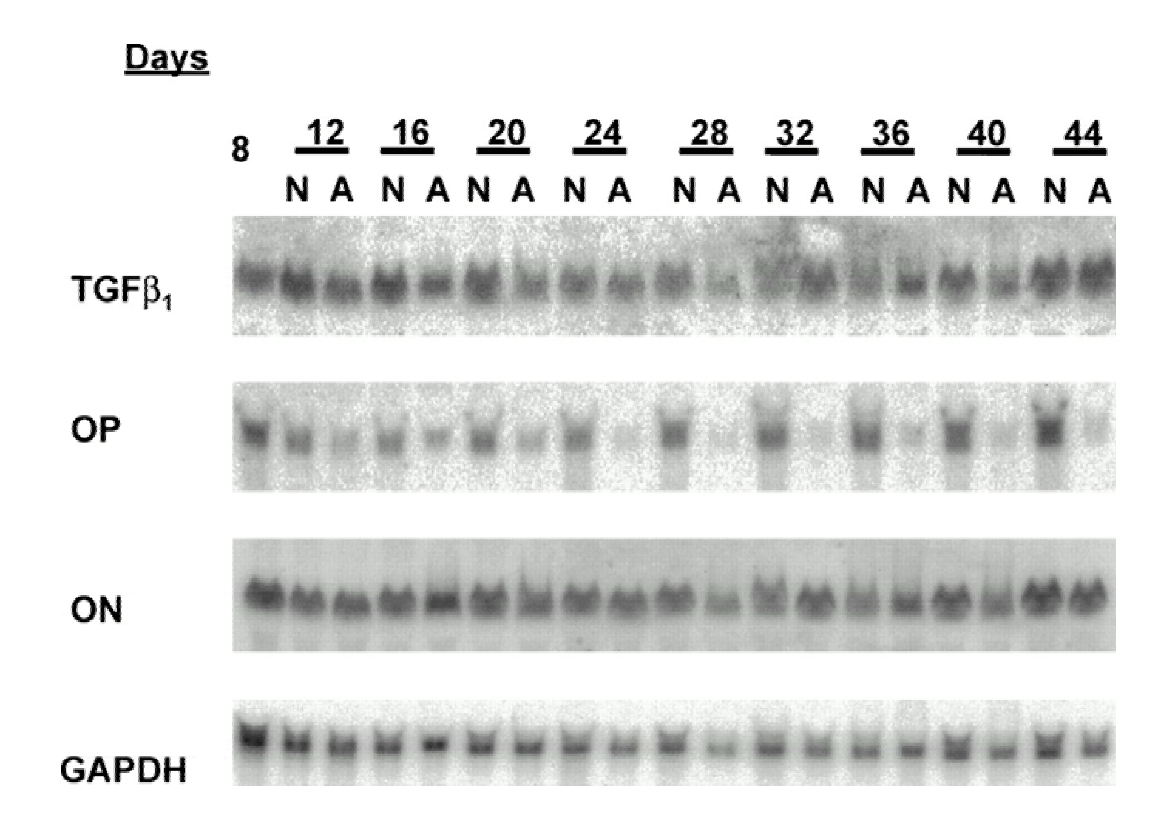


<u>Figure 1</u> Northern blot analysis of type I collagen mRNA expression in calvariae-derived osteoblasts incubated in acidic medium for 30 minutes. Adapted from Frick et al ⁹.



GAPDH

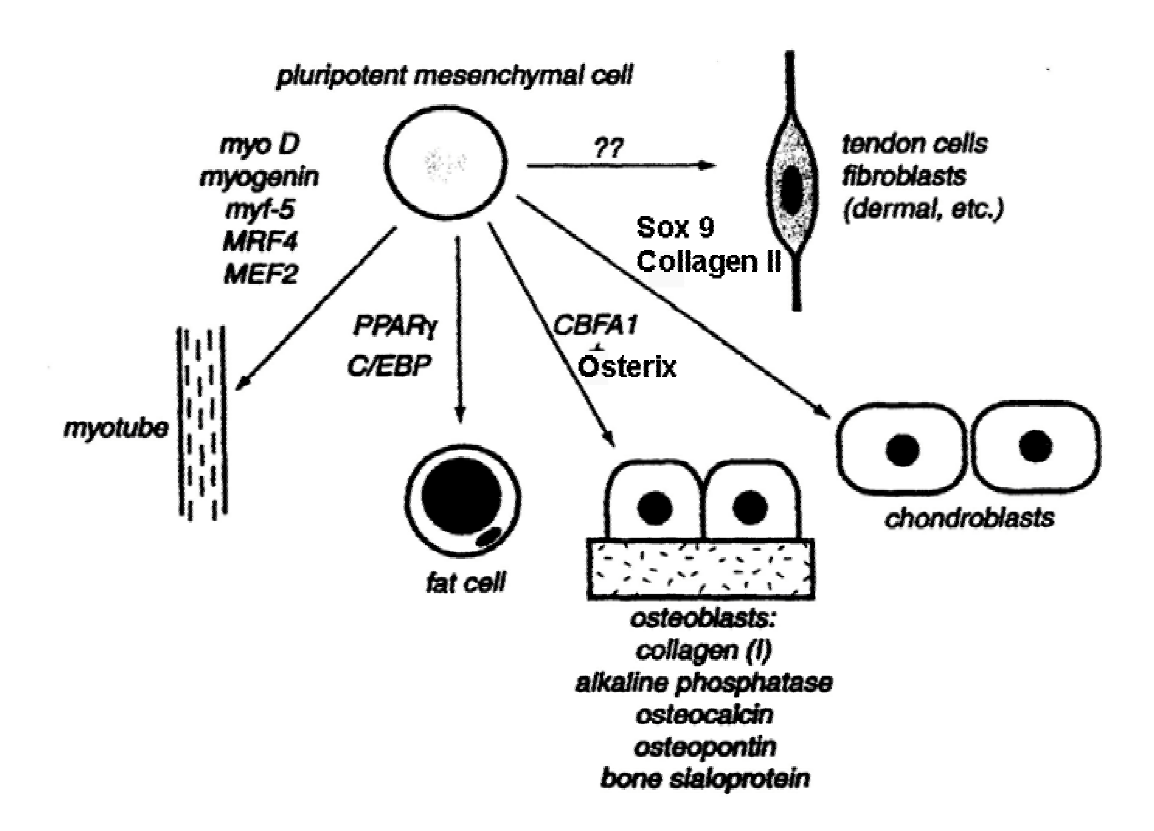
<u>Figure 2</u> Northern blot analysis of matrix Gla protein mRNA expression of calvariae-derived osteoblasts incubated in acidic medium for 11-42 days. N = N normal pH, N = N acidosis. Adapted from Frick et al N = N acidosis.



<u>Figure 3</u> Northern blot analysis showed mRNA expression of various bone matrix proteins of calvariae-derived osteoblasts incubated in acidic medium for 12-44 days. N = N normal pH, A = N acidosis, N = N osteopontin, N = N osteopontin. Adapted from Frick et al.

Osteoblasts originate from mesenchymal precursor cells (MSCs) in the bone marrow. These cells contribute to replacement of osteoblasts in bone turnover and fracture healing throughout life. Under appropriate conditions, multipotent MSCs can also differentiate into chondrocytes, adipocytes and fibroblasts. A wide variety of systemic and local factors appears to regulate osteoprogenitor proliferation and differentiation, a sequence that is characterized by a series of cellular and molecular events distinguished by differential expression of osteoblast-associated genes, including those for specific transcription factors and matrix proteins 11 (figure 3). In vitro, induction of osteogenic differentiation from MSCs can be achieved in the presence of dexamethasone (Dex). ßglycerophosphate (ß-GP) and ascorbate phosphate (Asp) 12. Mature osteoblasts synthesize and secrete bone matrix including type I collagen and various NCPs ready for subsequent mineralization. Of these NCPs, osteocalcin and osteonectin have been known to involve in the process of bone formation and mineralization 13-15, while osteopontin and bone sialoprotein play roles in bone resorption ¹⁶⁻¹⁹. Metabolic acidosis, through its effect on osteoblasts may alter the production of NCPs, resulting in the abnormal bone remodeling. Alkaline therapy may restore cellular functions and NCPs composition. Osteomalacia has been reported in 20-30% of patients with renal tubular acidosis ^{3, 20}. The diagnosis was mostly based on clinical and roentgenographic findings. Bone pain was relieved and osteomalacia improved after alkaline therapy 3, 21. Previously, we reported significant increase in osteoid volume and surface in bone of patients with dRTA, while there was no major increase in osteoid thickness. A detailed analysis on the parameters associated with mineralization was not performed.

In the first part of our study, we examined the NCP composition in non-decalcified bone sections of dRTA patients before and after alkaline therapy. Additional information on mineralization parameters will be analyzed by bone histomorphometry. In the second part of our study, we studied the sequential changes in the expression of osteoblastic genes in human MSCs cultured in normal and acidic environment during in vitro osteogenic induction.



<u>Figure 4</u> Multipotent MSCs can differentiate into osteoblasts, chondrocytes, adipocytes and myocytes under appropriate condition through the expression of lineage specific transcription factors.

Objectives

Part 1

- 1. To determine the presence of impaired bone matrix mineralization in dRTA patients
- 2. To determine whether alkaline therapy improves osteoblast function.
- 3. To examine the expression of various NCPs in bone sections of dRTA patients before and after alkaline therapy by immunohistochemistry

Part 2

- 1. To isolate and characterize bone marrow-derived MSCs by using flow cytometry and its ability to differentiate into osteoblasts and adipocytes in vitro
- 2. To determine the effect of chronic metabolic acidosis on MSCs cell proliferation
- 3. To determine the expression of various osteoblastic genes during in vitro osteogenic induction in normal and acidic condition by quantitative real-time RT-PCR
- 4. To examine he effect of chronic metabolic acidosis on bone matrix mineralization by von Kossa staining and calcium assay

Summary of results

Part 1

- 1. Bone matrix mineralization was impaired in majority of dRTA patients while fewer patients had histologic feature of adynamic bone disease
- 2. Alkaline therapy improved osteoblast function suggested by the increase in bone formation rate/number of osteoblasts.
- 3. The expression of osteocalcin increased significantly after alkaline therapy.
- 4. Osteopontin expression decreased in all but one patient.
- 5. There was no alteration in osteonectin and bone sialoprotein expression before and after alkaline therapy.

Part 2

- Isolated bone marrow-derived MSCs showed characteristic MSC surface marker profile and were able to differentiate into osteoblasts and adipocytes in vitro.
- 2. Chronic metabolic acidosis dose-dependently attenuated cellular proliferation
- Chronic metabolic acidosis enhanced the expression of early osteoblastic genes including cbfa-1 (a specific osteoblast transcription factor) and type I collagen (a major bone matrix protein).
- Chronic metabolic acidosis suppressed the expression of alkaline phosphatase mRNA as well as its enzyme activity.
- 5. The expression of osterix, another essential osteoblast transcription factor downstream of cbfa-1, was diminished by metabolic acidosis.
- 6. Metabolic acidosis impaired bone matrix mineralization.
- 7. We are still confirming the expression of mature osteoblastic gene, osteocalcin.

Conclusion

Part 1

Abnormal bone remodeling in patients with dRTA is characterized by low turnover bone disease with defective mineralization. Alteration of NCPs expression suggested the effect of metabolic acidosis on bone cells in vivo. Alkaline therapy improved bone formation through the restoration of bone mineral balance and perhaps enhanced osteoblast function.

Part 2

Chronic metabolic acidosis directly affects osteoblast differentiation from MSCs. Osteoblast differentiation is enhanced in the early stages, whereas bone matrix mineralization is impaired. The roles of heightened cbfa-1 mRNA on the expression of other osteoblastic genes will require further study.

Materials and Methods

Part 1

Patients

Subgroup of dRTA patients who completed one year of alkaline therapy with adequate bone specimens available for further examination by immunohistochemistry from our previous studies were included ^{4, 5}. These were idiopathic dRTA patients who were residents of Khon Kaen province, Thailand, where a very high incidence of dRTA has been reported ²⁰. Seven patients, three males and four females, who were diagnosed with dRTA on the presence of (1) persistent hyperchloremic metabolic acidosis with serum bicarbonate less than 18 mmol/L found in at least two occasions, one month apart, (2) failure to acidify urine (with urine pH > 5.5) or urinary excretion of ammonia less than 50 mEq/day in the presence of systemic acidosis, (3) absence of bicarboturia exceeding 15% of that filtered at normal plasma bicarbonate concentration, serum creatinine of less than 190 µmol/L and absence of proteinuria, Fanconi syndrome, chronic diarrhea, current usage of diuretics, carbonic anhydrase inhibitors, and all kinds of alkaline therapy were included in this study. The calcium intake of dRTA patients was 9.45 ± 3.35 mmol/day. All patients were then treated for one year with 60 mEg/day of potassium citrate in two-divided dose to keep the serum bicarbonate above 20 mmol/L throughout the study. For patients who initially failed to achieve the target serum bicarbonate level, the dosages of potassium citrate were increased in a stepwise fashion until reaching the desired serum bicarbonate level. No medication that might affect calcium and bone metabolism, for example, diuretics, vitamin D, estrogen, bisphosphonate, and calcium supplements, was allowed throughout the study.

Biochemical Analysis

Serum electrolytes, calcium, phosphate, intact PTH (iPTH) and 24-hour urine collections for sodium, potassium, calcium, phosphate and creatinine were obtained at the time of bone biopsy. Hypercalciuria was defined as urinary calcium excretion > 4.75 mmol/day in either sex ^{1, 22}. Serum iPTH was determined by an immunoradiometric assay (ELSA-PTH; CIS BioInternational, GIF-sur-Yvette Cedex, France). The normal serum iPTH was 10 to 60 pg/mL.

Bone mineral density

Bone mineral density (BMD; g/cm^2) was determined at vertebral (L2-L4), femoral neck, trochanter, and Wards' triangle by dual energy x-ray absorptiometry (Lunar Expert XL, Lunar Corp., USA). Precision of the BMD measurement in our laboratory at L2-L4, and neck of femur was 1.2 and 0.6% respectively. The control values of BMD were obtained from 28 normal farmers who were permanent residents of Khon Kaen province, age 32.9 \pm 11.2 years, weight 54.3 \pm 8.3 kg, height 1.55 \pm 0.05 m and male: female ratio 22:6.

Bone biopsy and histomorphometry

At the beginning of the study, transiliac crest bone biopsy was taken from the anterior superior iliac spine after tetracycline double labeling and again on the opposite side after one year of alkaline therapy using protocol reported previously ⁴. In brief, bone specimens of 5 mm in diameter and 20-30 mm in length were fixed for 24 hours in 70% ethanol, dehydrated in graded ethanol and

impregnated and embedded in the mixture of methylmethacrylate, dibutylphthalate and benzoyl peroxide at room temperature for 5 days and subsequently, in 42°C oven for 3 days. After polymerization, bone sections of 6 Jm thickness were cut using Reichert-Jung Polycut S (Cambridge Instruments, NuBloch, Germany) equipped with tungsten carbide-edge knife (Leica, Germany), mounted on coated slides and incubated at 42°C for 2 weeks. Undecalcified sections were stained with modified Masson-Goldner trichrome, aurin tricarboxylic acid (Aluminon), Von-Kossa and hematoxylin-eosin stain. If the specimen had a positive stain for aluminum, a further stain with Perls stain to exclude the cross-reaction with iron deposit was done. Unstained sections of 15-µ m thickness were prepared for examinations by a fluorescent light microscopy. All sections, both pre and post potassium citrate therapy, were studied qualitatively and quantitatively for static and dynamic parameters of bone formation and bone resorption by the same pathologist and technician who had no knowledge of the patients' clinical presentations and treatments. Histomorphometric measurements were carried out with a semiautomatic image analyzer (Osteomeasure; Osteometric Inc, Atlanta, USA). At least 30 different fields of the same bone biopsy specimen were analyzed. Histomorphometric parameters were expressed according to Parfitt et al's standardized nomenclature ²³. The reference values for normal histomorphometric parameters were obtained from 17 normal Thai adults without bone disease, eight men and nine women, age 35.1 ± 2.8 years (range 19 to 58), height 1.61 ± 0.06 m. and weight 59.2 ± 7.8 kg. Protocol of the study has been approved by ethical committee on research involving human subjects of Ramathibodi hospital, Mahidol University. Written informed consents were obtained from all subjects.

Antibodies

Rabbit polyclonal antibodies LF-32 (osteocalcin), LF-120 (bone sialoprotein), BON-I (osteonectin) and mouse monoclonal antibody LFMb-14 (osteopontin) were generous gifts from Dr Larry W. Fisher, National Institutes of Health (NIH), Bethesda, MD ²⁴.

Immunohistology

Immunohistochemistry was performed on the bone sections as described previously by Derkx et al ²⁵. Briefly, plasticized bone sections were deacrylated in three changes of 2-Ethoxyethylacetate (BDH, Poole, England) overnight, rinsed in xylene, rehydrated, decalcified with 1% acetic acid for 2 days and rinsed with distilled water for 30 min. Sections were stained using Universal LSAB2 Kits (Dako, CA, USA) according to manufacturer's recommendations with modifications. All steps were carried out at room temperature. Endogenous peroxidase activity was inhibited by 3%H₂O₂ in PBS for 30 min followed by 5 min wash in PBS. Subsequently, slides were blocked with 10% normal goat serum (Dako, CA, USA) in PBS for 1 hour. Excessive serum was removed. Sections were then incubated with primary antibodies including osteocalcin 1:1600, bone sialoprotein 1:800, osteonectin 1:800 and osteopontin 1:3200 diluted in goat serum for 2 hours and 30 min. The washings were carried out in PBS containing 0.05% tween (tween-PBS) for 10 min and PBS for additional 5 min. Primary antibodies were detected by incubation with ready-to-use biotinylated goat anti-immunoglobulin second antibody (detecting both mouse and rabbit antibodies) for 10 min and washed for 5 min each in tween-PBS and PBS. Next, peroxidase-conjugated biotin-

streptavidin complex was allowed to react with second antibody for 10 min and sections were washed for 5 min in tween-PBS and 30 min in PBS. Antibody complexes were visualized by incubation with diaminobenzidine obtained from Dako liquid DAB substrate-chromogen system. Sections were rinsed in distilled water for 5 min, counterstained with Mayer's hematoxylin, rinse in tap water, dehydrated with ascending alcohols, cleared with xylene, and mounted on glass slides with cover slips using Permount (Fisher Scientific, New Jersey, USA) mounting medium. Bone biopsy sections from pre and post alkaline treatment of the same patients were stained at the same time. Negative control sections were stained in the same fashion with omission of primary antibody.

Quantitative analysis of the NCPs

We performed quantitative analysis of the NCPs using similar protocol described previously by Derkx et al ²⁵. Briefly, a CCD color video camera (Sony, Japan) mounted on a microscope (Zeiss, Germany) with a 10x objective was used to transfer images of the immunostained samples to the computer. The KS-300 (version 2.00) digital image analysis system (Kontron, Munchen, Germany) was used to analyze at least 40 microscopic fields of trabecular bone area in two 6 µm sections cut at steps of 50-100 µm in the same bone biopsy. This has been shown previously to be sufficient to obtain representative data with a small confidence interval ²⁵. The threshold of positive staining (brown) was determined interactively and the determined threshold was used to automatically analyze the images of the section. The mineralized bone matrix area (purple) was determined by first, manually tracing the perimeter of the mineralized trabecular bone on the computer screen (in order to exclude the cells in the bone marrow, which also stain purple) and then allowing the analysis system to calculate the area. The ratio of the immunostained and the mineralized bone matrix area was calculated. Bone sections from the same patient obtained pre and post alkaline treatment were analyzed at the same time and two separate measurements were performed in all sections.

Part 2

Isolation and culture of bone marrow derived MSCs

Bone marrow samples were obtained using a bone marrow biopsy needle inserted through posterior iliac crest of a healthy bone marrow donor after an informed consent. Bone marrow mononuclear cells (BMMCs) were separated by density gradient centrifugation with 1.073 g/ml Percoll solution (Sigma, MO, USA). Briefly, 10 ml of heparinized bone marrow cells were mixed in an equal volume of Dulbecco's Modified Eagle's Medium (DMEM) (BioWhittaker, MD, USA) and centrifuged at 900g for 10 min at room temperature. The washed cells were resuspended in DMEM at a density of 4 x 10⁷ cells/ml, and 5 ml aliquot was layered over 1.073 g/ml Percoll solution and centrifuged at 1,000g for 30 min at room temperature. The interface mononuclear cells were collected and washed twice with DMEM. Total cell count and cell viability were evaluated by 0.2% Trypan blue exclusion. A total of 2 x 10⁶ cells/ml of BMMCs were cultured in DMEM complete medium supplemented with 10% fetal bovine serum (FBS) (GibcoBRL, NY, USA) and 1% penicillin-streptomycin (GibcoBRL) at 37°C in 5% CO₂ incubator. On day 3 of cultivation, non-adherent cells

were discarded and this process was repeated every 4 days. Upon 90% confluency, MSCs were trypsinized by 0.05% trypsin (Gibco BRL) and passaged for the next expansion. This study has been approved by ethical committee on Research Involving Human Subjects at Ramathibodi hospital, Mahidol University.

Flow cytometry analysis of cultured bone marrow derived MSCs

Bone marrow derived adherent cells (at the end of 4th passage) were trypsinized and adjusted to 5-10 x 10^6 cells/ml. 100 μ I of adjusted cells were incubated with 10 μ I of following monoclonal antibodies, CD-14PE, CD-34FITC, CD45-FITC, HLA-DR PE and CD-105FITC (Becton-Dickinson Pharmingen, Heidelberg, Germany) at 4° C in the dark. After 20 min of incubation, 2 ml of PBS/2% FBS solution was added to each monoclonal antibody-treated cells. The mixtures were then centrifuged at 2,500 rpm for 10 min followed by removal of supernatant. These steps were repeated again following fixation of the cells with 0.5% paraformaldehyde. Flow cytometry analysis was performed using Cellquest software program.

Osteogenic and adipogenic differentiation

Studies were performed in subconfluent culture of human MSCs between passages 4-8. These cells have previously been shown to remain undifferentiated through multiple passages and their osteogenic potential is preserved up until passage 10-15 26 . A normal karyotype and telomerase activity were found to be maintained even at passage 12 27 . MSCs were grown in multiwell tissue culture plates (Nunc, Denmark) until 50-60% confluency when DEX 100 nM (Sigma, MO, USA), β -GP 10 mM (Sigma) and Asp 0.1 mM (Sigma) were added to induce osteogenic differentiation (day 0). This medium will be referred to as osteogenic differentiation medium (OM). In the dose response experiments, concentrated hydrochloric acid (HCI) was added (at day 0) at the concentration of 1 μ II/mI of culture medium to achieve an approximate pH of 7.25 (HCL 1), 2 μ II/mI for pH 7.15 (HCL 2) and 3 μ II/mI for pH 7.0 (HCL 3). MSCs grown in the culture medium without HCI (HCL 0) served as control (pH 7.4). Time course experiments were performed with the cells grown in HCL 2 culture medium. MSCs cultivated in the absence of OM represent negative controls. For adipogenic differentiation, DEX 1 μ M, 3-isobutyl-1 methylxanthine 100 μ g/mI (Sigma) and insulin 10 μ g/mI (Sigma) were added to confluent culture of MSCs. Medium was changed twice weekly.

Cell proliferation assay

Cell proliferation was evaluated by MTT assay at various time intervals. The yellow tetrazolium MTT (Sigma, MO, USA) was reduced by metabolically active cells resulting in intracellular purple formazan, which was solubilized and quantified by spectrophotometric means. The experiments were performed in 12-well tissue culture plates. MSCs were grown in the presence of OM without HCI (HCL 0) and with HCI (HCL 1, HCL 2 and HCL 3). After the cells were rinsed twice with DMEM without phenol red, 1 ml of 0.5 mg/ml MTT solution was added to each well. After 3 hours of incubation at 37°C in CO2 incubator, the purple precipitate formed within the cells. MTT was removed and intracellular purple formazan was solubilized with 1 ml of 0.04 M HCl in absolute isopropanol. Absorbance was recorded at 570 nm with background subtraction at 650 nm.

Studies of osteoblastic gene expression by quantitative real-time RT-PCR.

Total RNA was isolated from culture cells at various time intervals using Trizol (Life Technologies, NY, USA) method as described by manufacturer. cDNAs were reverse transcribed from 1 µg of total RNA using Reverse Transcription System (Promega, WI, USA) with random hexamer as primer as described by manufacturer. cDNAs obtained from the reaction were diluted 1:5 in DNAse free water. Quantitative real-time RT-PCR was performed using ABI Prism 7000 Sequence Detection System (Applied Biosystems, CA, USA). 3-6 µl of cDNAs was analyzed in 25 μΙ reaction of Tagman® Universal PCR mastermix (Applied Biosystems). Multiplexed PCR reaction was performed with both target and reference genes (18S rRNA) in the same reaction. Each sample was analyzed in triplicate. The probe for 18S rRNA was fluorescently labeled with VIC and TAMRA (Applied Biosystems), whereas the probes for gene of interest were labeled with 6carboxyfluorescein (FAM) and TAMRA (Applied Biosystems). Primer concentrations were 300 nM except for type I collagen and 18S rRNA where the concentrations were 25 nM. Probe concentrations were 100-150 nM for the target genes and 50 nM for 18S rRNA. The nucleotide sequences of primers and probes for 18S rRNA, cbfa-1, type I collagen (Coll I), osterix (Osx), alkaline phosphatase (ALP) and osteocalcin (OC) are shown in Table 3. Relative expression levels of the gene of interest, normalized by the amount of 18S rRNA, were calculated by Sequence Detection Software version 1.2 (Applied Biosystems) using Relative Quantification Study approach. The average values of Δ Cts from each sample were used for statistical analysis.

Table 3 Primer and Probe Sequences

	Forward and reverse primers		
Gene	(5'-3')	Probe (5'-3')	
	(5 -3)		
18 S	CGGCTACCACATCCAAGGAA	TGCTGGCACCAGACTTGCCCTC	
rRNA	GCTGGAATTACCGCGGCT	TGCTGGCACCAGACTTGCCCTC	
Cbfa-1	GCCTTCAAGGTGGTAGCCC	CCACAGTCCCATCTGGTACCTCTCCG	
	CGTTACCCGCCATGACAGTA	CCACAGTCCCATCTGGTACCTCTCCG	
Coll I	CAGCCGCTTCACCTACAGC	000000000000000000000000000000000000000	
	TTTTGTATTCAATCACTGTCTTGCC	CCGGTGTGACTCGTGCAGCCATC	
Osx	CCCCACCTCTTGCAACCA	CCAGCATGTCTTGCCCCAAGATGTCTA	
	CCTTCTAGCTGCCCACTATTTCC		
ALP	GACCCTTGACCCCCACAAT	TGGACTACCTACTTGGGTCTCTTCGA	
	GCTCGTACTGCATGTCCCCT	GCCA	
ОС	GAAGCCCAGCGGTGCA	T004040444000T00400TTT00T	
	CACTACCTCGCTGCCCTCC	TGGACACAAAGGCTGCACCTTTGCT	

Alkaline phosphatase enzyme activity assay

Alkaline phosphatase enzyme activity was measured based on its ability to convert a substrate, *p*-nitrophenyl phosphate, to a yellow colored product, *p*-nitrophenol. The absorbance of *p*-

nitrophenol can be determined at 405 nm in a microtiter plate reader. The experiments were performed in 12-well tissue culture plates. After cell layers were rinsed twice with calcium and magnesium free PBS, 0.3 ml of 2 mg/ml *p*-nitrophenyl phosphate solution (Sigma) in 0.75 M AMP (Sigma) with 2 mM magnesium chloride, pH10.3, was added to each well. Cells were incubated in 37°C water bath for 30 min and the reaction was stopped by adding 0.3 ml of 50 mM NaOH to each well. Protein concentration was determined using Bradford Reagent (Sigma) as described by manufacturer. Absorbance of p-nitrophenol was normalized by protein concentration. Standard curve was constructed using p-nitrophenol standard solution (Sigma). For each sample and standard, assay was performed in duplicate.

Measurement of calcium content

The deposition of calcium in mineralization nodules was determined based on Calcium-o-Cresolphthalein Complexone method. Calcium yielded purple-colored product when formed complex with a chromogenic substrate, *o*-cresolphthalein Complexone, in an alkaline medium. The intensity of color, measured at 575 nm, is directly proportional to calcium concentration in the sample. The experiments were performed in 12-well tissue culture plates. All the glasswares were cleaned and soaked overnight in 3% HCl, rinsed with distilled water and dried before use. After cell layers were rinsed twice with calcium and magnesium free PBS, decalcification was performed by adding 200-500 μ l of 0.6 N HCl into each well. Cells were left overnight at 4°C and 50 μ l of samples were transferred to the test tubes containing 1 ml of colored solution (0.1% *o*-cresolphthalein complexone (Sigma) and 1% 8-hydroxyquinoline (Sigma)) the next morning. To provide an alkaline environment, 1 ml of AMP, pH 10.7, was added to each tube and the mixtures were incubated at room temperature for 5 min before measurement. Absorbance of calcium was normalized by protein concentration. Serially diluted stock CaCO₃ was used as standards. For each sample and standard, assay was performed in duplicate.

Von Kossa staining

The experiments were performed in 25 mm² tissue culture dishes. MSCs were allowed to grow in the presence of OM with or without HCl until mineralization appeared. After washing the cells twice in calcium and magnesium free PBS, cell layers were fixed with 10% formalin for 30 min, washed thoroughly with distilled water and incubated with 2% silver nitrate in front of 60 watt lamp for 15 min. Aluminum foil was placed around the dish and the lamp in order to reflect the light.

Statistical Analysis

Results are presented as mean \pm standard deviation (SD) on the first part of the study of dRTA patients and as mean \pm standard error of measurement (SEM) on the second part of the study on MSCs. Student t test was used to compare group means of two samples. The difference was considered significant at P value below 0.05.

Results

Part 1

Patient characteristics are shown in Table 4. All the patients were acidemic with impaired urine ammonium excretion (urine ammonium < 50 mEq/day) and relatively high urine pH (> 5.5). Blood and urine chemistries for dRTA patients are presented in Table 5. Full details on blood and 24-hour urine chemistries before and after potassium citrate therapy have been reported previously ⁵. Hypokalemia (3.4 ± 0.8 mmol/L), hypophosphatemia and low serum iPTH levels were observed at baseline. None of the patients had hypercalciuria. During alkaline therapy with potassium citrate, all dRTA patients could maintain their serum bicarbonate above 20 mmol/L. After treatment, serum potassium (4.1 ± 0.4 mmol/L), bicarbonate, phosphate and iPTH levels rose significantly above the corresponding baseline values. There were no significant alterations in serum calcium, urine calcium and urine phosphate after the treatment.

Table 4 Patient characteristics at presentation

Patient No	Age years	Height cm	Weight <i>kg</i>	Sex	Blood/Urine pH	Urine Ammonium meq/day	Duration ^a months
1	16	157	44	F	7.31/7.0	36	8
2	35	145	46.7	F	7.30/6.0	29	18
3	30	170	65	М	7.29/6.2	30	36
4	50	146	50	F	7.31/6.8	30	60
5	42	158	53	М	7.28/6.4	32	120
6	20	136	32.3	М	7.30/6.9	24	144
7	25	148	39.5	F	7.32/6.5	31	24
Mean	31.1	151.4	47.2		7.3/6.5	30.3	58.6
SD	12.1	11.1	10.4		0.01/0.4	3.6	53.2

^aduration of symptoms, for example, muscle weakness, renal stone or fracture

Table 5 Blood (per liter) and urine (per day) chemistries of dRTA patients

	Baseline		After Treatment		Normal ^c	
	Serum	Urine	Serum	Urine	Serum	Urine
Creatinine μ mol	99 ± 18	974 ± 160	93.7±11.2	700 ± 100	91.5 ± 38	1061 ± 71
Sodium mmol	139.9 ± 2.4	97.9 ± 44.9	141.6 ± 2.6	113.2 ± 26	138 ± 5.1	110.6 ± 90
Bicarbonate mmol	16.5 ± 3.3	-	22.6 ± 2.4 ^a	-	25 ± 1.5	-
Calcium mmol	2.1 ± 0.1	2.6 ± 1.6	2.3 ± 0.2	2.9 ± 1.7	2.3 ± 0.5	2.75 ± 1.7
Phosphate mmol	0.8 ± 0.2	11.3 ± 4.2	1.1 ± 0.2 ^a	10.2 ± 2.9	1.2 ± 0.1	10.6 ± 5.5
iPTH pg/mL	12.9 ± 5.6	-	24.1 ± 10 ^b	-	-	-

 $^{^{}a}$ Significant difference when compared to the corresponding baseline value (P < 0.05)

^bSignificant difference when compared to the corresponding baseline value (P < 0.01)

^cData obtained from the 28 normal farmers who were permanent residents of Khon Kaen province

Table 6 Bone mineral density (g/cm²) of dRTA patients

	dRTA patients	Name	
Area	Baseline	After Treatment	Normal
L2-L4	1.05 ± 0.23	1.08 ± 0.17	1.15 ± 0.25
Total femur	0.89 ± 0.16	0.98 ± 0.17^{a}	1.05 ± 0.29
Neck	0.85 ± 0.15	0.88 ± 0.18	1.00 ± 0.25
Wards	0.68 ± 0.20	0.72 ± 0.17	0.89 ± 0.30
Trochanter	0.67 ± 0.14	0.75 ± 0.13 ^a	0.81 ± 0.27

^aP < 0.05 compared to baseline BMD in dRTA patients

Bone mineral densities at baseline and the end of the study period are shown in Table 6. The basal BMD values of dRTA patients were lower than those of normal controls in all studied areas. After one year of alkaline therapy, there were significant elevations in the BMDs of total femur and trochanter of femur (P < 0.05). Bone histomorphometric data before and after the treatment is presented in Table 7. At baseline, there were significant elevations in the osteoid volume and surface (P < 0.05) compared to the corresponding parameters in normal controls. Osteoid thickness was slightly but insignificantly elevated. Osteoblastic and osteoclastic surfaces were decreased but the differences were not significant. Eroded surface was not different from controls. The reductions in the mineral apposition rate, mineralizing surface/osteoid surface and adjusted apposition rate were accompanied by the prolongation of mineralization lag time (P < 0.05). Bone formation rate per bone surface was suppressed at baseline (P < 0.05). While bone formation rate per osteoblast number was lower than that of normal controls, the difference did not reach statistical significance. After potassium citrate therapy, bone volume and osteoblastic and osteoclastic surfaces were modestly increased, but the differences were not significant. A slight decrease in osteoid volume was observed. Osteoid surface and thickness were not significantly altered. Dynamic parameters showed significant improvement in the mineral apposition rate, mineralizing surface and adjusted apposition rate compared to the baseline values (P < 0.05). Mineralization lag time also declined significantly (P< 0.05). Bone formation rate per bone surface and bone formation rate per osteoblast number increased significantly after the treatment (P < 0.05). On regression analysis, a tendency toward negative correlation between the osteoid thickness and adjusted apposition rate was observed (r = -0.717, P = 0.07; Fig 5). No positive staining for the aluminum was found in any of the bone specimens.

Table 7 Bone histomorphometry of dRTA patients at baseline and after alkaline treatment

History and a matric parameters	dR	Reference value	
Histomorphometric parameters	Baseline	After treatment	range)
Bone volume (BV/TV) %	20.32 ± 3.54	24.91 ± 2.80	26.44 ± 7.21
	(15.63 - 25.56)	(20.64 - 28.00)	(12.72 – 36.88)
Osteoid volume (OV/TV) %	2.50 ± 1.65 ^a	1.83 ± 1.30	0.92 ± 1.05
	(0.18 - 4.53)	(0.42 - 4.2)	(0.2 - 3.06)
Osteoid surface (OS/BS) %	25.10 ± 21.4 ^a	24.02 ± 20.5 ^a	5.79 ± 4.39
	(3.27 - 39.8)	(7.12 - 32.16)	(0.30 – 15.86)
Osteoid thickness (O.th) μm	10.11 ± 3.2	10.16 ± 4.09	8.69 ± 2.14
	(5.29 - 14.34)	(6.12 - 17.5)	(5.53 – 15.87)
Osteoblastic surface (Ob.S/BS) %	1.05 ± 0.93	2.03 ± 1.92	2.6 ± 1.1
	(0 - 2.43)	(0.15 - 5.45)	(0.51 - 4.80)
Osteoclastic surface (Oc.S/BS) %	0.04 ± 0.33	0.06 ± 0.06	0.13 ± 0.23
	(0 - 0.08)	(0 - 0.16)	(0.01 - 0.59)
Osteoclast number (N.Oc/T.Ar)/mm²	0.14 ± 0.11	0.15 ± 0.14	0.24 ± 0.31
	(0 - 0.32)	(0 - 0.32)	(0.01 - 0.83)
Eroded surface (ES/BS) %	5.79 ± 3.02	4.32 ± 3.07	5.68 ± 2.32
	(1.78 - 9.71)	(1.69 - 7.94)	(2.08 - 10.06)
Mineral apposition rate (MAR) μ m/d	0.74 ± 0.39^{a}	1.20 ± 0.42 ^b	1.32 ± 0.69
·	(0.30 - 1.27)	(0.43 - 1.63)	(0.48 - 2.94)
Mineralizing surface/osteoid surface	20.59 ± 26.7 ^a	39.83 ± 31.33 ^{a,b}	81.15 ± 23.66
(MS/OS) %	(3.51 - 71.82)	(8.41 - 89.79)	(36.84 - 97.79)
Adjusted apposition rate ^c (Aj.AR) <i>μm/d</i>	0.13 ± 0.17 ^a	0.52 ± 0.46 ^b	0.78 ± 0.59
	(0.03 - 0.49)	(0.04 - 1.24)	(0.35 - 1.93)
Mineralization lag time ^d (Mlt) days	240.93 ± 167.55 ^a	90.68 ± 172.67 ^b	15.42 ± 11.64
	(13.89 - 424.3)	(5.63 - 479.94)	(1.77 - 30.94)
Bone formation rate per bone surface e	5.97 ± 5.51 ^a	28.05 ± 15.96 ^b	29.83 ± 20.42
(BFR/BS) $\mu m^3/\mu m^2/y$	(2.15 – 17.92)	(4.28 – 44.9)	(8.35 – 44.47)
Bone formation rate per osteoblast	55.57 ± 41.82	91.46 ± 30.98 ^b	88.64 ± 93.29
number (BFR/N.Ob) μm^2 /cell/d	(10.89 - 120.76)	(39.22 -127.48)	(21.12 - 272.35)

 $^{^{\}rm a}$ Significant difference when compared to the corresponding normal value (P < 0.05)

 $^{^{\}mathrm{b}}$ Significant difference when compared to the corresponding baseline value (P < 0.05)

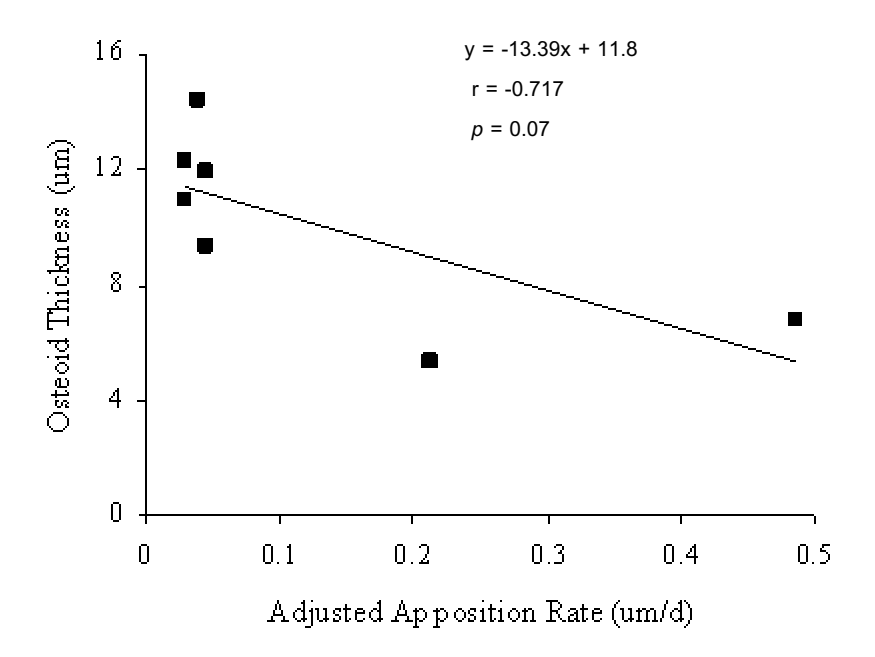
^cAj.AR was calculated from : Aj.AR = [(MS/OS) x MAR]/100

^dMlt was calculated from : Mlt = O.th/Aj.AR

^eBFR/BS was calculated from : BFR/BS = [(MS/BS) x MAR]/100, where MS/BS (mineralizing surface, %) was the extent of tetracycline labeled surface (double plus half single labeled surface) as a percentage of total trabecular bone surface

 $^{^{}f}$ BFR/N.Ob was calculated from BFR/N.Ob = MAR x [osteoid perimeter (μ m)/number of osteoblasts]

<u>Figure 5</u> Relationship between osteoid thickness (μ m) and adjusted apposition rate (μ m/day) of dRTA patients before treatment with alkaline.



All the NCPs strongly stained the mineralized bone matrix compartment but variably stained osteoid and cellular components, including osteoblasts, osteoclasts, osteocytes and lining cells (Fig 2). Negative controls were devoid of staining. Each protein had a specific pattern of distribution, but an overlap in localization between the proteins was observed. As shown in figure 6, osteocalcin (Fig 6A and B) stained more intensely in the outer than inner lamellae osteon, while osteopontin stained diffusely and distinctively in the area of bone surface adjacent to the bone marrow (lamina limitans) (Fig 6C and D). A significant increase in the area of osteocalcin staining from $16.65 \pm 9.25\%$ in bone biopsy at initial diagnosis to $22.26 \pm 8.16\%$ after alkaline treatment (P < 0.04) was observed (Fig 7A). Six of seven patients showed decreased expression of osteopontin with an average of $28.91 \pm 10.4\%$ at initial biopsy to $22.3 \pm 3.76\%$ post alkaline (P = 0.16) (Fig 7B). Osteonectin and bone sialoprotein diffusely stained the bone matrix and cement lines (Fig 6E and F). The area of staining of osteonectin ($19.46 \pm 10.92\%$ and $21.62 \pm 9.52\%$, P = 0.5) and bone sialoprotein ($11.94 \pm 4.37\%$ and $12 \pm 3.76\%$, P = 0.98) were not significantly different post alkaline therapy (Fig 7C and D). After a careful examination of the sections obtained from initial biopsy and one year after alkaline treatment, there was no alteration in the distribution of any of the proteins.

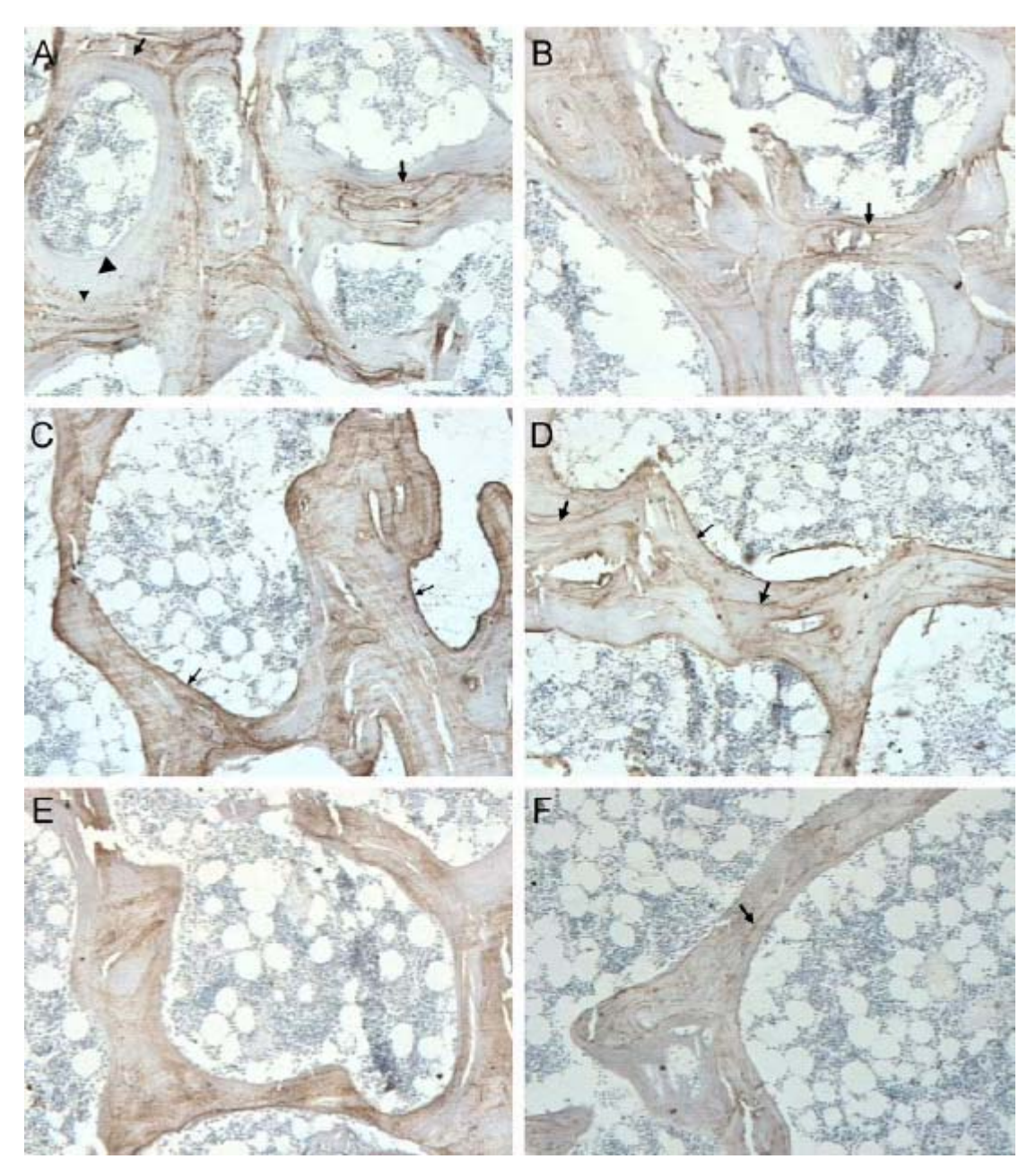
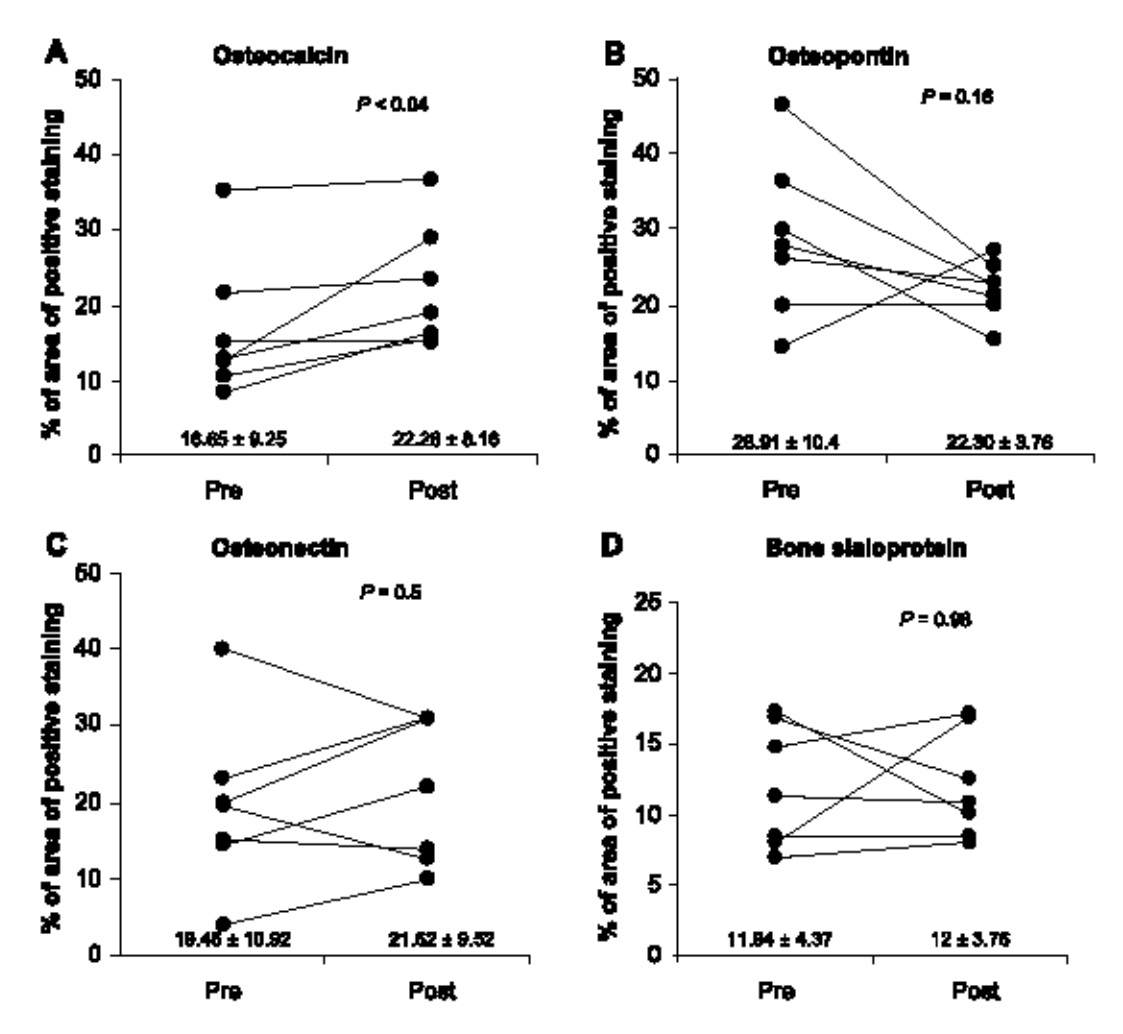


Figure 6 Immunohistochemistry of NCPs in bone sections of patients with dRTA pre and post alkaline treatment. Each protein has specific pattern of distribution but an overlap in localization between the proteins was observed. (A) Osteocalcin pre-alkaline; (B) Osteocalcin one year post-alkaline treatment. Osteocalcin was detected in the cement lines and more in the outer than the inner lamellae osteon. Note the increase in osteocalcin expression in the bone section after alkaline treatment. (C) Osteopontin pre-alkaline; (D) Osteopontin post-alkaline. Osteopontin expressed more diffusely and most prominently in the area of the bone surface adjacent to the bone marrow (lamina limitans). Note the decrease in osteopontin expression in the bone section after alkaline treatment. (E) Osteonectin. Osteonectin diffusely expressed in the bone matrix but minimally in the cement lines (F) Bone sialoprotein. Bone sialoprotein also diffusely stained the bone matrix and presented in the cement lines. Large arrowhead = inner lamellae osteon; small arrowhead = outer lamellae osteon; large arrow = cement lines; small arrow = lamina limitans. Original magnification, x100.



<u>Figure 7</u> Quantitation of NCPs expression using digital image analysis pre and post-alkaline treatment. Data was expressed as percentage of area of positive staining/mineralized bone matrix area (A) Osteocalcin; (B) Osteopontin; (C) Osteonectin; (D) Bone sialoprotein. Osteocalcin expression significantly increased after alkaline treatment. Six of seven patients had decreased osteopontin expression.

Part 2

First, we isolated and characterized MSCs derived from bone marrow aspiration specimen. After BMMCs isolated from Percoll gradient were plated, the adherent MSCs gave rise to colonies and exhibited characteristic spindle-shaped morphology (Figure 8A). Flow cytometry analysis of the **4**th the passage revealed characteristic MSC surface (CD14^{neg}CD45^{neg}CD34^{neg}HLA-DR^{neg}CD105^{pos}) ²⁷(Figure 9A–D). To determine the ability of MSCs to differentiate into osteoblasts and adipocytes, MSCs were cultivated in the presence of OM and adipogenic inducing medium respectively. After 20 days in culture, cell colonies displayed bone-like nodular aggregates of matrix mineralization (Figure 8B) noticeable on von Kossa staining (Figure 13). MSCs cultivated in the absence of OM never mineralized (data not shown). Lipid-rich vacuoles were observed after 7 days of adipogenic induction (Figure 8D). Cell proliferation of cultured human MSCs in the presence of OM with (HCL 1, 2 and 3) and without (HCL 0) HCl was determined by MTT assay (Figure 10). Increasing metabolic acidosis below pH 7.25 resulted in a decline in cell proliferation.

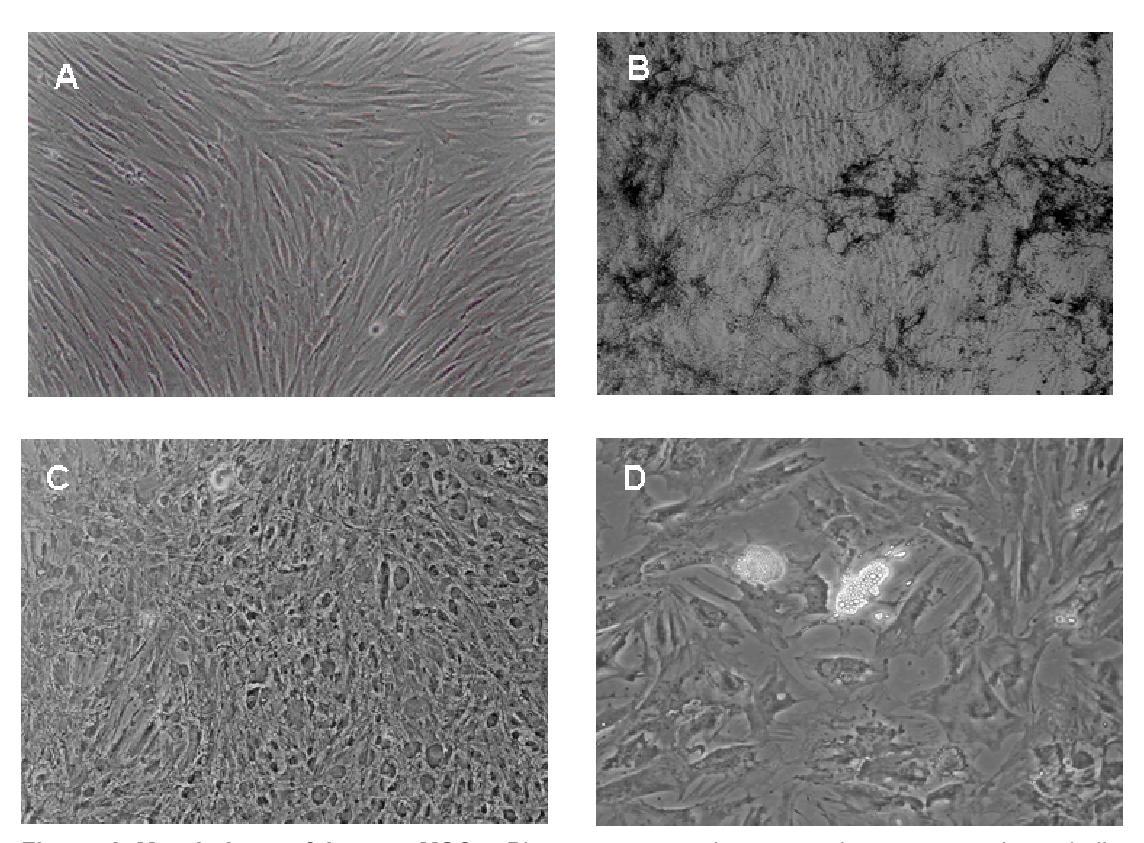


Figure 8 Morphology of human MSCs. Phase contrast microscopy demonstrates the spindle-shaped morphology of MSCs grown in the absence of OM (A), nodular aggregates of mineralization in the presence of OM for 28 days (B), cuboidal-shaped osteoblasts without nodular aggregates in the presence of OM with HCl 3 μ I/ml (HCL 3, pH ~ 7) for 28 days (C) and adipocytes with lipid-rich vacuoles (D).

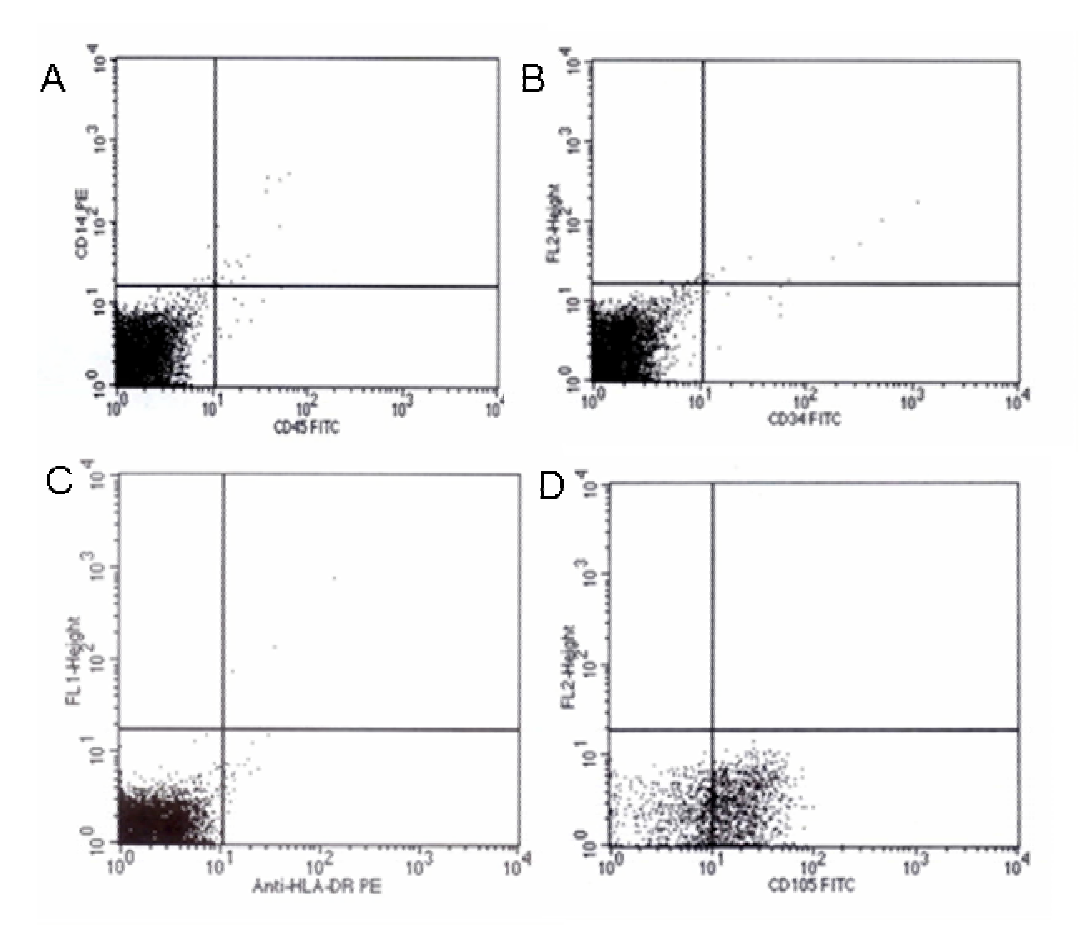
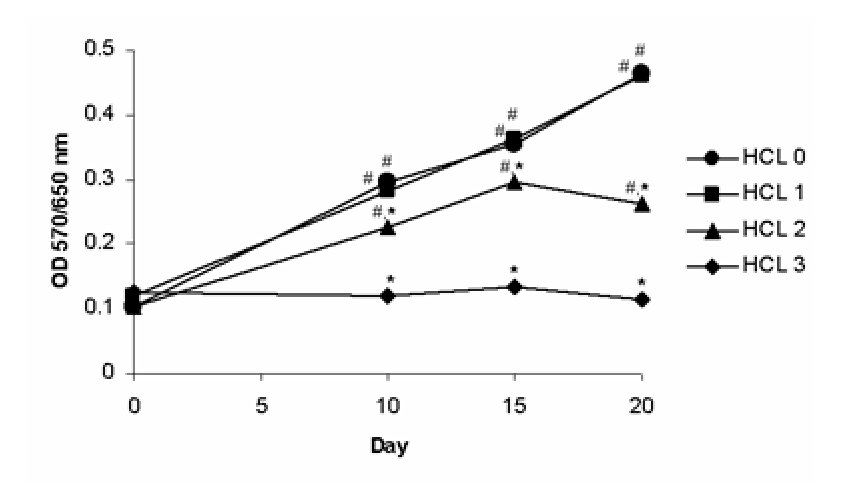


Figure 9 Flow cytometry analysis of human MSCs



<u>Figure 10</u> Cell proliferation assay MSCs were grown in the presence of OM without HCl (HCL 0, pH ~ 7.4) and with HCl 1 μl/1 ml of OM (HCL 1, pH ~ 7.25), 2 μl/ml (HCL 2, pH ~ 7.15) and 3 μ l/ml (HCL 3, pH ~ 7). Cell proliferation was evaluated by MTT assay. Results represent an average of 3 experiments. $^{\#}P$ < 0.05 compared to day 0, $^{*}P$ < 0.05 compared to HCL 0.

Next, we examined the effect of chronic metabolic acidosis on the expression of early osteoblastic genes, cbfa-1, an essential transcription factor required for osteoblast differentiation, ²⁸

and type I collagen, a major bone matrix protein produced by osteoblasts 29 . Half-confluent cultures of human MSCs were cultivated in the presence OM with (HCL 2) and without (HCL 0) HCl. Negative control cells were grown in the absence of osteogenic stimulation with (Negative control HCL 2) and without (Negative control HCL 0) HCl. Cells were harvested for RNA extraction at day 0, 5, 10, 15 and 20 for quantitative real-time RT-PCR analysis. As shown in Figure 11A and B, the expression of cbfa-1 and type I collagen mRNA was enhanced upto 6.2 fold in the presence of OM. Less than 1.6 fold increase for cbfa-1 and 3.7 fold increase for type I collagen were observed in negative controls. In HCL 0, maximal expression of both genes was noted at day 10-15. The mRNA levels were greater in HCL 2 than in HCL 0 from day 5 through 15 (P < 0.05). At day 15, the expression of both genes appeared to reach plateau; however, the robust increase in expression was observed in HCL 2 at day 20 (cbfa-1 = 6 ± 0.1 vs. 3.3 ± 0.2, type I collagen = 6.2 ± 0.3 vs. 2.8 ± 0.4, P < 0.05). Dose response experiments, performed at day 10, showed a progressive rise in cbfa-1 and type I collagen expression with increasing acidosis (Figure 12A and B). The fold increases from HCL 0 for HCL 3 cultures were 2 ± 0.2 for cbfa-1 and 2.8 ± 0.2 for type I collagen (P < 0.05 vs. HCL 0, HCL 1 and HCL 2).

Due to the enhanced expression of early osteoblast markers during acidosis, the expression of osterix, another essential osteoblast transcription factor downstream of cbfa-1 30, and alkaline phosphatase, an osteoblastic gene upregulated during an intermediate phase of osteoblast differentiation, was subsequently examined ²⁹. Figure 11C displayed a continuing rise in alkaline phosphatase mRNA upto 24.4 fold in the presence of OM, whereas less than 4.6 fold increase was observed in negative controls. Unlike cbfa-1 and type I collagen, metabolic acidosis suppressed alkaline phosphatase mRNA expression. In HCL 2, despite the gradual increase in alkaline phosphatase mRNA with time, the levels were less than those of HCL 0 at all time points (P < 0.05). Likewise, dose response experiments demonstrated a progressive decline in alkaline phosphatase mRNA with increasing acidosis (Figure 12C). The fold difference (relative to the lowest baseline HCL 3) of alkaline phosphatase mRNA for HCL 0, HCL 1, HCL 2 and HCL 3 were 2 ± 0.1, 1.4 ± 0.2 (P < 0.05 vs. HCL 0), 1 ± 0.2 (P < 0.05 vs. HCL 0) and 1 ± 0.2 (P < 0.05 vs. HCL 0) respectively. The product of alkaline phosphatase gene was also examined by evaluating the enzyme activity. As shown in Figure 13, exposure to acidic medium suppressed alkaline phosphatase enzyme activity correlating with the decreased amount of mRNA expression. In HCL 0 and HCL 1, the enzyme activity rose rapidly reaching plateau by day 10, whereas the rise was more indolent in HCL 2 and HCL 3. At day 10, when the differences were greatest, the enzyme activities for HCL 0, HCL 1, HCL 2 and HCL 3 were 47.6 ± 4.3 nmol, 35.6 ± 4.5 nmol (P < 0.05 vs. HCL 0), 20.8 ± 2.7 nmol (P < 0.05vs. HCL 0 and HCL 1) and 13.6 \pm 0.9 nmol (P < 0.05 vs. HCL 0, HCL 1 and HCL 2) respectively. A slight increase in enzyme activity was noted in Negative control HCL 0. As for osterix, the expression attained its peak at day 15, approximately 4.3 fold above baseline (Figure 11E). The mRNA levels of osterix in HCL 2 were lower than those of HCL 0 at all time points and the difference reached statistical significance at day 15 (1.7 ± 0.5 vs. 4.3 ± 0.6, P < 0.05). Dose response experiments showed a progressive decline in osterix mRNA with increasing acidosis (Figure 12E). The fold difference (relative to the lowest baseline HCL 3) of osterix mRNA for HCL 0, HCL 1, HCL 2 and HCL 3 were 7.1 \pm 1.1, 4.1 \pm 1 (P = NS), 4.9 \pm 0.8 (P = NS) and 1 \pm 0.3 (P < 0.05 vs. HCL 0 and HCL 2) respectively.

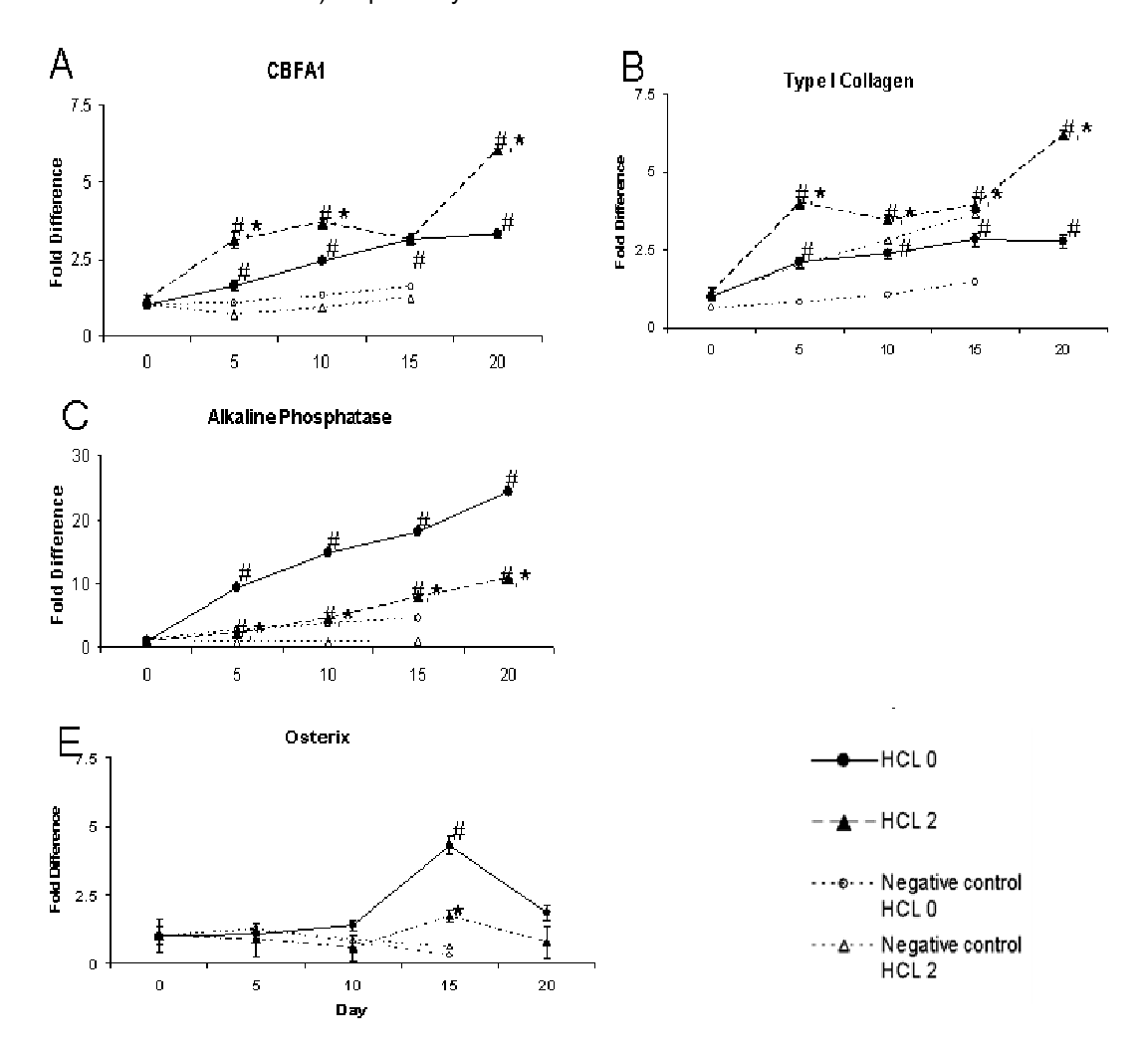


Figure 11 Time course of the effect of chronic metabolic acidosis on mRNA levels of osteoblastic genes. MSCs were grown in the presence of OM without HCl (HCL 0, pH \sim 7.4) and with HCl 2 μ I/1 ml of OM (HCL 2, pH \sim 7.15). Negative controls were cultivated in the absence of osteogenic stimulation. Relative gene expressions were determined by quantitative real-time RT-PCR. Expression levels are expressed as fold increase from the corresponding baseline values at day 0. Results represent an average of 4-6 experiments for HCLs and one experiment for negative controls. $^{\#}P$ < 0.05 compared to day 0, $^{*}P$ < 0.05 compared to HCL 0.

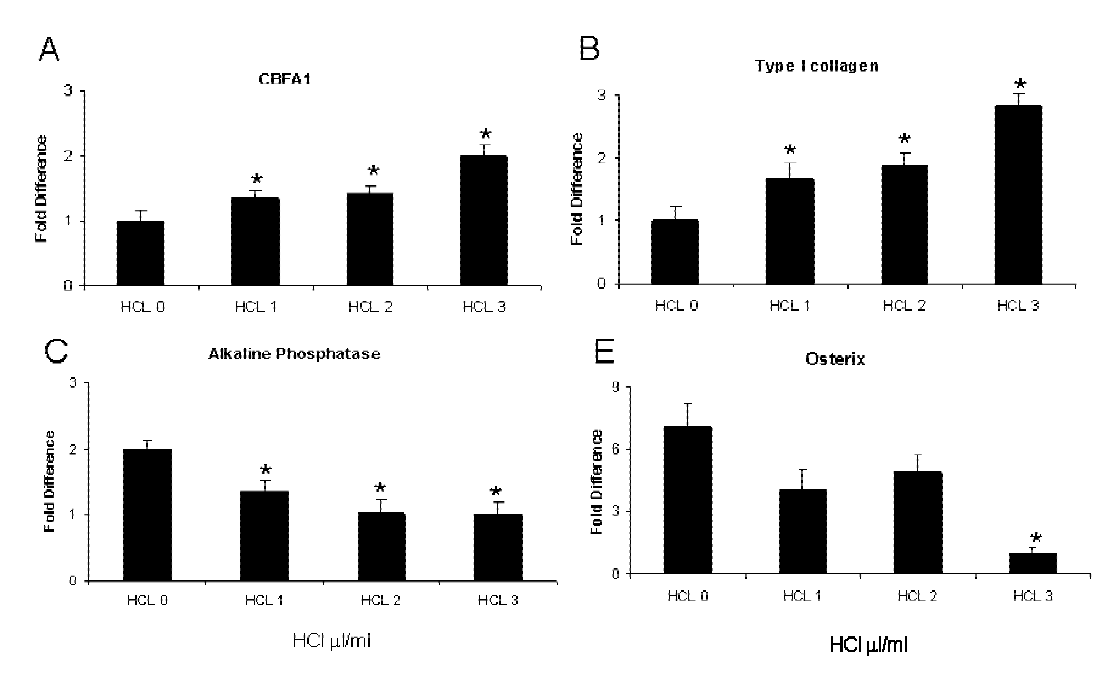
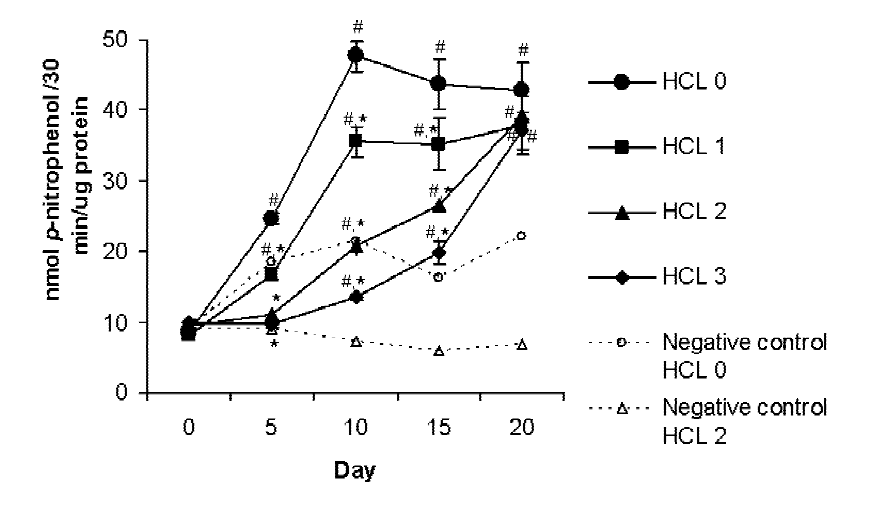


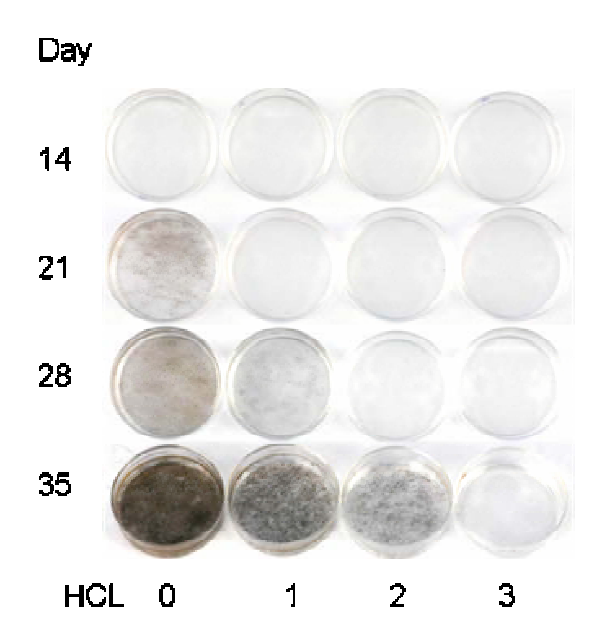
Figure 12 Dose response of the effect of chronic metabolic acidosis on mRNA levels of osteoblastic genes. MSCs were grown in the presence of OM without HCl (HCL 0, pH ~ 7.4) and with HCl 1 μ I/1 ml of OM (HCL 1, pH ~ 7.25), 2 μ I/ml (HCL 2, pH ~ 7.15) and 3 μ I/ml (HCL 3, pH ~ 7). Cells were harvested for RNA extraction at day 10 for cbfa-1, type I collagen and alkaline phosphatase and day 15 for osterix. Relative gene expressions were determined by quantitative real-time RT-PCR Expression levels are expressed as fold increase from the lowest baseline (HCL 0 or HCL 3 wherever applicable). Results represent an average of 4-6 experiments. *P < 0.05 compared to HCL 0.



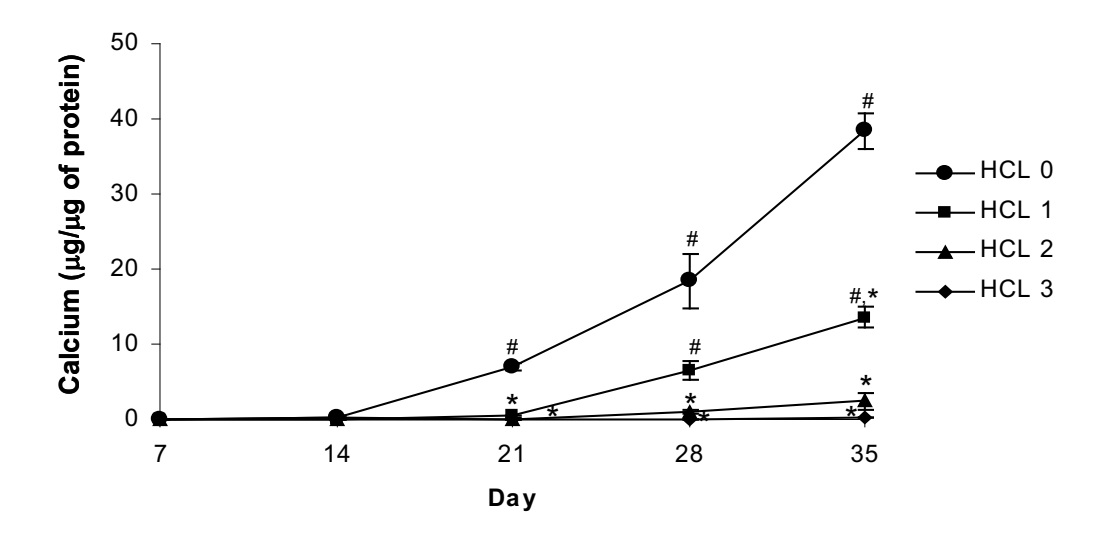
<u>Figure 13</u> Alkaline phosphatase enzyme activity. MSCs were grown in the presence of OM without HCl (HCL 0, pH ~ 7.4) and with HCl 1 μl/1 ml of OM (HCL 1, pH ~ 7.25), 2 μl/ml (HCL 2, pH ~ 7.15) and 3 μl/ml (HCL 3, pH ~ 7). Alkaline phosphatase enzyme activities were determined by calorimetric assay and normalized by protein content. Results represent an average of 6 experiments for HCLs and one experiment for negative controls. $^{\#}P$ < 0.05 compared to day 0, $^{*}P$ < 0.05 compared to HCL 0.

In order to determine whether MSCs were able to differentiate into mature osteoblasts during chronic metabolic acidosis, the expression of osteocalcin, a mature osteoblastic gene 29 , is being evaluated.

Finally, we determined whether chronic metabolic acidosis impaired bone matrix mineralization. Von Kossa staining of mineral deposition revealed the presence of mineralized nodules starting from day 21 in HCL 0 (figure 14). Metabolic acidosis delayed bone matrix mineralization in HCL1, HCL 2 and HCL 3 cultures. Mineralization occurred at day 28 in HCL 1, day 35 in HCL 2 and never appeared at all in HCL 3 up to 45 days in culture (Figure 8C and 14). Quantification of bone matrix mineralization was performed by measurement of calcium content in the bone nodules (figure 15). In HCL 0, calcium deposition was measurable at day 14 (0.2 \pm 0.03 μ g) and progressively increased through day 35 (38.4 \pm 4.7 μ g, P < 0.05 vs. day 7, 14, 21 and 28). In contrast, the amount of calcium deposit for HCL 1, HCL 2 and HCL 3 at day 35 were 13.6 \pm 2.7 μ g (P < 0.05 vs. HCL 0), 2.4 \pm 2.3 μ g (P < 0.05 vs. HCL 0, and HCL 1) and 0.2 \pm 0.1 μ g (P < 0.05 vs. HCL 0, HCL 1 and HCL 2) respectively.



<u>Figure 14</u> Von Kossa staining of bone matrix mineralization. MSCs were grown in the presence of OM without HCl (HCL 0, pH \sim 7.4) and with HCl 1 μ l/1 ml of OM (HCL 1, pH \sim 7.25), 2 μ l/ml (HCL 2, pH \sim 7.15) and 3 μ l/ml (HCL 3, pH \sim 7). Cultures were fixed and stained for mineral deposition by von Kossa technique.



<u>Figure 15</u> The amount of calcium deposition in mineralization nodules. MSCs were grown in the presence of OM without HCl (HCL 0, pH ~ 7.4) and with HCl 1 μl/1 ml of OM (HCL 1, pH ~ 7.25), 2 μl/ml (HCL 2, pH ~ 7.15) and 3 μl/ml (HCL 3, pH ~ 7). The amount of calcium deposition was measured by Calcium-o-Cresolphthalein Complexone method and normalized by protein content. Results represent an average of 6 experiments. $^{\#}P$ < 0.05 compared to day 7, $^{*}P$ < 0.05 compared to HCL 0.

Discussion

Part 1

These seven patients have compatible characteristics of dRTA as described previously. Successful correction of metabolic acidosis with potassium citrate resulted in the increase in serum potassium, phosphate and iPTH 4, 5. Earlier studies demonstrated that chronic metabolic acidosis induced by exogenous or endogenous acid loads resulted in physicochemical dissolution of the bone and enhanced osteoclastic bone resorption accompanied by marked elevation in the urinary calcium excretion $^{31-33}$. In our patients, however, hypercalciuria was not observed. The difference in the urinary calcium excretion might be a result of the difference in the chronicity of the disease and the relatively low calcium intake in this group of Thai population. In a study by Lemann et al, all subjects had a rather short period of acidosis of less than a month when compared with our patients, who had suffered from metabolic acidosis for many years. Nevertheless, our findings were consistent with that of Coe et al ³⁴. In Coe's study, chronic metabolic acidosis produced no hypercalciuria when dietary sodium intake was restricted. When sodium intake was increased, while maintaining the same acid load, hypercalciuria appeared ³⁴. The urinary sodium excretion in our patients was rather low and approximately half of the amount of urinary sodium excretion associated with hypercalciuria found in Coe's study. Therefore, the low urinary sodium excretion might contribute partly to the relatively low urinary calcium excretion. Another possible explanation is the histomorphometric finding of suppressed osteoclast population and activity, which suggests against a presence of significant process of bone resorption in our patients. Metabolic acidosis has been known to result in renal phosphate wasting through the reduction in proximal tubular phosphate reabsorption 35, 36. In our patients, serum phosphate was low at baseline; however, the urinary phosphate excretion was unaltered compared to the healthy subjects. The prolonged negative phosphate balance and the chronically suppressed PTH levels might be responsible for the absence of phosphaturia. Correction of metabolic acidosis normalized the phosphate balance and serum phosphate.

The combination of negative calcium balance, phosphate depletion and suppressed PTH during metabolic acidosis explains the findings of low bone density and the feature of low turnover bone disease, characterized by low bone volume, low osteoblast and osteoclast numbers, decreased mineralizing surface, and normal bone eroded surface, demonstrated by histomorphometry. In addition, the alteration in vitamin D metabolism might play a contributory role. Several studies reported inconsistent results on the levels of 1,25-(OH)₂ vitamin D during metabolic acidosis ranged from increased to unchanged to decreased ³⁶⁻³⁸. In human, Krapf et al demonstrated an increase in 1,25-(OH)₂D level secondary to phosphate depletion in an experimental NH₄CL induced acidosis. The production rate of 1,25-(OH)₂ vitamin D was stimulated and PTH decreased secondarily ³⁶. We did not measure the 1,25-(OH)₂D levels in our patients; nevertheless, the finding of low PTH in our study is consistent with that of Krapf's. Correction of metabolic acidosis normalized the calcium balance, serum phosphorus, and PTH resulting in an increase in bone mass. The elevated osteoid surface and volume, the reduction in mineralizing surface, the falls in mineral apposition rate and adjusted apposition rate, and the prolonged mineralization lag time suggest toward a presence of

mineralization defect in dRTA. Nevertheless, the degree of increased osteoid thickness, together with its negative correlation with the adjusted apposition rate, a cardinal feature of osteomalacia, was only borderline significant ³⁹. The explanation may be the high variability of the osteoid thickness among our patients, which in turn suggests the presence of heterogeneity of bone disease in dRTA. Previously, both osteomalacia and osteoporosis have been reported in association with metabolic acidosis 20, 40. Our findings also indicate that some patients have a histological feature of osteomalacia associated with an increased osteoid thickness while others fall in a group of low bone turnover osteopenia accompanied by a normal to decreased osteoid thickness. The existence of diversity of bone disease in dRTA is further supported by the wide range of values reported on the mineralizing surface and mineralization lag time. The most likely causative factors for the defective mineralization in our patients were phosphate depletion and, perhaps, abnormal vitamin D metabolism. After successful correction of metabolic acidosis, the parameters associated with mineralization and bone formation improved considerably. In addition, alkaline therapy might also improve osteoblast function suggested by the increase in bone formation rate per osteoblast. While the negative calcium and phosphate balance and perhaps impaired osteoblast function contributed to the low bone mass, cell-mediated bone resorption did not seem to play a major role. Previous in vitro studies demonstrated enhanced osteoclastic bone resorption during metabolic acidosis 41, 42 Later on, Frick et al discovered that RANKL RNA expression was upregulated in mouse calvariae incubated in acidic media, suggesting that metabolic acidosis stimulates osteoclast differentiation 43. In addition to the proliferative effect on bone cells, PTH is also a potent stimulation for RANKL expression and osteoclast differentiation 44, 45. Thus, the absence of enhanced bone resorption in our patients could be explained by the presence of low PTH resulting in the reduction in osteoblast and osteoclast populations and the suppression of osteoclast differentiation. Substantial evidence suggested that growth hormone/insulin-like growth factor axis was suppressed during metabolic acidosis 46, 47. Therefore, in addition to the low PTH, the impaired growth hormone/insulin-like growth factor system, whose effect directly promotes cellular proliferation and differentiation, might also be responsible for the overall reduction in bone cell populations. After alkaline therapy, the parameters associated with bone resorption were unchanged. One would have expected the reduction in osteoclast number and/or activity after correction of acidosis; however, such findings might have been prevented by the rise of the PTH.

Additional analysis on the bone matrix proteins demonstrated a significant increase in osteocalcin expression within the bone matrix after correction of metabolic acidosis. Osteocalcin, produced and secreted almost exclusively by cells of osteoblast origin, is well-known as a marker of osteoblast function and its serum level correlates with bone formation ^{13, 48}. The increased osteocalcin expression, which might have occurred secondarily to the enhanced osteoblast function after correction of metabolic acidosis, corresponded to the improvement in bone formation and mineralization. In vitro studies using osteoblast culture model demonstrated the inhibition of osteoblast function by metabolic acidosis; for example, metabolic acidosis impaired osteoblastic collagen synthesis ⁸ and reversibly inhibited the expression of osteoblastic genes including type I

collagen, matrix Gla protein and osteopontin ¹⁰. Our finding provides in vivo evidence on the inhibitory effect of metabolic acidosis on osteoblastic gene expression and its improvement after alkaline therapy. In support of our result, others have found an increase in serum osteocalcin after correction of metabolic acidosis corresponding to the improvement in bone mineral balance ^{49,50}.

Osteonectin is another NCP that involves in the process of bone formation. Osteonectin deficient mice have decreased bone formation and profound osteopenia ¹⁵. Culture of bone marrow stromal cells and osteoblasts obtained from these animals revealed compromised osteoblast formation, maturation and survival ⁵¹. Previous in vitro study using osteoblast culture model in acidic medium found no alteration in the expression of osteonectin mRNA compared to control culture at neutral pH ¹⁰. We also found no significant difference in the expression of osteonectin within the bone matrix before and after alkaline therapy, suggesting that the effect of metabolic acidosis on bone matrix protein expression might be selective.

Osteopontin and bone sialoprotein belong to the same family protein, which contains an RGD (Arg-Gly-Asp) cell attachment sequence, therefore play roles in the regulation of adhesion and the attachment and spreading of osteoclasts to the bone surface ⁵². Osteopontin mRNA was found in both osteoblasts and osteoclasts ¹⁶ and especially highly expressed in the resorption lacunae and in the osteoclasts at immediate resorption surfaces ¹⁷. In a study by Ihara et al, PTH-induced increase in TRAP-positive cells was absent in osteopontin-deficient bones 44, emphasizing the role of osteopontin in differentiation of osteoclasts and bone resorption. In our study, six of seven patients had decreased osteopontin expression within the bone matrix after alkaline therapy. The expression of bone sialoprotein was not significantly altered. The discrepancy between our result and that of Frick et al, who found decreased osteopontin mRNA in osteoblasts cultured in acidic media ¹⁰, could be due to the fact that osteopontin production is almost undetectable in osteoblasts actively expressing osteocalcin ²⁹; therefore, the reduction in its expression might be secondary to the decreased production by osteoclasts rather than osteoblasts. Since RANKL is upregulated during metabolic acidosis; thus, the reduction in RANKL stimulated osteoclast differentiation might be the reason for decreased osteopontin expression after alkaline therapy. PTH has been known to stimulate RANKL and osteopontin expression 45, 53; therefore, the increase in PTH levels after acidosis correction could attenuate the alterations in osteopontin expression and histomorphometric parameters related to bone resorption.

We found no significant alteration in the distribution of NCPs before and after alkaline therapy, suggesting minor roles of the distribution of the proteins in abnormal bone remodeling in patients with dRTA. The variability in the expression of NCPs among different patients might be due to sex and age differences in the composition of bone matrix ⁵⁴. This observation, however, will require further study in a larger number of patients.

Our study confirmed previous reports of preserved antigenicity within the mineralized compartment of the bone embedded in plastic $^{25, 55}$. The staining within the cellular components could be improved with embedding and polymerization performed at lower temperature (-15 to -20° C) 56 . The data on NCPs was limited by the semi-quantitative nature of immunohistochemistry;

however, the method we applied required measurements of at least 40 trabecular bone areas in multiple bone sections cut at different levels, which have been shown previously to be sufficient to obtain representative data with a small confidence intervals ²⁵.

In summary, our data demonstrated abnormal bone remodeling in patients with dRTA characterized by low turnover bone disease with defective mineralization. Alteration of NCPs expression suggested the effect of metabolic acidosis on bone cells in vivo. Alkaline therapy improved bone formation through the restoration of bone mineral balance and perhaps enhanced osteoblast function. Further studies are required to elucidate the effect of chronic metabolic acidosis on bone resorption in vivo.

Part 2

Bone marrow contains at least two types of stem cells: hematopoietic stem cells and MSCs. When plating BMMCs on the plastic dish, MSCs are able to attach to the dish and propagate while hematopoietic stem cells are non-adherent and can be discarded. MSCs are identified based on the positivity of a set of marker proteins on their surface, including CD105 and CD 73, and the negativity for other markers of hematopoietic cells such as CD14, CD45 and CD34. They are also characterized by the ability to differentiate into multiple mesenchymal lineages, including osteocytes, chondrocytes and adipocytes ²⁷. Our isolated cultured MSCs showed characteristic surface marker profiles and were able to undergo osteogenic and adipogenic differentiation under appropriate conditions.

In our study of experimental acidosis, we observed that cellular proliferation was suppressed at pH 7.15 or below. The expression of multiple osteoblastic genes, which are sequentially upregulated during different stages of osteoblast differentiation, was altered by metabolic acidosis. First, we observed the enhanced expression of cbfa-1, an essential transcription factor necessary for osteoblast commitment, by metabolic acidosis. Cbfa-1 is required during osteogenesis and its expression is upregulated in the early proliferative period of osteoblast differentiation. Homozygous mutation of cbfa-1 resulted in a complete lack of bone formation with arrest of osteoblast differentiation ²⁸. The upregulation of cbfa-1 in chronic metabolic acidosis suggests accelerated osteoblast differentiation during the early period. This was further supported by the finding of heightened type I collagen mRNA expression. Type I collagen is the most abundant matrix protein in bone and the expression of its transcript usually peaks in the early period of osteoblast differentiation following that of cbfa-1 11, 29. Moreover, the expression of type I collagen mRNA appeared to follow the same pattern to that of cbfa-1 especially the robust increase at day 20, when downregulation of both genes are to be expected in normal condition (figure 3A and 3B). Since the promoter of type I collagen gene has a binding site for cbfa-1 ⁵⁷, the binding of cbfa-1 to this cis-acting element may be responsible for the increase in type I collagen transcripts. On the other hand, metabolic acidosis could also affect other transcription proteins upstream of both cbfa-1 and type I collagen.

The period of bone matrix synthesis and maturation follows the early proliferative period of osteoblast differentiation. During this time, genes associated with bone cell phenotype and other noncollagenous bone matrix proteins emerged For example, alkaline phosphatase mRNA expression and enzyme activity are usually increased upto 10 fold. Later on in the mineralization period, the upregulation of osteocalcin mRNA signifies terminally differentiated osteoblast ²⁹. In contrast to the stimulatory effect on early osteoblastic genes, chronic metabolic acidosis suppressed alkaline phosphatase mRNA and its enzyme activity. At present, we are trying to confirm the expression of osteocalcin to determine whether terminal osteoblast differentiation is augmented or attenuated by metabolic acidosis.

Recently, another transcription factor necessary for osteoblast differentiation, osterix, has been identified. Osterix null mice completely lack bone formation due to the absence of osteoblasts. Osterix expression is absent in cbfa-1 null mice, although cbfa-1 is detected in osterix null mice suggesting that osterix acts downstream of cbfa-1 ³⁰. Little is known as to how osterix regulates osteoblast differentiation. It has been suggested that osterix is required for directing MSCs away from chondrocyte lineage and toward the osteoblast lineage. The reduction in osterix mRNA in our study may represent a negative feedback control from increased expression of cbfa-1. This, however, will require further study.

Metabolic acidosis has been known to impair bone matrix mineralization both in vitro and in vivo 10, 20, 58, 59. The skeletal demineralization was presumed to be secondary to both physicochemical bone dissolution and cell-mediated process 7, 8, 41, 42, 60. In our study, bone matrix mineralization was also impaired in the cell layers cultured in acidic environment. The attenuation of osteoblast maturation may be partly responsible the impaired mineralization. The possibility of osteoblast dedifferentiation during chronic metabolic acidosis was also suggested by the results from Frick et al's study demonstrating diminished expression of osteoblastic genes, matrix Gla protein and osteopontin, in calvariae-derived osteoblasts grown in acidic medium 10.

Our study is the first to show sequential changes of osteoblastic gene expression during chronic metabolic acidosis. Osteoblast differentiation is accelerated in the early stages. Our findings confirm that of other studies in demonstrating the reduction of alkaline phosphatase enzyme activity and impaired bone matrix mineralization during acidosis ^{8, 42}. Conflicting data exists on type I collagen. In a previous study, mouse calvarial bone cells exposed to acidic medium for 30 minutes had decreased type I collagen mRNA ⁹, whereas in our study its expression was enhanced. This discrepancy may be due to different effect of acute versus chronic metabolic acidosis on protein and gene expression.

In conclusion, chronic metabolic acidosis directly affects osteoblast differentiation from MSCs. Osteoblast differentiation is enhanced in the early stages, whereas matrix mineralization is impaired. The roles of heightened cbfa-1 mRNA on the expression of other osteoblastic genes will require further study.

Bibliography

- 1. Caruana RJ, Buckalew VM, Jr. The syndrome of distal (type 1) renal tubular acidosis. Clinical and laboratory findings in 58 cases. Medicine (Baltimore) 1988;67(2):84-99.
- 2. Wrong OM, Feest TG. The natural history of distal renal tubular acidosis. Contrib Nephrol 1980;21:137-44.
- 3. Richards P, Chamberlain MJ, Wrong OM. Treatment of osteomalacia of renal tubular acidosis by sodium bicarbonate alone. Lancet 1972;2(7785):994-7.
- 4. Domrongkitchaiporn S, Pongsakul C, Stitchantrakul W, Sirikulchayanonta V, Ongphiphadhanakul B, Radinahamed P, et al. Bone mineral density and histology in distal renal tubular acidosis. Kidney Int 2001;59(3):1086-93.
- 5. Domrongkitchaiporn S, Pongskul C, Sirikulchayanonta V, Stitchantrakul W, Leeprasert V, Ongphiphadhanakul B, et al. Bone histology and bone mineral density after correction of acidosis in distal renal tubular acidosis. Kidney Int 2002;62(6):2160-6.
- 6. Bushinsky DA, Krieger NS, Geisser DI, Grossman EB, Coe FL. Effects of pH on bone calcium and proton fluxes in vitro. Am J Physiol 1983;245(2):F204-9.
- 7. Bushinsky DA, Lechleider RJ. Mechanism of proton-induced bone calcium release: calcium carbonate-dissolution. Am J Physiol 1987;253(5 Pt 2):F998-1005.
- 8. Krieger NS, Sessler NE, Bushinsky DA. Acidosis inhibits osteoblastic and stimulates osteoclastic activity in vitro. Am J Physiol 1992;262(3 Pt 2):F442-8.
- 9. Frick KK, Jiang L, Bushinsky DA. Acute metabolic acidosis inhibits the induction of osteoblastic egr-1 and type 1 collagen. Am J Physiol 1997;272(5 Pt 1):C1450-6.
- 10. Frick KK, Bushinsky DA. Chronic metabolic acidosis reversibly inhibits extracellular matrix gene expression in mouse osteoblasts. Am J Physiol 1998;275(5 Pt 2):F840-7.
- 11. Aubin JE. Regulation of osteoblast formation and function. Rev Endocr Metab Disord 2001;2(1):81-94.
- 12. Maniatopoulos C, Sodek J, Melcher AH. Bone formation in vitro by stromal cells obtained from bone marrow of young adult rats. Cell Tissue Res 1988;254(2):317-30.
- 13. Garcia-Carrasco M, Gruson M, de Vernejoul MC, Denne MA, Miravet L. Osteocalcin and bone morphometric parameters in adults without bone disease. Calcif Tissue Int 1988;42(1):13-7.
- 14. Gundberg CM, Lian JB, Gallop PM, Steinberg JJ. Urinary gamma-carboxyglutamic acid and serum osteocalcin as bone markers: studies in osteoporosis and Paget's disease. J Clin Endocrinol Metab 1983;57(6):1221-5.
- 15. Delany AM, Amling M, Priemel M, Howe C, Baron R, Canalis E. Osteopenia and decreased bone formation in osteonectin-deficient mice. J Clin Invest 2000;105(7):915-23.
- 16. Merry K, Dodds R, Littlewood A, Gowen M. Expression of osteopontin mRNA by osteoclasts and osteoblasts in modelling adult human bone. J Cell Sci 1993;104 (Pt 4):1013-20.
- 17. Dodds RA, Connor JR, James IE, Rykaczewski EL, Appelbaum E, Dul E, et al. Human osteoclasts, not osteoblasts, deposit osteopontin onto resorption surfaces: an in vitro and ex vivo study of remodeling bone. J Bone Miner Res 1995;10(11):1666-80.

- 18. Yoshitake H, Rittling SR, Denhardt DT, Noda M. Osteopontin-deficient mice are resistant to ovariectomy-induced bone resorption. Proc Natl Acad Sci U S A 1999;96(14):8156-60.
- 19. Raynal C, Delmas PD, Chenu C. Bone sialoprotein stimulates in vitro bone resorption. Endocrinology 1996;137(6):2347-54.
- 20. Nilwarangkur S, Nimmannit S, Chaovakul V, Susaengrat W, Ong-aj-Yooth S, Vasuvattakul S, et al. Endemic primary distal renal tubular acidosis in Thailand. Q J Med 1990;74(275):289-301.
- 21. Mautalen C, Montoreano R, Labarrere C. Early skeletal effect of alkali therapy upon the osteomalacia of renal tubular acidosis. J Clin Endocrinol Metab 1976;42(5):875-81.
- 22. Henneman PH, Benedict PH, Forbes AP, Dudley HR. Idiopathic hypercaicuria. N Engl J Med 1958;259(17):802-7.
- 23. Parfitt AM, Drezner MK, Glorieux FH, Kanis JA, Malluche H, Meunier PJ, et al. Bone histomorphometry: standardization of nomenclature, symbols, and units. Report of the ASBMR Histomorphometry Nomenclature Committee. J Bone Miner Res 1987;2(6):595-610.
- 24. Fisher LW, Stubbs JT, 3rd, Young MF. Antisera and cDNA probes to human and certain animal model bone matrix noncollagenous proteins. Acta Orthop Scand Suppl 1995;266:61-5.
- 25. Derkx P, Nigg AL, Bosman FT, Birkenhager-Frenkel DH, Houtsmuller AB, Pols HA, et al. Immunolocalization and quantification of noncollagenous bone matrix proteins in methylmethacrylate-embedded adult human bone in combination with histomorphometry. Bone 1998;22(4):367-73.
- 26. Bruder SP, Jaiswal N, Haynesworth SE. Growth kinetics, self-renewal, and the osteogenic potential of purified human mesenchymal stem cells during extensive subcultivation and following cryopreservation. J Cell Biochem 1997;64(2):278-94.
- 27. Pittenger MF, Mackay AM, Beck SC, Jaiswal RK, Douglas R, Mosca JD, et al. Multilineage potential of adult human mesenchymal stem cells. Science 1999;284(5411):143-7.
- 28. Komori T, Yagi H, Nomura S, Yamaguchi A, Sasaki K, Deguchi K, et al. Targeted disruption of Cbfa1 results in a complete lack of bone formation owing to maturational arrest of osteoblasts. Cell 1997;89(5):755-64.
- 29. Stein GS, Lian JB. Molecular mechanisms mediating proliferation/differentiation interrelationships during progressive development of the osteoblast phenotype. Endocr Rev 1993;14 (4):424-42.
- 30. Nakashima K, Zhou X, Kunkel G, Zhang Z, Deng JM, Behringer RR, et al. The novel zinc finger-containing transcription factor osterix is required for osteoblast differentiation and bone formation. Cell 2002;108(1):17-29.
- 31. Bleich HL, Moore MJ, Lemann J, Jr., Adams ND, Gray RW. Urinary calcium excretion in human beings. N Engl J Med 1979;301(10):535-41.
- 32. Lemann J, Jr., Litzow JR, Lennon EJ. The effects of chronic acid loads in normal man: further evidence for the participation of bone mineral in the defense against chronic metabolic acidosis. J Clin Invest 1966;45(10):1608-14.
- 33. Kraut JA, Mishler DR, Singer FR, Goodman WG. The effects of metabolic acidosis on bone formation and bone resorption in the rat. Kidney Int 1986;30(5):694-700.

- 34. Coe FL, Firpo JJ, Jr. Evidence for mild reversible hyperparathyroidism in distal renal tubular acidosis. Arch Intern Med 1975;135(11):1485-9.
- 35. Ambuhl PM, Zajicek HK, Wang H, Puttaparthi K, Levi M. Regulation of renal phosphate transport by acute and chronic metabolic acidosis in the rat. Kidney Int 1998;53(5):1288-98.
- 36. Krapf R, Vetsch R, Vetsch W, Hulter HN. Chronic metabolic acidosis increases the serum concentration of 1,25-dihydroxyvitamin D in humans by stimulating its production rate. Critical role of acidosis-induced renal hypophosphatemia. J Clin Invest 1992;90(6):2456-63.
- 37. Kraut JA, Gordon EM, Ransom JC, Horst R, Slatopolsky E, Coburn JW, et al. Effect of chronic metabolic acidosis on vitamin D metabolism in humans. Kidney Int 1983;24(5):644-8.
- 38. Reddy GS, Jones G, Kooh SW, Fraser D. Inhibition of 25-hydroxyvitamin D3-1-hydroxylase by chronic metabolic acidosis. Am J Physiol 1982;243(4):E265-71.
- 39. Parfitt AM. Osteomalacia and Related Disorders. In: Avioli LV, Krane SM, editors. Metabolic Bone Disease and Clinically Related Disorders. 3rd ed. San Diego: Academic Press; 1997. p. 327-386.
- 40. Weger W, Kotanko P, Weger M, Deutschmann H, Skrabal F. Prevalence and characterization of renal tubular acidosis in patients with osteopenia and osteoporosis and in non-porotic controls. Nephrol Dial Transplant 2000;15(7):975-80.
- 41. Meghji S, Morrison MS, Henderson B, Arnett TR. pH dependence of bone resorption: mouse calvarial osteoclasts are activated by acidosis. Am J Physiol Endocrinol Metab 2001;280 (1):E112-9.
- 42. Bushinsky DA. Stimulated osteoclastic and suppressed osteoblastic activity in metabolic but not respiratory acidosis. Am J Physiol 1995;268(1 Pt 1):C80-8.
- 43. Frick KK, Bushinsky DA. Metabolic acidosis stimulates RANKL RNA expression in bone through a cyclo-oxygenase-dependent mechanism. J Bone Miner Res 2003;18(7):1317-25.
- 44. Ihara H, Denhardt DT, Furuya K, Yamashita T, Muguruma Y, Tsuji K, et al. Parathyroid hormone-induced bone resorption does not occur in the absence of osteopontin. J Biol Chem 2001;276(16):13065-71.
- 45. Huang JC, Sakata T, Pfleger LL, Bencsik M, Halloran BP, Bikle DD, et al. PTH differentially regulates expression of RANKL and OPG. J Bone Miner Res 2004;19(2):235-44.
- 46. Green J, Maor G. Effect of metabolic acidosis on the growth hormone/IGF-I endocrine axis in skeletal growth centers. Kidney Int 2000;57(6):2258-67.
- 47. Brungger M, Hulter HN, Krapf R. Effect of chronic metabolic acidosis on the growth hormone/IGF-1 endocrine axis: new cause of growth hormone insensitivity in humans. Kidney Int 1997;51(1):216-21.
- 48. Price PA. Gla-containing proteins of bone. Connect Tissue Res 1989;21(1-4):51-7; discussion 57-60.
- 49. Lin YF, Shieh SD, Diang LK, Lin SH, Chyr SH, Li BL, et al. Influence of rapid correction of metabolic acidosis on serum osteocalcin level in chronic renal failure. Asaio J 1994;40(3):M440-4.

- 50. Sebastian A, Harris ST, Ottaway JH, Todd KM, Morris RC, Jr. Improved mineral balance and skeletal metabolism in postmenopausal women treated with potassium bicarbonate. N Engl J Med 1994;330(25):1776-81.
- 51. Delany AM, Kalajzic I, Bradshaw AD, Sage EH, Canalis E. Osteonectin-null mutation compromises osteoblast formation, maturation, and survival. Endocrinology 2003;144(6):2588-96.
- 52. Young MF. Bone matrix proteins: their function, regulation, and relationship to osteoporosis. Osteoporos Int 2003;14 Suppl 3:S35-42.
- 53. Gopalakrishnan R, Ouyang H, Somerman MJ, McCauley LK, Franceschi RT. Matrix gamma-carboxyglutamic acid protein is a key regulator of PTH-mediated inhibition of mineralization in MC3T3-E1 osteoblast-like cells. Endocrinology 2001;142(10):4379-88.
- 54. Aerssens J, Boonen S, Joly J, Dequeker J. Variations in trabecular bone composition with anatomical site and age: potential implications for bone quality assessment. J Endocrinol 1997;155 (3):411-21.
- 55. Ingram RT, Clarke BL, Fisher LW, Fitzpatrick LA. Distribution of noncollagenous proteins in the matrix of adult human bone: evidence of anatomic and functional heterogeneity. J Bone Miner Res 1993;8(9):1019-29.
- 56. Erben RG. Embedding of bone samples in methylmethacrylate: an improved method suitable for bone histomorphometry, histochemistry, and immunohistochemistry. J Histochem Cytochem 1997;45(2):307-13.
- 57. Ducy P, Zhang R, Geoffroy V, Ridall AL, Karsenty G. Osf2/Cbfa1: a transcriptional activator of osteoblast differentiation. Cell 1997;89(5):747-54.
- 58. Phelps KR, Einhorn TA, Vigorita VJ, Lieberman RL, Uribarri J. Acidosis-induced osteomalacia: metabolic studies and skeletal histomorphometry. Bone 1986;7(3):171-9.
- 59. Disthabanchong S, Domrongkitchaiporn S, Sirikulchayanonta V, Stitchantrakul W, Karnsombut P, Rajatanavin R. Alteration of noncollagenous bone matrix proteins in distal renal tubular acidosis. Bone 2004;35(3):604-13.
- 60. Bushinsky DA, Wolbach W, Sessler NE, Mogilevsky R, Levi-Setti R. Physicochemical effects of acidosis on bone calcium flux and surface ion composition. J Bone Miner Res 1993;8 (1):93-102.

Suggestions for future research projects

The mechanisms underlying how chronic metabolic acidosis enhanced osteoblast differentiation in the earlier stages but inhibiting further maturation are still mysterious. The increased expression of cbfa-1 could be partly responsible for the delayed maturation of osteoblasts. In order to elucidate the role of cbfa-1 in osteoblast maturation, one possibility is using cbfa-1-targeted siRNA to suppress the gene expression during metabolic acidosis. The restoration of osteoblast maturation as determined by the expression of mature osteoblastic genes will confirm the role of cbfa-1 in osteoblast differentiation during acidosis. Nevertheless, this does not rule out the fact that metabolic acidosis may also affect other genes that influence the expression of cbfa-1, type I collagen and alkaline phosphatase, for example, msx-2, AJ-18 and dlx-5 among others. Further examination of these genes can be performed and its impact on other osteoblastic genes can be explored.

Output

1. ผลงานตีพิมพ์ในวารสารวิชาการนานาชาติ

- 1.1. Disthabanchong S, Domrongkitchaiporn S, Sirikulchayanonta V, Stitchantrakul V, Karnsombut P, Rajatanavin R. Alteration of Noncollagenous Bone Matrix Proteins in Distal Renal Tubular Acidosis. Bone 2004; 35(3):604-613 (ผลงานนี้ได้รับทุนส่วนหนึ่งจากเมธีวิจัยอาวุโส ศ.นพ.รัชตะ รัชตะนาวิน)
- 1.2. **Disthabanchong S**, Radinahamed P, Hongeng S, Rajatanavin R. Chronic Metabolic Acidosis Enhances Osteoblast Differentiation from Mesenchymal Precursor Cells. (Manuscript in preparation)

2. การนำผลงานวิจัยไปใช้ประโยชน์

- 2.1. เชิงสาธารณะ
 - ผลงานวิจัยนี้ได้ก่อให้เกิดเครือข่ายความร่วมมือในการทำวิจัยเกี่ยวกับโรคกระดูก ระหว่างคณะ แพทยศาสตร์รพ.รามาธิบดี กับ คณะวิทยาศาสตร์มหาวิทยาลัยมหิดล นำไปสู่การสร้างกระแสความ สนใจในวงกว้าง
- 2.2. เชิงวิชาการ
 ผลงานวิจัยนี้สามารถใช้ในการพัฒนาการเรียนการสอน, เพิ่มศักยภาพของผู้ทำวิจัย และเผยแพร่ให้
 กับนักวิจัยรุ่นใหม่และนักศึกษาได้เรียนรู้และใช้เป็นแบบอย่าง เช่น ในการสร้างสมมุติฐาน และออก
 แบบระเบียบวิธีวิจัย
- 2.3. อื่นๆ การเสนอผลงานในที่ประชุมวิชาการ และ หนังสือ
 - 2.3.1. Disthabanchong S, Radinahamed P, Hongeng S, Domrongkitchaiporn S, Rajatanavin R. Chronic Metabolic Acidosis Enhances Early Osteoblast Differentiation while Inhibiting Late Maturation. Submitted for a presentation at the American Society of Nephrology Annual Meeting, Philadelphia, PA, USA 2005
 - 2.3.2. Disthabanchong S, Domrongkitchaiporn S, Sirikulchayanonta V, Rajatanavin R. Differential Expression of Noncollagenous Bone Matrix Proteins in Cortical and Trabecular Bone. Abstract POO1. Accepted for a poster presentation at the 31st European Symposium on Calcified Tissues, Nice, France, 2004
 - 2.3.3. Disthabanchong S, Domrongkitchaiporn S, Sirikulchayanont V, Rajatanavin R. Effect of Alkaline Therapy on Bone Matrix Protein Composition in Distal Renal Tubular Acidosis. PUB560 Journal of the American Society of Nephrology 2003; 14:894A

ภาคผนวก

1. Manuscript in preparation

"Chronic metabolic acidosis enhances osteoblast differentiation from mesenchymal precursor cells"

2. Reprint of manuscript

[&]quot;Alteration of noncollagenous bone matrix proteins in distal renal tubular acidosis"

(This is an unfinished manuscript. Please do not reproduce.)
Chronic Metabolic Acidosis Enhances
Osteoblast Differentiation from
Mesenchymal Precursor Cells

By

Sinee Disthabanchong, M.D.*, Piyanuch Radinahamed, M.S.*, Suradej Hongeng, M.D.† and Rajata Rajatanavin, M.D.§

*Division of Nephrology, Department of Medicine; †
Department of Pediatrics; and §Division of
Endocrinology, Department of Medicine, Ramathibodi
Hospital, Mahidol University, Bangkok, Thailand

Category – original study

Corresponding author
Sinee Disthabanchong, M.D.
Division of Nephrology
Department of Medicine
Ramathibodi Hospital
7th floor research building,
Rama VI Rd,
Bangkok, 10400
Thailand
Pharma (((2) 201 1022)

Phone: (662) 201-1922 Fax: (662) 201-1715

E-mail: sineemd@hotmail.com

Abstract

Distal renal tubular acidosis (dRTA) is characterized by impairment of distal tubular acid secretion resulting in persistent metabolic acidosis. Recent examination of bone histology of dRTA patients showed markedly decreased bone formation with impaired bone matrix mineralization that is not entirely explained by an alteration in the mineral balance. Data from in vitro studies suggests a direct inhibitory effect of metabolic acidosis on osteoblast function. We investigated the effects of chronic metabolic acidosis on osteoblast differentiation from mesenchymal precursor cells (MSCs). Human MSCs isolated from bone marrow aspiration specimen were induced to differentiate into osteoblasts in culture. Concentrated hydrochloric acid was added to the medium to lower the bicarbonate concentration and pH. The mRNA expression of various osteoblastic genes, alkaline phosphatase enzyme activity and bone matrix mineralization were examined periodically. Chronic metabolic acidosis was found to enhance the mRNA expression of early osteoblast transcription factor, cbfa-1, and the major constituent of bone matrix protein, type I collagen, in a dose dependent manner. In contrast, the mRNA expression of osterix (a transcription factor downstream of cbfa-1), alkaline phosphatase (an enzyme normally upregulated in intermediately mature osteoblasts) was suppressed. Alkaline phosphatase enzyme activity was also found to be decreased, correlating with the reduced amount of mRNA expression. Finally, impaired bone matrix mineralization was demonstrated by a reduction in both calcium deposition and number of bone nodules visualized by von Kossa staining. In conclusion, chronic metabolic acidosis enhanced early osteoblast differentiation while impaired bone matrix mineralization.

Keywords: acidosis, osteoblast, bone, osteoblast differentiation, mesenchymal

Introduction

Distal renal tubular acidosis (dRTA) is a clinical syndrome characterized by impaired renal excretion of ammonium and titrable acid resulting in persistent metabolic acidosis. The presence of chronic metabolic acidosis results in various metabolic consequences, including hypokalemia, hypercalciuria, hypophosphatemia and abnormal bone metabolism ¹⁻³. Recent bone histologic studies of dRTA patients from our laboratory revealed findings of osteopenia, suppressed bone formation and some degree of impaired bone matrix mineralization ^{4,59}. Although the abnormal bone remodeling may largely be due to an alteration in mineral balance, the effect of metabolic acidosis on bone cells may also play a significant role. We searched for evidence of this by examining the expression of various bone matrix proteins in dRTA. Since bone matrix proteins are mostly produced by osteoblasts ²⁹; their alterations would suggest an influence of metabolic acidosis on osteoblast function. Immunohistochemical staining of the bone sections obtained from patients with dRTA before and after alkaline therapy revealed heightened expression of osteocalcin after correction of acidosis ⁵⁹. As osteocalcin is a marker of mature osteoblast, its restoration by alkaline therapy suggests the possibility of impaired osteoblast differentiation and/or maturation by metabolic acidosis.

Using an in vitro model of bone organ culture derived from neonatal mouse calvariae, Krieger et al observed that short-term incubation of calvariae in acidic medium suppressed type I collagen synthesis and lowered alkaline phosphatase enzyme activity ⁸. In a later study, the same group examined the effect of acute metabolic acidosis on primary bone cells. Incubation of calvariae-derived osteoblasts in acidic medium for 30 minutes resulted in marked decrease in erg-1 and type I collagen gene expression ⁹. Furthermore, chronic metabolic acidosis diminished the expression of matrix Gla protein and osteopontin mRNA of primary osteoblasts derived from the same source and impaired bone matrix mineralization ¹⁰. This evidence supports the existence of a direct inhibitory effect of metabolic acidosis on osteoblasts.

Osteoblasts originate from mesenchymal precursor cells (MSCs) in the bone marrow. These cells contribute to replacement of osteoblasts in bone turnover and fracture healing throughout life. Under appropriate conditions, multipotent MSCs can also differentiate into chondrocytes, adipocytes and fibroblasts. A wide variety of systemic and local factors appears to regulate osteoprogenitor proliferation and differentiation, a sequence that is characterized by a series of cellular and molecular events distinguished by differential expression of osteoblast-associated genes, including those for specific transcription factors and matrix proteins 11 . In vitro, the induction of osteogenic differentiation can be achieved in the presence of dexamethasone (Dex), β -glycerophosphate (β -GP) and ascorbate phosphate (Asp) 12 . Since metabolic acidosis may have an inhibitory effect on osteoblasts and possibly interfere with osteoblast maturation, we studied the sequential changes in the expression of osteoblastic genes in human MSCs during osteogenic induction to examine the effect of chronic metabolic acidosis on osteoblast differentiation.

Materials and Methods

Isolation and culture of bone marrow derived MSCs

Bone marrow samples were obtained using a bone marrow biopsy needle inserted through posterior iliac crest of a healthy bone marrow donor after an

informed consent. Bone marrow mononuclear cells (BMMCs) were separated by density gradient centrifugation with 1.073 g/ml Percoll solution (Sigma, MO, USA). Briefly, 10 ml of heparinized bone marrow cells were mixed in an equal volume of Dulbecco's Modified Eagle's Medium (DMEM) (BioWhittaker, MD, USA) and centrifuged at 900g for 10 min at room temperature. The washed cells were resuspended in DMEM at a density of 4 x 10⁷ cells/ml, and 5 ml aliquot was layered over 1.073 g/ml Percoll solution and centrifuged at 1,000g for 30 min at room temperature. The interface mononuclear cells were collected and washed twice with DMEM. Total cell count and cell viability were evaluated by 0.2% Trypan blue exclusion. A total of 2 x 10⁶ cells/ml of BMMCs were cultured in DMEM complete medium supplemented with 10% fetal bovine serum (FBS) (GibcoBRL, NY, USA) and 1% penicillin-streptomycin (GibcoBRL) at 37°C in 5% CO₂ incubator. On day 3 of cultivation, non-adherent cells were discarded and this process was repeated every 4 days. Upon 90% confluency, MSCs were trypsinized by 0.05% trypsin (Gibco BRL) and passaged for the next expansion. This study has been approved by ethical committee on Research Involving Human Subjects at Ramathibodi hospital, Mahidol University.

Flow cytometry analysis of cultured bone marrow derived MSCs

Bone marrow derived adherent cells (at the end of 4th passage) were trypsinized and adjusted to 5-10 x 10⁶ cells/ml. 100 µl of adjusted cells were incubated with 10 µl of following monoclonal antibodies, CD-14PE, CD-34FITC, CD45-FITC, HLA-DR PE and CD-105FITC (Becton-Dickinson Pharmingen, Heidelberg, Germany) at 4°C in the dark. After 20 min of incubation, 2 ml of PBS/2% FBS solution was added to each monoclonal antibody-treated cells. The mixtures were then centrifuged at 2,500 rpm for 10 min followed by removal of supernatant. These steps were repeated again following fixation of the cells with 0.5% paraformaldehyde. Flow cytometry analysis was performed using Cellquest software program.

Osteogenic and adipogenic differentiation

Studies were performed in subconfluent culture of human MSCs between passages 4-8. These cells have previously been shown to remain undifferentiated through multiple passages and their osteogenic potential is preserved up until passage 10-15 ²⁶. A normal karyotype and telomerase activity were found to be maintained even at passage 12 ²⁷. MSCs were grown in multi-well tissue culture plates (Nunc, Denmark) until 50-60% confluency when DEX 100 nM (Sigma, MO, USA), β-GP 10 mM (Sigma) and Asp 0.1 mM (Sigma) were added to induce osteogenic differentiation (day 0). This medium will be referred to as osteogenic differentiation medium (OM). In the dose response experiments, concentrated hydrochloric acid (HCl) was added (at day 0) at the concentration of 1µl/1ml of culture medium to achieve an approximate pH of 7.25 (HCL 1), 2 µl/ml for pH 7.15 (HCL 2) and 3 µ 1/ml for pH 7.0 (HCL 3). MSCs grown in the culture medium without HCl (HCL 0) served as control (pH 7.4). Time course experiments were performed with the cells grown in HCL 2 culture medium. MSCs cultivated in the absence of OM represent negative controls. For adipogenic differentiation, DEX 1 µM, 3-isobutyl-1 methylxanthine 100 µg/ml (Sigma) and insulin 10 µg/ml (Sigma) were added to confluent culture of MSCs. Medium was changed twice weekly.

Cell proliferation assay

Cell proliferation was evaluated by MTT assay at various time intervals. The yellow tetrazolium MTT (Sigma, MO, USA) was reduced by metabolically active cells resulting in intracellular purple formazan, which was solubilized and quantified by spectrophotometric means. The experiments were performed in 12-well tissue culture plates. MSCs were grown in the presence of OM without HCl (HCL 0) and with HCl (HCL 1, HCL 2 and HCL 3). After the cells were rinsed twice with DMEM without phenol red, 1 ml of 0.5 mg/ml MTT solution was added to each well. After 3 hours of incubation at 37°C in CO₂ incubator, the purple precipitate formed within the cells. MTT was removed and intracellular purple formazan was solubilized with 1 ml of 0.04 M HCl in absolute isopropanol. Absorbance was recorded at 570 nm with background subtraction at 650 nm.

Studies of osteoblastic gene expression by quantitative real-time RT-PCR.

Total RNA was isolated from culture cells at various time intervals using Trizol (Life Technologies, NY, USA) method as described by manufacturer. cDNAs were reverse transcribed from 1 µg of total RNA using Reverse Transcription System (Promega, WI, USA) with random hexamer as primer as described by manufacturer. cDNAs obtained from the reaction were diluted 1:5 in DNAse free water. Quantitative real-time RT-PCR was performed using ABI Prism 7000 Sequence Detection System (Applied Biosystems, CA, USA). 3-6 µl of cDNAs were analyzed in 25 µl reaction of Tagman® Universal PCR mastermix (Applied Biosystems). Multiplexed PCR reaction was performed with both target and reference genes (18S rRNA) in the same reaction. Each sample was analyzed in triplicate. The probe for 18S rRNA was fluorescently labeled with VICTM and TAMRA (Applied Biosystems), whereas the probes for gene of interest were labeled with 6-carboxyfluorescein (FAM) and TAMRA (Applied Biosystems). Primer concentrations were 300 nM except for type I collagen and 18S rRNA where the concentrations were 25 nM. Probe concentrations were 100-150 nM for the target genes and 50 nM for 18S rRNA. The nucleotide sequences of primers and probes for 18S rRNA, cbfa-1, type I collagen (Coll I), osterix (Osx), alkaline phosphatase (ALP) and osteocalcin (OC) are shown in Table I. Relative expression levels of the gene of interest, normalized by the amount of 18S rRNA, were calculated by Sequence Detection Software version 1.2 (Applied Biosystems) using Relative Quantification Study approach. The average values of Δ Cts from each sample were used for statistical analysis.

Alkaline phosphatase enzyme activity assay

Alkaline phosphatase enzyme activity was measured based on its ability to convert a substrate, *p*-nitrophenyl phosphate, to a yellow colored product, *p*-nitrophenol. The absorbance of *p*-nitrophenol can be determined at 405 nm in a microtiter plate reader. The experiments were performed in 12-well tissue culture plates. After cell layers were rinsed twice with calcium and magnesium free PBS, 0.3 ml of 2 mg/ml *p*-nitrophenyl phosphate solution (Sigma) in 0.75 M AMP (Sigma) with 2 mM magnesium chloride, pH10.3, was added to each well. Cells were incubated in 37°C water bath for 30 min and the reaction was stopped by adding 0.3 ml of 50 mM NaOH to each well. Protein concentration was determined using Bradford Reagent (Sigma) as described by manufacturer. Absorbance of *p*-nitrophenol was normalized by protein concentration. Standard curve was constructed using *p*-nitrophenol standard solution (Sigma). For each sample and standard, assay was performed in duplicate.

Measurement of calcium content

The deposition of calcium in mineralization nodules was determined based on Calcium-o-Cresolphthalein Complexone method. Calcium vielded purple-colored product when formed complex with a chromogenic substrate, o-cresolphthalein Complexone, in an alkaline medium. The intensity of color, measured at 575 nm, is directly proportional to calcium concentration in the sample. The experiments were performed in 12-well tissue culture plates. All the glasswares were cleaned and soaked overnight in 3% HCl, rinsed with distilled water and dried before use. After cell layers were rinsed twice with calcium and magnesium free PBS, decalcification was performed by adding 200-500 ul of 0.6 N HCl into each well. Cells were left overnight at 4°C and 50 µl of samples were transferred to the test tubes containing 1 ml of colored solution (0.1% o-cresolphthalein complexone (Sigma) and 1% 8hydroxyquinoline (Sigma)) the next morning. To provide an alkaline environment, 1 ml of AMP, pH 10.7, was added to each tube and the mixtures were incubated at room temperature for 5 min before measurement. Absorbance of calcium was normalized by protein concentration. Serially diluted stock CaCO₃ was used as standards. For each sample and standard, assay was performed in duplicate.

Von Kossa staining

The experiments were performed in 25 mm² tissue culture dishes. MSCs were allowed to grow in the presence of OM with or without HCl until mineralization appeared. After washing the cells twice in calcium and magnesium free PBS, cell layers were fixed with 10% formalin for 30 min, washed thoroughly with distilled water and incubated with 2% silver nitrate in front of 60 watt lamp for 15 min. Aluminum foil was placed around the dish and the lamp in order to reflect the light.

Statistical Analysis

Results are presented as mean \pm SEM. Student t test was used to compare group means of two samples. The difference was considered significant at P value below 0.05.

Results

First, we isolated and characterized MSCs derived from bone marrow aspiration specimen. After BMMCs isolated from Percoll gradient were plated, the adherent MSCs gave rise to colonies and exhibited characteristic spindle-shaped morphology (figure 1A). Flow cytometry analysis of the cells in the 4th passage revealed characteristic MSC surface marker profile (CD14^{neg}CD45^{neg}CD34^{neg}HLA-DR^{neg}CD105^{pos}) ²⁷(figure 2A–2D). To determine the ability of MSCs to differentiate into osteoblasts and adipocytes, MSCs were cultivated in the presence of OM and adipogenic inducing medium respectively. After 20 days in culture, cell colonies displayed bone-like nodular aggregates of matrix mineralization (figure 1B) noticeable on von Kossa staining (figure 7). MSCs cultivated in the absence of OM never mineralized (data not shown). Lipid-rich vacuoles were observed after 7 days of adipogenic induction (figure 1D). Cell proliferation of cultured human MSCs in the presence of OM with (HCL 1, 2 and 3) and without (HCL 0) HCl was determined by MTT assay (figure 3). Increasing metabolic acidosis below pH 7.25 resulted in a decline in cell proliferation.

Next, we examined the effect of chronic metabolic acidosis on the expression of early osteoblastic genes, cbfa-1, an essential transcription factor required for osteoblast differentiation, ²⁸ and type I collagen, a major bone matrix protein

produced by osteoblasts ²⁹. Half-confluent cultures of human MSCs were cultivated in the presence OM with (HCL 2) and without (HCL 0) HCl. Negative control cells were grown in the absence of osteogenic stimulation with (Negative control HCL 2) and without (Negative control HCL 0) HCl. Cells were harvested for RNA extraction at day 0, 5, 10, 15 and 20 for quantitative real-time RT-PCR analysis. As shown in figure 4A and 4B, the expression of cbfa-1 and type I collagen mRNA was enhanced upto 6.2 fold in the presence of OM. Less than 1.6 fold increase for cbfa-1 and 3.7 fold increase for type I collagen were observed in negative controls. In HCL 0, maximal expression of both genes was noted at day 10-15. The mRNA levels were greater in HCL 2 than in HCL 0 from day 5 through 15 (P < 0.05). At day 15, the expression of both genes appeared to reach plateau; however, the robust increase in expression was observed in HCL 2 at day 20 (cbfa-1 = 6 ± 0.1 vs. 3.3 ± 0.2 , type I collagen = 6.2 ± 0.3 vs. 2.8 ± 0.4 , P < 0.05). Dose response experiments, performed at day 10, showed a progressive rise in cbfa-1 and type I collagen expression with increasing acidosis (figure 5A and 5B). The fold increases from HCL 0 for HCL 3 cultures were 2 ± 0.2 for cbfa-1 and 2.8 ± 0.2 for type I collagen (P < 0.05 vs. HCL 0, HCL 1 and HCL 2).

Due to the enhanced expression of early osteoblast markers during acidosis. the expression of osterix, another essential osteoblast transcription factor downstream of cbfa-1 ³⁰, and alkaline phosphatase, an osteoblastic gene upregulated during an intermediate phase of osteoblast differentiation, was subsequently examined ²⁹. Figure 11C displayed a continuing rise in alkaline phosphatase mRNA upto 24.4 fold in the presence of OM, whereas less than 4.6 fold increase was observed in negative controls. Unlike cbfa-1 and type I collagen, metabolic acidosis suppressed alkaline phosphatase mRNA expression. In HCL 2, despite the gradual increase in alkaline phosphatase mRNA with time, the levels were less than those of HCL 0 at all time points (P < 0.05). Likewise, dose response experiments demonstrated a progressive decline in alkaline phosphatase mRNA with increasing acidosis (figure 12C). The fold difference (relative to the lowest baseline HCL 3) of alkaline phosphatase mRNA for HCL 0, HCL 1, HCL 2 and HCL 3 were 2 ± 0.1 , 1.4 ± 0.2 (P < 0.05 vs. HCL 0), $1 \pm$ 0.2 (P < 0.05 vs. HCL 0) and $1 \pm 0.2 (P < 0.05 \text{ vs. HCL } 0)$ respectively. The product of alkaline phosphatase gene was also examined by evaluating the enzyme activity. As shown in Figure 13, exposure to acidic medium suppressed alkaline phosphatase enzyme activity correlating with the decreased amount of mRNA expression. In HCL 0 and HCL 1, the enzyme activity rose rapidly reaching plateau by day 10, whereas the rise was more indolent in HCL 2 and HCL 3. At day 10, when the differences were greatest, the enzyme activities for HCL 0, HCL 1, HCL 2 and HCL 3 were 47.6 \pm 4.3 nmol, 35.6 \pm 4.5 nmol (P < 0.05 vs. HCL 0), 20.8 \pm 2.7 nmol (P < 0.05 vs. HCL 0 and HCL 1) and 13.6 \pm 0.9 nmol (P < 0.05 vs. HCL 0, HCL 1 and HCL 2) respectively. A slight increase in enzyme activity was noted in Negative control HCL 0. As for osterix, the expression attained its peak at day 15, approximately 4.3 fold above baseline (figure 11E). The mRNA levels of osterix in HCL 2 were lower than those of HCL 0 at all time points and the difference reached statistical significance at day 15 (1.7 \pm 0.5 vs. 4.3 \pm 0.6, P < 0.05). Dose response experiments showed a progressive decline in osterix mRNA with increasing acidosis (figure 12E). The fold difference (relative to the lowest baseline HCL 3) of osterix mRNA for HCL 0, HCL 1, HCL 2 and HCL 3 were 7.1 ± 1.1 , 4.1 ± 1 (P = NS), 4.9 ± 0.8 (P = NS) and 1 ± 0.3 (P < 0.05 vs. HCL 0 and HCL 2) respectively.

In order to determine whether MSCs were able to differentiate into mature osteoblasts during chronic metabolic acidosis, the expression of osteocalcin, a mature osteoblastic gene ²⁹, is being evaluated.

Finally, we determined whether chronic metabolic acidosis impaired bone matrix mineralization. Von Kossa staining of mineral deposition revealed the presence of mineralized nodules starting from day 21 in HCL 0 (figure 7). Metabolic acidosis delayed bone matrix mineralization in HCL1, HCL 2 and HCL 3 cultures. Mineralization occurred at day 28 in HCL 1, day 35 in HCL 2 and never appeared at all in HCL 3 up to 45 days in culture (figure 1C and 7). Quantification of bone matrix mineralization was performed by measurement of calcium content in the bone nodules (figure 8). In HCL 0, calcium deposition was measurable at day 14 (0.2 \pm 0.03 μ g) and progressively increased through day 35 (38.4 \pm 4.7 μ g, P < 0.05 vs. day 7, 14, 21 and 28). In contrast, the amount of calcium deposit for HCL 1, HCL 2 and HCL 3 at day 35 were 13.6 \pm 2.7 μ g (P < 0.05 vs. HCL 0), 2.4 \pm 2.3 μ g (P < 0.05 vs. HCL 0, and HCL 1) and 0.2 \pm 0.1 μ g (P < 0.05 vs. HCL 0, HCL 1 and HCL 2) respectively.

Discussion

Bone marrow contains at least two types of stem cells: hematopoietic stem cells and MSCs. When plating BMMCs on the plastic dish, MSCs are able to attach to the dish and propagate while hematopoietic stem cells are non-adherent and can be discarded. MSCs are identified based on the positivity of a set of marker proteins on their surface, including CD105 and CD 73, and the negativity for other markers of hematopoietic cells such as CD14, CD45 and CD34. They are also characterized by the ability to differentiate into multiple mesenchymal lineages, including osteocytes, chondrocytes and adipocytes ²⁷. Our isolated cultured MSCs showed characteristic surface marker profiles and were able to undergo osteogenic and adipogenic differentiation under appropriate conditions.

In our study of experimental acidosis, we observed that cellular proliferation was suppressed at pH 7.15 or below. The expression of multiple osteoblastic genes, which are sequentially upregulated during different stages of osteoblast differentiation, was altered by metabolic acidosis. First, we observed the enhanced expression of cbfa-1, an essential transcription factor necessary for osteoblast commitment, by metabolic acidosis. Cbfa-1 is required during osteogenesis and its expression is upregulated in the early proliferative period of osteoblast differentiation. Homozygous mutation of cbfa-1 resulted in a complete lack of bone formation with arrest of osteoblast differentiation ²⁸. The upregulation of cbfa-1 in chronic metabolic acidosis suggests accelerated osteoblast differentiation during the early period. This was further supported by the finding of heightened type I collagen mRNA expression. Type I collagen is the most abundant matrix protein in bone and the expression of its transcript usually peaks in the early period of osteoblast differentiation following that of cbfa-1 ^{11, 29}. Moreover, the expression of type I collagen mRNA appeared to follow the same pattern to that of cbfa-1 especially the robust increase at day 20, when downregulation of both genes are to be expected in normal condition (figure 3A and 3B). Since the promoter of type I collagen gene has a binding site for cbfa-1 ⁵⁷, the binding of cbfa-1 to this cis-acting element may be responsible for the increase in type I collagen transcripts. On the other hand, metabolic acidosis could also affect other transcription proteins upstream of both cbfa-1 and type I collagen.

The period of bone matrix synthesis and maturation follows the early proliferative period of osteoblast differentiation. During this time, genes associated

with bone cell phenotype and other noncollagenous bone matrix proteins emerged For example, alkaline phosphatase mRNA expression and enzyme activity are usually increased upto 10 fold. Later on in the mineralization period, the upregulation of osteocalcin mRNA signifies terminally differentiated osteoblast ²⁹. In contrast to the stimulatory effect on early osteoblastic genes, chronic metabolic acidosis suppressed alkaline phosphatase mRNA and its enzyme activity. At present, we are trying to confirm the expression of osteocalcin to determine whether terminal osteoblast differentiation is augmented or attenuated by metabolic acidosis.

Recently, another transcription factor necessary for osteoblast differentiation, osterix, has been identified. Osterix null mice completely lack bone formation due to the absence of osteoblasts. Osterix expression is absent in cbfa-1 null mice, although cbfa-1 is detected in osterix null mice suggesting that osterix acts downstream of cbfa-1 ³⁰. Little is known as to how osterix regulates osteoblast differentiation. It has been suggested that osterix is required for directing MSCs away from chondrocyte lineage and toward the osteoblast lineage. The reduction in osterix mRNA in our study may represent a negative feedback control from increased expression of cbfa-1. This, however, will require further study.

Metabolic acidosis has been known to impair bone matrix mineralization both in vitro and in vivo ^{10, 20, 58, 59}. The skeletal demineralization was presumed to be secondary to both physico-chemical bone dissolution and cell-mediated process ^{7, 8, 41, 42, 60}. In our study, bone matrix mineralization was also impaired in the cell layers cultured in acidic environment. The attenuation of osteoblast maturation may be partly responsible the impaired mineralization. The possibility of osteoblast dedifferentiation during chronic metabolic acidosis was also suggested by the results from Frick et al's study demonstrating diminished expression of osteoblastic genes, matrix Gla protein and osteopontin, in calvariae-derived osteoblasts grown in acidic medium ¹⁰.

Our study is the first to show sequential changes of osteoblastic gene expression during chronic metabolic acidosis. Osteoblast differentiation is accelerated in the early stages. Our findings confirm that of other studies in demonstrating the reduction of alkaline phosphatase enzyme activity and impaired bone matrix mineralization during acidosis ^{8,42}. Conflicting data exists on type I collagen. In a previous study, mouse calvarial bone cells exposed to acidic medium for 30 minutes had decreased type I collagen mRNA ⁹, whereas in our study its expression was enhanced. This discrepancy may be due to different effect of acute versus chronic metabolic acidosis on protein and gene expression.

In conclusion, chronic metabolic acidosis directly affects osteoblast differentiation from MSCs. Osteoblast differentiation is enhanced in the early stages, whereas matrix mineralization is impaired. The role of heightened cbfa-1 mRNA on the expression of other osteoblastic genes will require further study.

Acknowledgement

This work was supported by Thailand research fund. We thank Dr. Jinny Tavee for advice and assistance with the manuscript.

Table I Primer and Probe Sequences

1 dole 1	1 Timer and 1 1000 bequences		
Gene	Forward and reverse primers $(5'-3')$	Probe (5'-3')	
18 S	CGGCTACCACATCCAAGGAA	TGCTGGCACCAGACTTGCCCTC	
rRNA	GCTGGAATTACCGCGGCT		
Cbfa-1	GCCTTCAAGGTGGTAGCCC	CCACAGTCCCATCTGGTACCTCTCCG	
	CGTTACCCGCCATGACAGTA	cenendiceenielooineeleleeo	
Coll I	CAGCCGCTTCACCTACAGC	CCGGTGTGACTCGTGCAGCCATC	
	TTTTGTATTCAATCACTGTCTTGCC	CCGGTGTGACTCGTGCAGCCATC	
Osx	CCCCACCTCTTGCAACCA	CCAGCATGTCTTGCCCCAAGATGTCT	
	CCTTCTAGCTGCCCACTATTTCC	CCAGCATGTCTTGCCCCAAGATGTCTA	
ALP	GACCCTTGACCCCCACAAT	TGGACTACCTACCTATTGGGTCTCTTCG	
	GCTCGTACTGCATGTCCCCT	AGCCA	
OC	GAAGCCCAGCGGTGCA	TGGACACAAAGGCTGCACCTTTGCT	
	CACTACCTCGCTGCCCTCC	TOUACACAAAOUCTUCACCTTTUCT	

Figure legends

Figure 1 Morphology of human MSCs. Phase contrast microscopy demonstrates the spindle-shaped morphology of MSCs grown in the absence of OM (A), nodular aggregates of mineralization in the presence of OM for 28 days (B), cuboidal-shaped osteoblasts without nodular aggregates in the presence of OM with HCl 3 μ ml (HCL 3, pH \sim 7) for 28 days (C) and adipocytes with lipid-rich vacuoles (D).

Figure 2 Flow cytometry analysis of human MSCs

Figure 3 Cell proliferation assay MSCs were grown in the presence of OM without HCl (HCL 0, pH \sim 7.4) and with HCl 1 μ l/1 ml of OM (HCL 1, pH \sim 7.25), 2 μ l/ml (HCL 2, pH \sim 7.15) and 3 μ l/ml (HCL 3, pH \sim 7). Cell proliferation was evaluated by MTT assay. Results represent an average of 3 experiments. **P < 0.05 compared to day 0, *P < 0.05 compared to HCL 0.

Figure 4 Time course of the effect of chronic metabolic acidosis on mRNA levels of osteoblastic genes. MSCs were grown in the presence of OM without HCl (HCL 0, pH \sim 7.4) and with HCl 2 μ l/1 ml of OM (HCL 2, pH \sim 7.15). Negative controls were cultivated in the absence of osteogenic stimulation. Relative gene expressions were determined by quantitative real-time RT-PCR. Expression levels are expressed as fold increase from the corresponding baseline values at day 0. Results represent an average of 4-6 experiments for HCLs and one experiment for negative controls. $^{\#}P < 0.05$ compared to day 0, $^{*}P < 0.05$ compared to HCL 0.

Figure 5 Dose response of the effect of chronic metabolic acidosis on mRNA levels of osteoblastic genes. MSCs were grown in the presence of OM without HCl (HCL 0, pH \sim 7.4) and with HCl 1 μ l/1 ml of OM (HCL 1, pH \sim 7.25), 2 μ l/ml (HCL 2, pH \sim 7.15) and 3 μ l/ml (HCL 3, pH \sim 7). Cells were harvested for RNA extraction at day 10 for cbfa-1, type I collagen and alkaline phosphatase and day 15 for osterix and osteocalcin. Relative gene expressions were determined by quantitative real-time RT-PCR Expression levels are expressed as fold increase from the lowest baseline (HCL 0 or HCL 3 wherever applicable). Results represent an average of 4-6 experiments. *P < 0.05 compared to HCL 0.

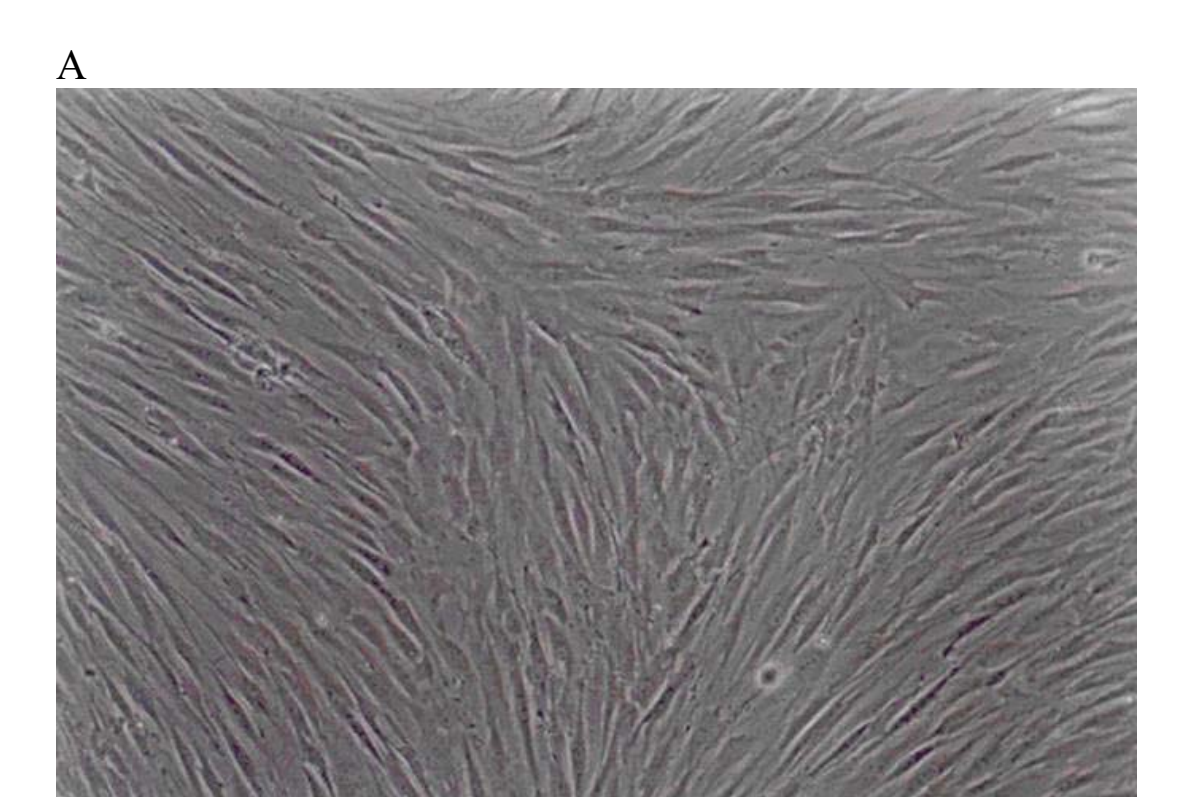
Figure 6 Alkaline phosphatase enzyme activity. MSCs were grown in the presence of OM without HCl (HCL 0, pH \sim 7.4) and with HCl 1 μ l/1 ml of OM (HCL 1, pH \sim 7.25), 2 μ l/ml (HCL 2, pH \sim 7.15) and 3 μ l/ml (HCL 3, pH \sim 7). Alkaline phosphatase enzyme activities were determined by calorimetric assay and normalized by protein content. Results represent an average of 6 experiments for HCLs and one experiment for negative controls. *#P < 0.05 compared to day 0, *P < 0.05 compared to HCL 0.

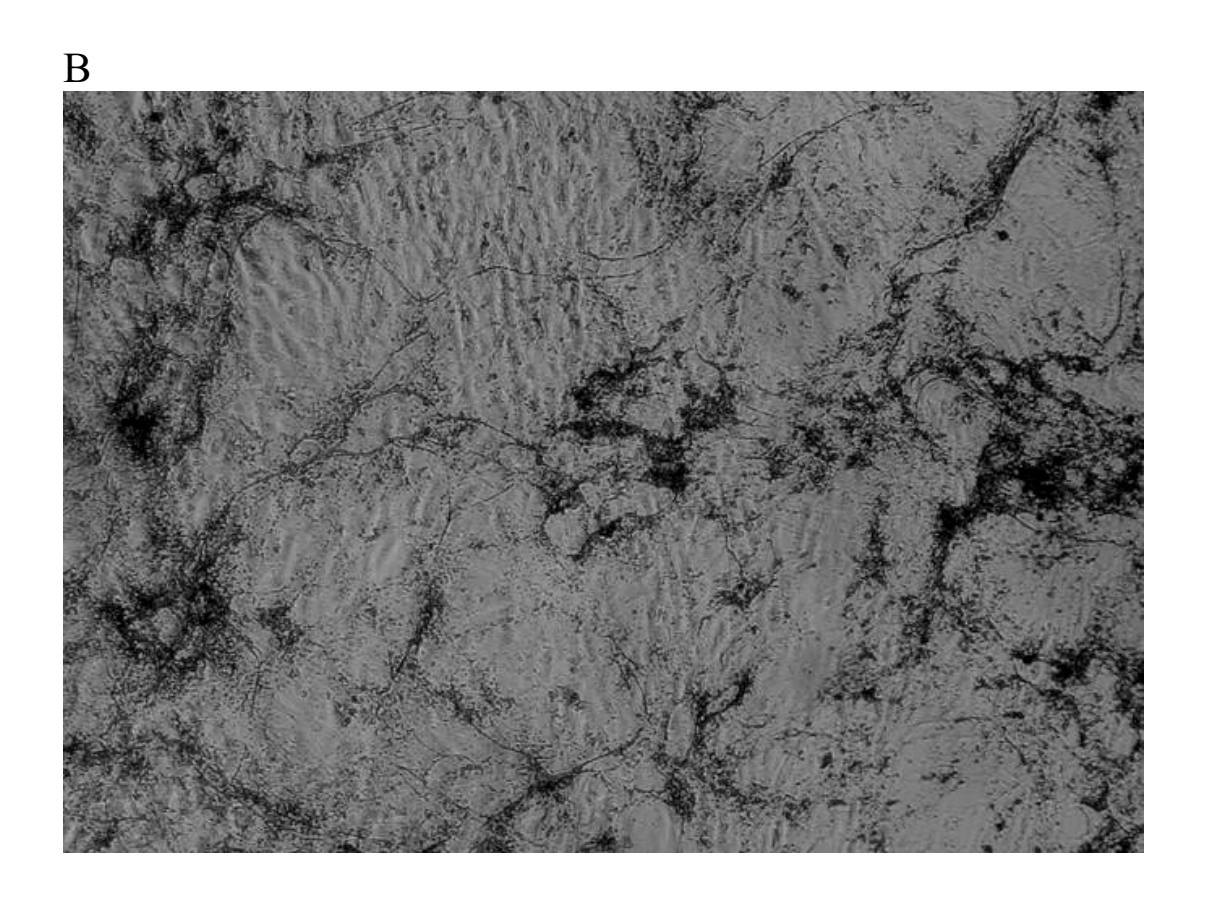
Figure 7 Von Kossa staining of bone matrix mineralization. MSCs were grown in the presence of OM without HCl (HCL 0, pH \sim 7.4) and with HCl 1 μ l/1 ml of OM (HCL 1, pH \sim 7.25), 2 μ l/ml (HCL 2, pH \sim 7.15) and 3 μ l/ml (HCL 3, pH \sim 7). Cultures were fixed and stained for mineral deposition by von Kossa technique.

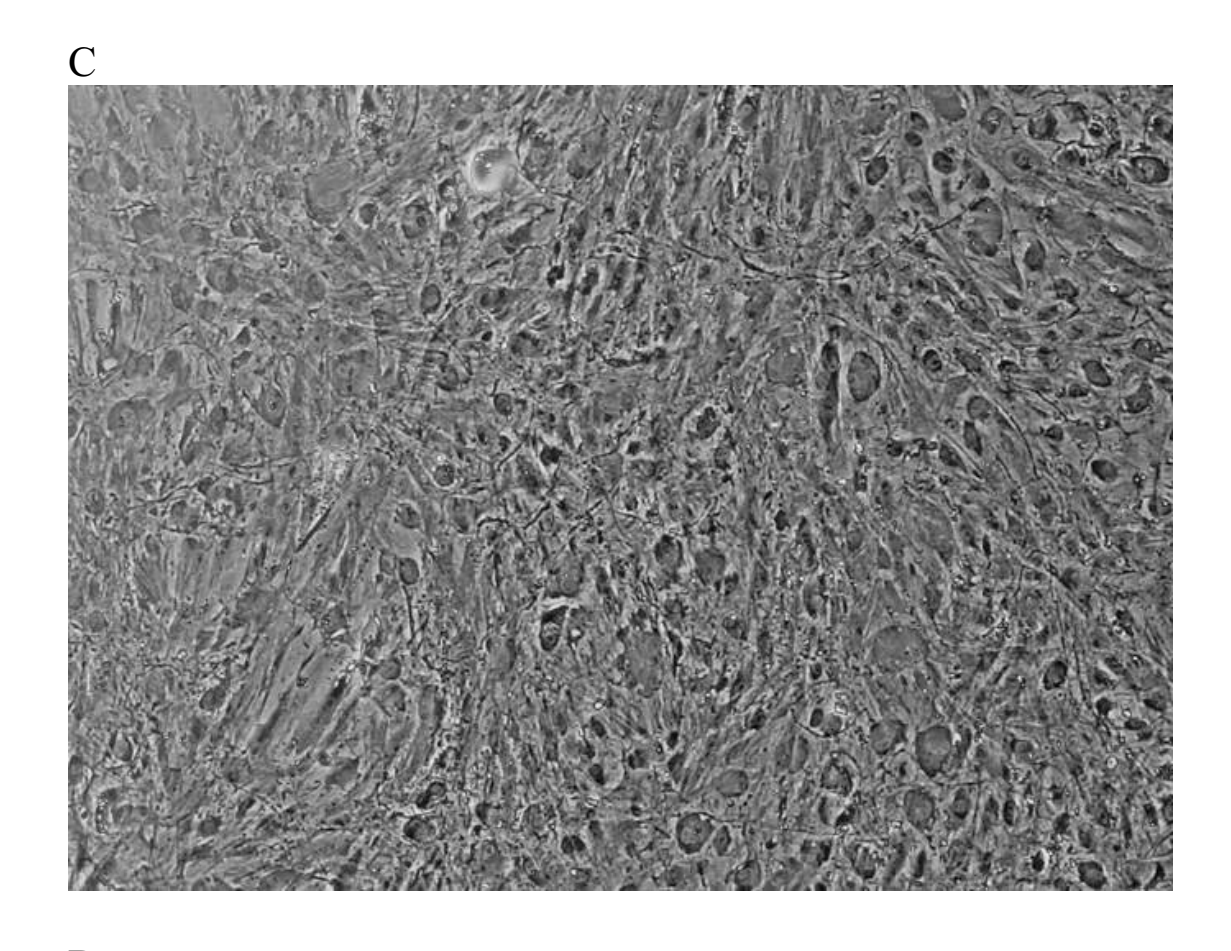
Figure 8 The amount of calcium deposition in mineralization nodules. MSCs were grown in the presence of OM without HCl (HCL 0, pH \sim 7.4) and with HCl 1 μ

l/1 ml of OM (HCL 1, pH ~ 7.25), 2 μ l/ml (HCL 2, pH ~ 7.15) and 3 μ l/ml (HCL 3, pH ~ 7). The amount of calcium deposition was measured by Calcium-o-Cresolphthalein Complexone method and normalized by protein content. Results represent an average of 6 experiments. $^{\#}P$ < 0.05 compared to day 7, $^{*}P$ < 0.05 compared to HCL 0.

Figure 1







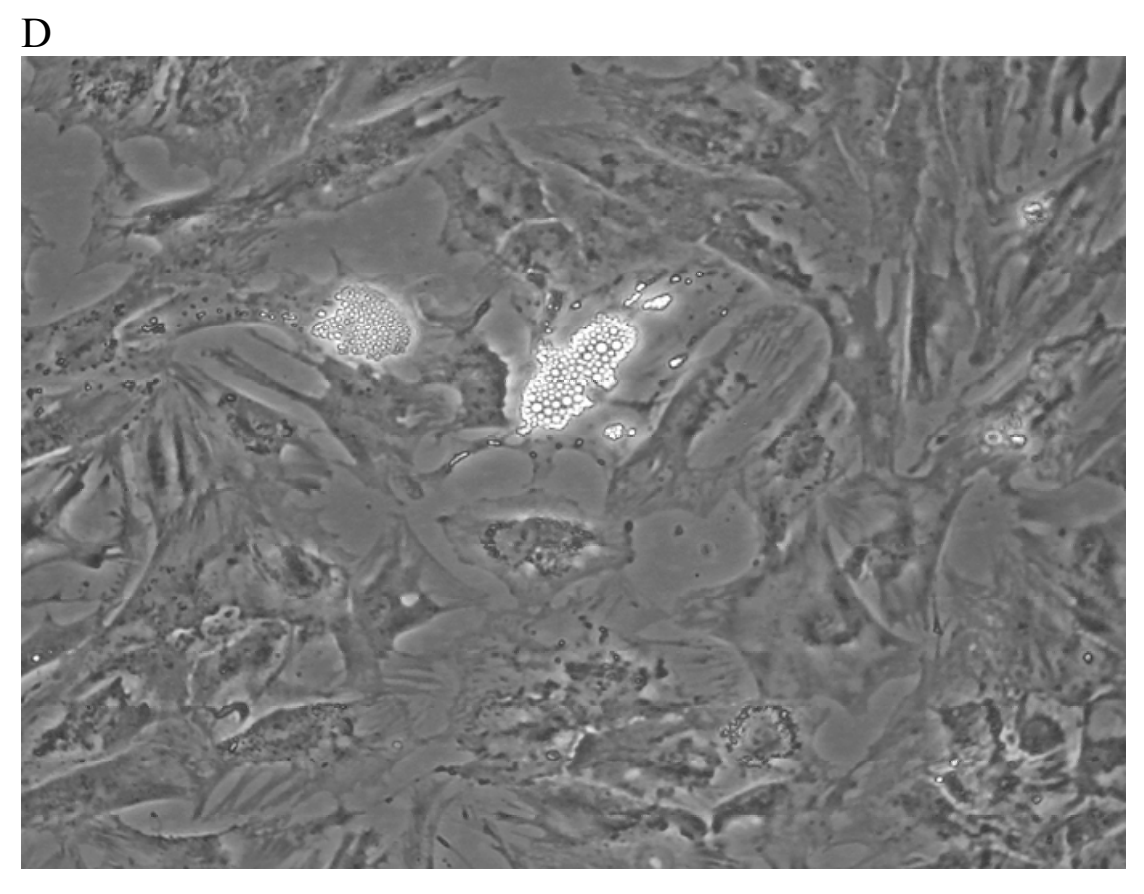


Figure 2

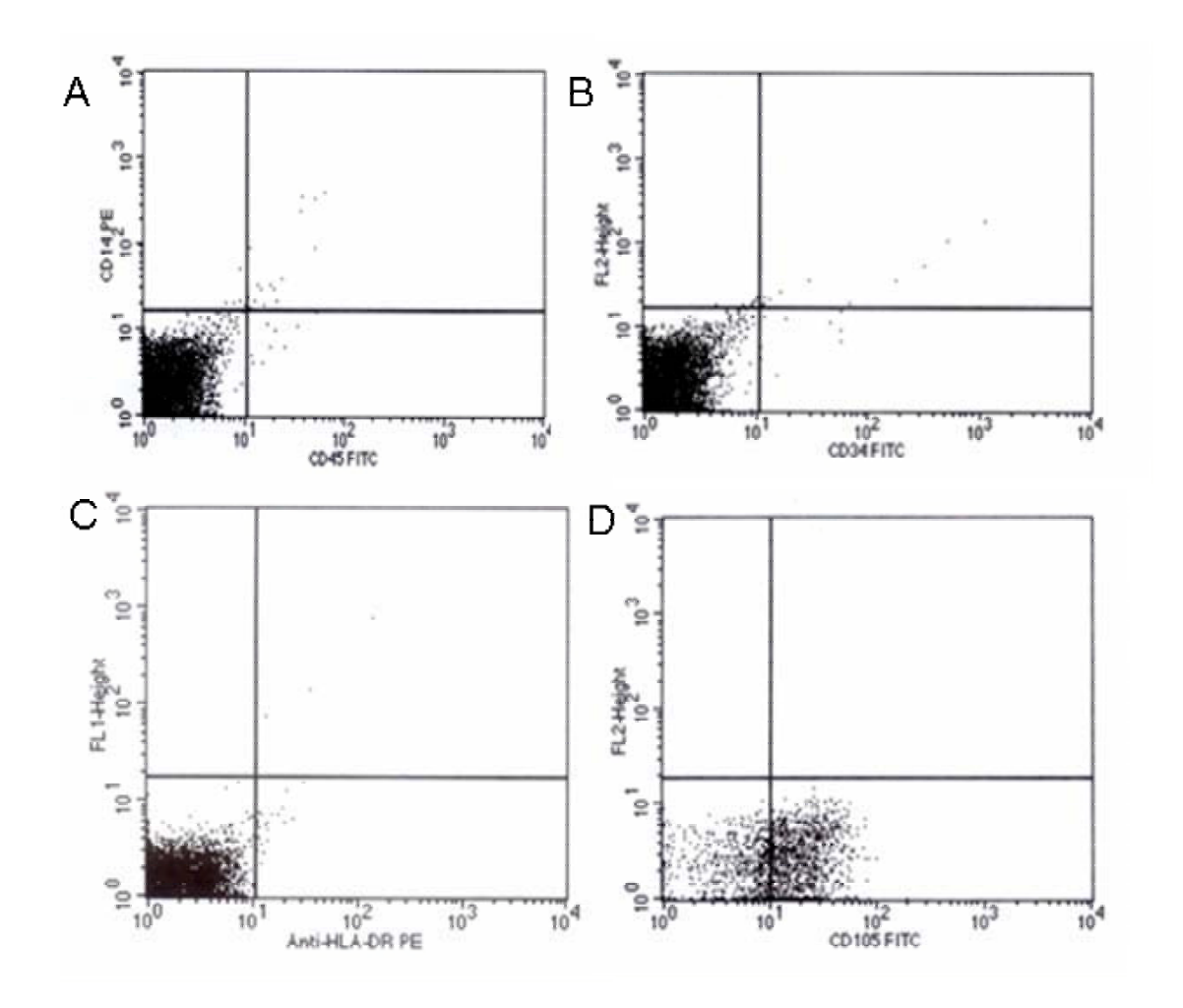


Figure 3

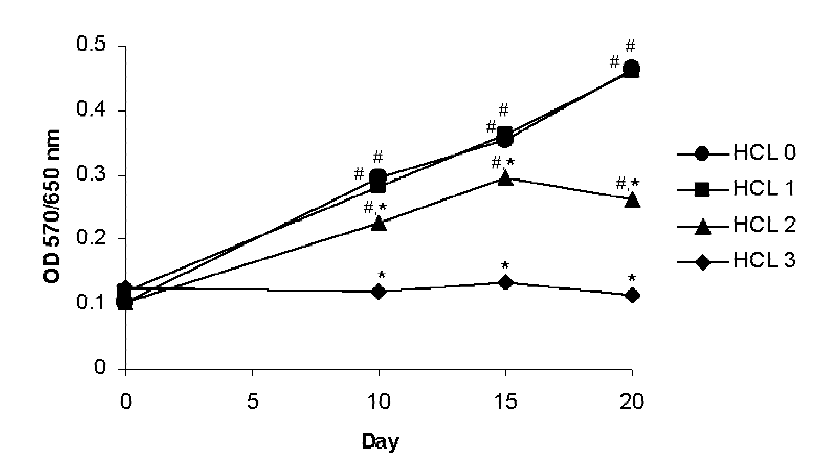
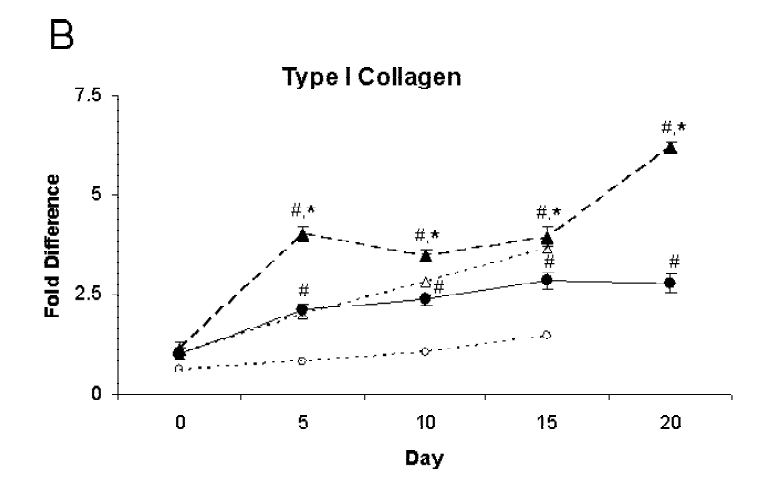
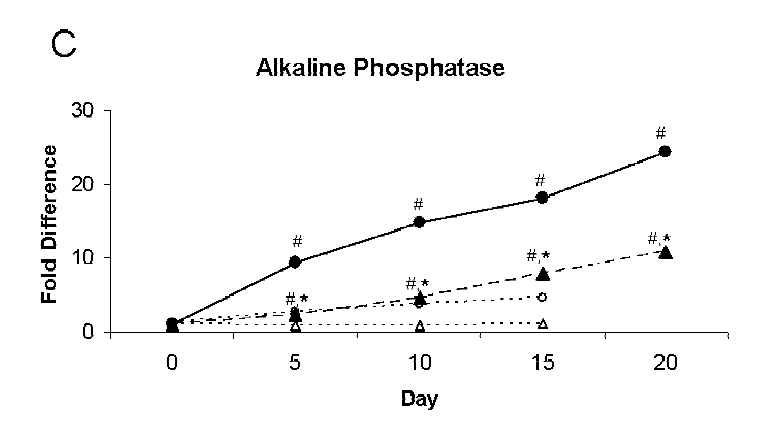


Figure 4





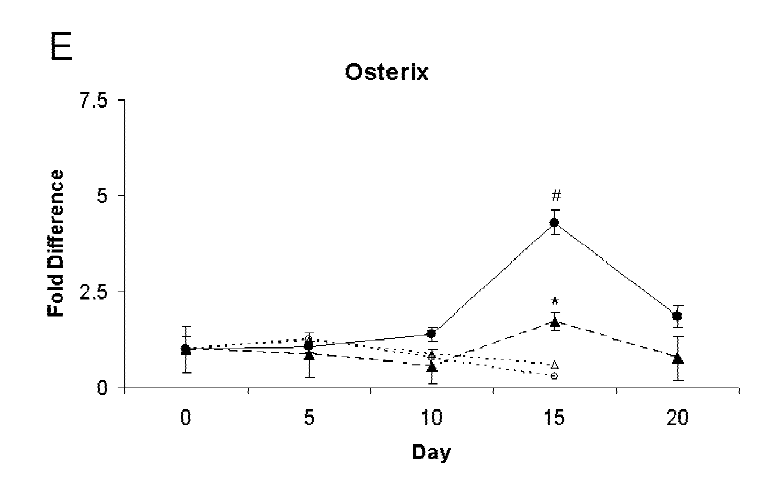
→ HCL 0

- ★ - HCL 2

...e. Negative control HCL 0

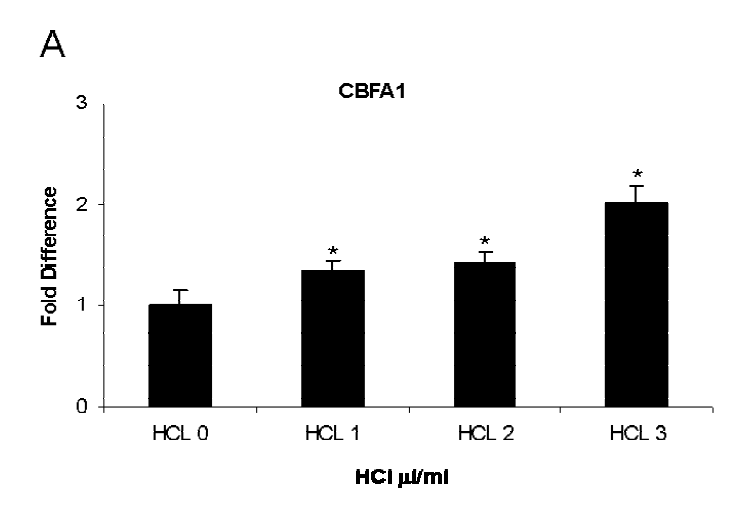
...Δ. Negative control HCL 2

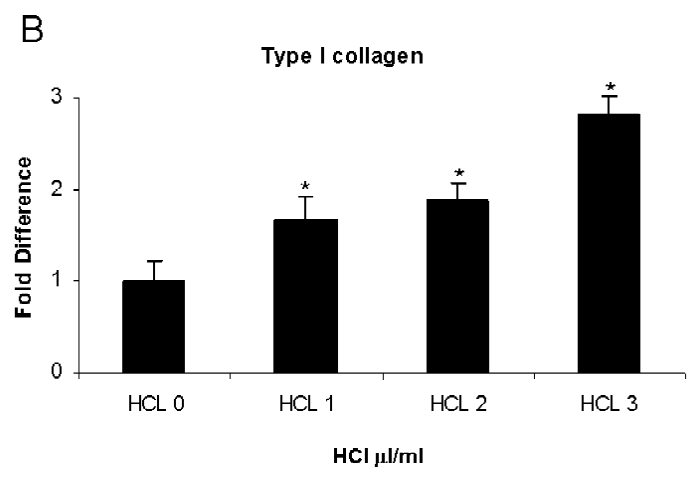
Figure 4



- —←HCL 0
- <u>★</u> HCL 2
- ···•··· Negative control HCL 0
- ···-∆···· Negative control HCL 2

Figure 5





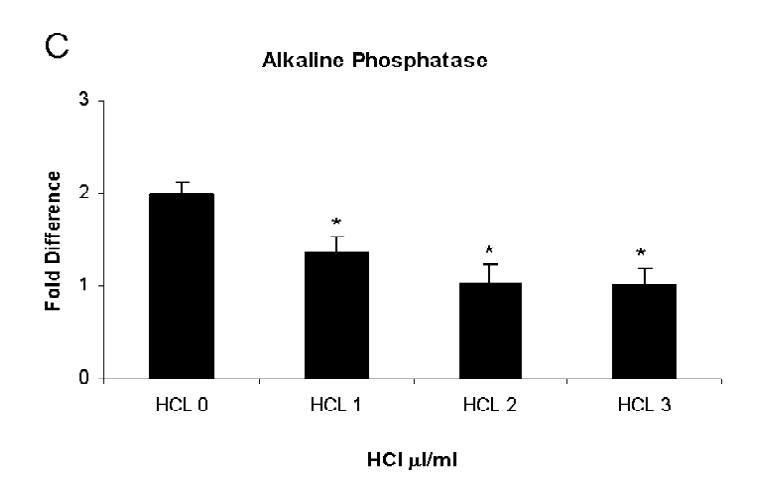


Figure 5

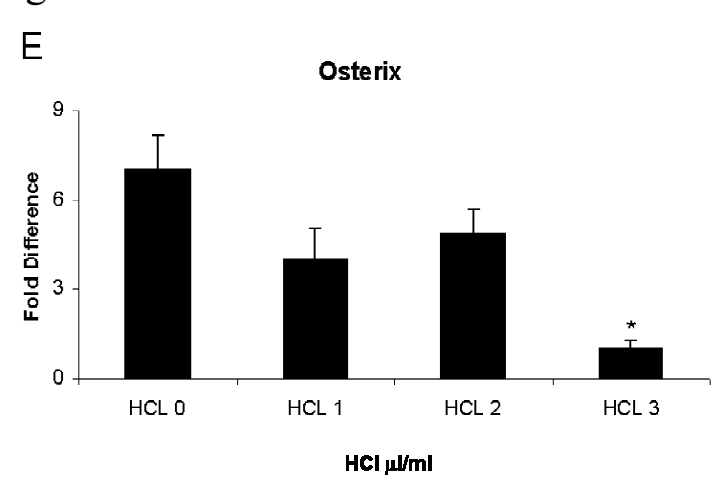


Figure 6

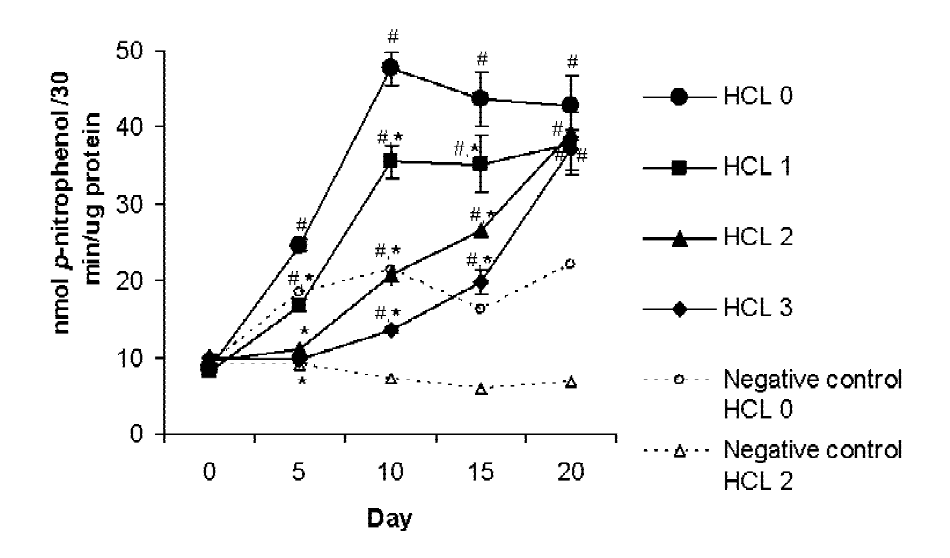


Figure 7

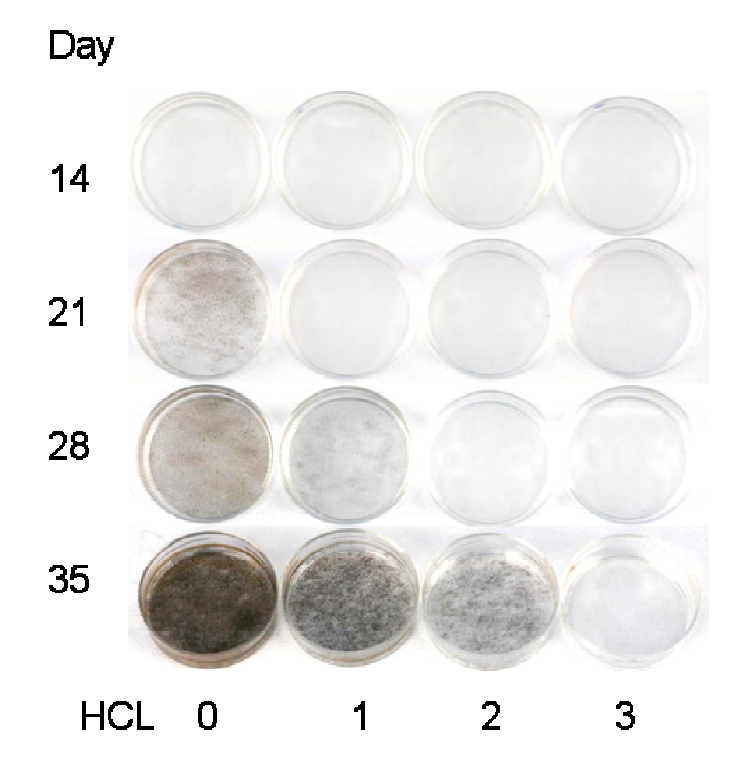
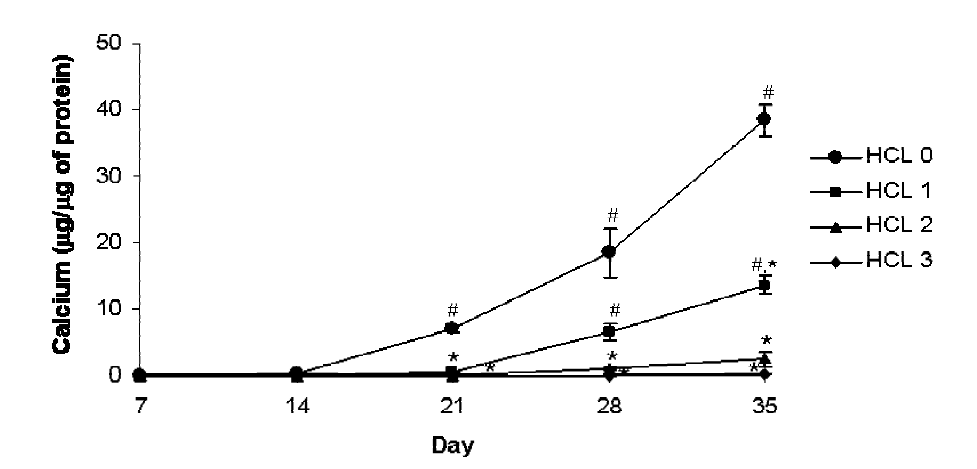


Figure 8





Bone 35 (2004) 604-613



www.elsevier.com/locate/bone

Alteration of noncollagenous bone matrix proteins in distal renal tubular acidosis

Sinee Disthabanchong, ^{a,*} Somnuek Domrongkitchaiporn, ^a Vorachai Sirikulchayanonta, ^b Wasana Stitchantrakul, ^a Patcharee Karnsombut, ^b and Rajata Rajatanavin ^c

^a Division of Nephrology, Department of Medicine, Ramathibodi Hospital, Mahidol University, Bangkok, Thailand

Received 13 October 2003; revised 1 April 2004; accepted 30 April 2004

Abstract

Our previous report on bone histomorphometry in patients with distal renal tubular acidosis (dRTA) revealed decreased bone formation rate (BFR) when compared to healthy subjects. The abnormality improved significantly after alkaline therapy. The modest increase in osteoblastic surface, after correction of metabolic acidosis, could not explain the striking improvement in bone formation, suggesting additional influence of metabolic acidosis on osteoblast function and/or bone matrix mineralization. Osteoblasts and, to a lesser extent, osteoclasts synthesize and secrete bone matrix including type I collagen and various noncollagenous proteins (NCPs). Substantial evidence suggested diverse functions of NCPs related to bone formation, resorption, and mineralization. Metabolic acidosis, through its effect on bone cells, may result in an alteration in the production of NCPs. Our study examined bone histomorphometry with detailed analysis on the mineralization parameters and NCPs expression within the bone matrix of patients with dRTA before and after treatment with alkaline. Seven dRTA patients underwent bone biopsy at their initial diagnosis and again 12 months after alkaline therapy. Bone mineral density (BMD) and bone histomorphometry were obtained at baseline and after the treatment. The expression of NCPs was examined by immunohistochemistry, quantitated by digital image analysis, and reported as a percentage of area of positive staining or mineralized trabecular bone area. Alkaline therapy normalized the low serum phosphate and PTH during acidosis. The reduction in BMD at baseline improved significantly by the treatment. Bone histomorphometry demonstrated the increase in osteoid surface and volume without significant alteration after acidosis correction. In comparison to the normal subjects, osteoid thickness was slightly but insignificantly elevated. Osteoblast and osteoclast populations and their activities were suppressed. The reduction in mineral apposition rate and adjusted apposition rate were observed in conjunction with the prolongation of mineralization lag time. Alkaline therapy improved the mineralization parameters considerably. In addition to the increase in BFR relative osteoblast number after acidosis correction, osteocalcin expression in the bone matrix increased significantly from 16.7% to 22.3%. Six of seven patients had decreased osteopontin expression. In conclusion, the abnormal bone remodeling in dRTA is characterized by low turnover bone disease with some degree of defective mineralization. Alteration of NCPs expression suggested the effect of metabolic acidosis on bone cells. Alkaline therapy increased bone mass through the restoration of bone mineral balance and, perhaps, improved osteoblast function. © 2004 Elsevier Inc. All rights reserved.

Keywords: Acidosis; Bone matrix; Osteoblasts; Osteoclasts

Introduction

Distal renal tubular acidosis (dRTA) is a clinical syndrome characterized by impaired ammonium and titrable

E-mail address: sineemd@hotmail.com (S. Disthabanchong).

acid excretion by the kidney resulting in persistent metabolic acidosis while excreting relatively alkaline urine. The presence of chronic metabolic acidosis results in various metabolic consequences, including hypokalemia, hypophosphatemia, and abnormal bone metabolism [1–3]. Recent studies from our laboratory revealed the findings of osteopenia and suppressed bone formation in patients with dRTA when compared to healthy controls. Correction of metabolic acidosis with alkaline improved the abnormality.

^bDivision of Nephrology, Department of Pathology, Ramathibodi Hospital, Mahidol University, Bangkok, Thailand

^c Division of Endocrinology, Department of Medicine, Ramathibodi Hospital, Mahidol University, Bangkok, Thailand

^{*} Corresponding author. Division of Nephrology, Department of Medicine, Ramathibodi Hospital, 7th Floor Research Building, Rama VI Road, Bangkok, 10400, Thailand. Fax: +662-201-1715.

The modest decrease in osteoblastic surface at baseline, which only improved slightly after alkaline treatment, could not explain the striking improvement in bone formation, suggesting the possibility of additional influence of metabolic acidosis on osteoblast function and/or bone matrix mineralization [4,5]. Previously, Bushinsky et al. [6,7] investigated the effect of metabolic acidosis on bone and discovered that metabolic acidosis resulted in skeletal demineralization through physicochemical dissolution of the bone as excess protons were buffered by bone carbonate. Later on, the effect of metabolic acidosis on bone cells was examined. Using cell culture model of neonatal mouse calvariae, the same group discovered that metabolic acidosis inhibited osteoblastic collagen synthesis while enhancing osteoclastic β-glucoronidase activity [8,9]. The opposite findings were observed when the incubation was performed in alkaline medium [10]. This data provided evidence regarding the effect of metabolic acidosis on both cellular and noncellular components of the bone.

Osteoblasts and, to a lesser extent, osteoclasts synthesize and secrete bone matrix, which include type I collagen and various noncollagenous proteins (NCPs). Of these NCPs, osteocalcin and osteonectin secreted mostly by osteoblasts have been known to involve in the process of bone formation and mineralization [11–13], while osteopontin and bone sialoprotein secreted by both osteoblasts and osteoclasts play roles in bone resorption [14–17]. Metabolic acidosis, through its effect on osteoblasts and osteoclasts, may alter the production of NCPs, resulting in the abnormal bone remodeling. Alkaline therapy may restore cellular functions and NCPs composition.

Osteomalacia has been reported in 20–30% of patients with renal tubular acidosis [3,18]. The diagnosis was mostly based on clinical and roentgenographic findings. Bone pain was relieved and osteomalacia improved after alkaline therapy [3,19]. Previously, we reported significant increase in osteoid volume and surface in bone of patients with dRTA, while there was no major increase in osteoid thickness. A detailed analysis on the parameters associated with mineralization was not performed. In a present study, we examined bone histomorphometry with detailed analysis on the mineralization parameters and osteoblastic activity in patients with dRTA before and after alkaline treatment. Composition of NCPs in the bone matrix was examined by immunohistochemistry.

Materials and methods

Patients

Subgroup of dRTA patients who completed 1 year of alkaline therapy with adequate bone specimens available for further examination by immunohistochemistry from our previous studies were included [4,5]. These were idiopathic dRTA patients who were residents of Khon Kaen province,

Thailand, where a very high incidence of dRTA has been reported [18]. Seven patients, three males, and four females, who were diagnosed with dRTA on the presence of (1) persistent hyperchloremic metabolic acidosis with serum bicarbonate less than 18 mmol/l found in at least two occasions, 1 month apart, (2) failure to acidify urine (with urine pH > 5.5) or urinary excretion of ammonia less than 50 mEq/day in the presence of systemic acidosis, (3) absence of bicarboturia exceeding 15% of that filtered at normal plasma bicarbonate concentration, serum creatinine of less than 190 µmol/l, and absence of proteinuria, Fanconi syndrome, chronic diarrhea, current usage of diuretics, carbonic anhydrase inhibitors, and all kinds of alkaline therapy were included in this study. The calcium intake of dRTA patients was 9.45 ± 3.35 mmol/day. All patients were then treated for 1 year with 60 mEg/day of potassium citrate in two divided doses to keep the serum bicarbonate above 20 mmol/ 1 throughout the study. For patients who initially failed to achieve the target serum bicarbonate level, the dosages of potassium citrate were increased in a stepwise fashion until reaching the desired serum bicarbonate level. No medication that might affect calcium and bone metabolism, for example, diuretics, vitamin D, estrogen, bisphosphonate, and calcium supplements, was allowed throughout the study.

Biochemical analysis

Serum electrolytes, calcium, phosphate, intact PTH (iPTH), and 24-h urine collections for sodium, potassium, calcium, phosphate, and creatinine were obtained at the time of bone biopsy. Hypercalciuria was defined as urinary calcium excretion > 4.75 mmol/day in either sex [1,20]. Serum iPTH was determined by an immunoradiometric assay (ELSA-PTH; CIS BioInternational, GIF-sur-Yvette Cedex, France). The normal serum iPTH was 10-60 pg/ml.

Bone mineral density

Bone mineral density (BMD; g/cm²) was determined at vertebral (L2–L4), femoral neck, trochanter, and Wards' triangle by dual energy X-ray absorptiometry (Lunar Expert XL, Lunar Corp., USA). Precision of the BMD measurement in our laboratory at L2–L4, and neck of femur was 1.2 and 0.6%, respectively. The control values of BMD were obtained from 28 normal farmers who were permanent residents of Khon Kaen province, age, 32.9 \pm 11.2 years, weight, 54.3 \pm 8.3 kg, height, 1.55 \pm 0.05 m, and male–female ratio, 22:6.

Bone biopsy and histomorphometry

At the beginning of the study, transiliac crest bone biopsy was taken from the anterior superior iliac spine after tetracycline double labeling and again on the opposite side after 1 year of alkaline therapy using protocol reported previously [4]. In brief, bone specimens of 5 mm in diameter and 20-30 mm in length were fixed for 24 h in 70% ethanol, dehydrated in graded ethanol, and impregnated and embedded in the mixture of methylmethacrylate, dibutylphthalate, and benzoyl peroxide at room temperature for 5 days and subsequently in 42°C oven for 3 days. After polymerization, bone sections of 6-µm thickness were cut using Reichert-Jung Polycut S (Cambridge Instruments, NuBloch, Germany) equipped with tungsten carbide-edge knife (Leica, Germany), mounted on coated slides and incubated at 42°C for 2 weeks. Undecalcified sections were stained with modified Masson-Goldner trichrome, aurin tricarboxylic acid (Aluminon), Von-Kossa, and hematoxylin-eosin stain. If the specimen had a positive stain for aluminum, a further stain with Perls stain to exclude the cross-reaction with iron deposit was done. Unstained sections of 15-µm thickness were prepared for examinations by a fluorescent light microscopy. All sections, both pre- and post-potassium citrate therapy, were studied qualitatively and quantitatively for static and dynamic parameters of bone formation and bone resorption by the same pathologist and technician who had no knowledge of the patients' clinical presentations and treatments. Histomorphometric measurements were carried out with a semiautomatic image analyzer (Osteomeasure; Osteometric Inc, Atlanta, USA). At least 30 different fields of the same bone biopsy specimen were analyzed. Histomorphometric parameters were expressed according to Parfitt et al.'s [21] standardized nomenclature. The reference values for normal histomorphometric parameters were obtained from 17 normal Thai adults without bone disease, eight men and nine women, age, 35.1 ± 2.8 years (range, 19-58), height, 1.61 ± 0.06 m, and weight, $59.2 \pm 7.8 \text{ kg}$.

Protocol of the study has been approved by ethical committee on research involving human subjects of Ramathibodi hospital, Mahidol University. Written informed consents were obtained from all subjects.

Antibodies

Rabbit polyclonal antibodies LF-32 (osteocalcin), LF-120 (bone sialoprotein), BON-I (osteonectin), and mouse

monoclonal antibody LFMb-14 (osteopontin) were generous gifts from Dr. Larry W. Fisher, National Institutes of Health (NIH), Bethesda, MD [22].

Immunohistology

Immunohistochemistry was performed on the bone sections as described previously by Derkx et al. [23]. Briefly, plasticized bone sections were deacrylated in three changes of 2-Ethoxyethylacetate (BDH, Poole, England) overnight, rinsed in xylene, rehydrated, decalcified with 1% acetic acid for 2 days, and rinsed with distilled water for 30 min. Sections were stained using Universal LSAB2 Kits (Dako, CA, USA) according to manufacturer's recommendations with modifications. All steps were carried out at room temperature. Endogenous peroxidase activity was inhibited by 3% H₂O₂ in PBS for 30 min followed by 5-min wash in PBS. Subsequently, slides were blocked with 10% normal goat serum (Dako, CA, USA) in PBS for 1 h. Excessive serum was removed. Sections were then incubated with primary antibodies including osteocalcin 1:1600, bone sialoprotein 1:800, osteonectin 1:800, and osteopontin 1:3200 diluted in goat serum for 2 h and 30 min. The washings were carried out in PBS containing 0.05% tween (tween-PBS) for 10 min and PBS for additional 5 min. Primary antibodies were detected by incubation with readyto-use biotinylated goat anti-immunoglobulin second antibody (detecting both mouse and rabbit antibodies) for 10 min and washed for 5 min each in tween-PBS and PBS. Next, peroxidase-conjugated biotin-streptavidin complex was allowed to react with second antibody for 10 min and sections were washed for 5 min in tween-PBS and 30 min in PBS. Antibody complexes were visualized by incubation with diaminobenzidine obtained from Dako liquid DAB substrate-chromogen system. Sections were rinsed in distilled water for 5 min, counterstained with Mayer's hematoxylin, rinsed in tap water, dehydrated with ascending alcohols, cleared with xylene, and mounted on glass slides with cover slips using Permount (Fisher Scientific, New Jersey, USA) mounting medium. Bone biopsy sections from pre- and post-alkaline treatment of the same patients were stained at the same time. Negative control

Table 1 Patient characteristics at presentation

Patient no.	Age years	Height (cm)	Weight (kg)	Sex	Blood/urine pH	Urine ammonium (mEq/day)	Duration ^a (months)
1	16	157	44	F	7.31/7.0	36	8
2	35	145	46.7	F	7.30/6.0	29	18
3	30	170	65	M	7.29/6.2	30	36
4	50	146	50	F	7.31/6.8	30	60
5	42	158	53	M	7.28/6.4	32	120
6	20	136	32.3	M	7.30/6.9	24	144
7	25	148	39.5	F	7.32/6.5	31	24
Mean	31.1	151.4	47.2		7.3/6.5	30.3	58.6
SD	12.1	11.1	10.4		0.01/0.4	3.6	53.2

^a Duration of symptoms, for example, muscle weakness, renal stone, or fracture.

Table 2 Blood (per liter) and urine (per day) chemistries of dRTA patients

	Baseline		After treatment		Normal ^a	
	Serum	Urine	Serum	Urine	Serum	Urine
Creatinine (µmol)	99 ± 18	974 ± 160	93.7±11.2	700 ± 100	91.5 ± 38	1061 ± 71
Sodium (mmol)	139.9 ± 2.4	97.9 ± 44.9	141.6 ± 2.6	113.2 ± 26	138 ± 5.1	110.6 ± 90
Bicarbonate (mmol)	16.5 ± 3.3	_	22.6 ± 2.4^{b}	_	25 ± 1.5	_
Calcium (mmol)	2.1 ± 0.1	2.6 ± 1.6	2.3 ± 0.2	2.9 ± 1.7	2.3 ± 0.5	2.75 ± 1.7
Phosphate (mmol)	0.8 ± 0.2	11.3 ± 4.2	1.1 ± 0.2^{b}	10.2 ± 2.9	1.2 ± 0.1	10.6 ± 5.5
iPTH (pg/ml)	12.9 ± 5.6	_	24.1 ± 10^{c}	_	_	_

^a Data obtained from the 28 normal farmers who were permanent residents of Khon Kaen province.

sections were stained in the same fashion with omission of primary antibody.

Quantitative analysis of the NCPs

We performed quantitative analysis of the NCPs using similar protocol described previously by Derkx et al. [23]. Briefly, a CCD color video camera (Sony, Japan) mounted on a microscope (Zeiss, Germany) with a 10× objective was used to transfer images of the immunostained samples to the computer. The KS-300 (version 2.00) digital image analysis system (Kontron, Munchen, Germany) was used to analyze at least 40 microscopic fields of trabecular bone area in two 6-μm sections cut at steps of 50-100 μm in the same bone biopsy. This has been shown previously to be sufficient to obtain representative data with a small confidence interval [23]. The threshold of positive staining (brown) was determined interactively and the determined threshold was used to automatically analyze the images of the section. The mineralized bone matrix area (purple) was determined by first, manually tracing the perimeter of the mineralized trabecular bone on the computer screen (to exclude the cells in the bone marrow, which also stain purple) and then allowing the analysis system to calculate the area. The ratio of the immunostained and the mineralized bone matrix area was calculated. Bone sections from the same patient obtained pre- and post-alkaline treatment were analyzed at the same time and two separate measurements were performed in all sections.

Statistical analysis

Results were presented as mean \pm standard deviation. Comparison between the group means was performed using paired and unpaired Student's t test. Differences between groups were considered significant when P < 0.05.

Results

Patient characteristics are shown in Table 1. All the patients were acidemic with impaired urine ammonium excretion (urine ammonium < 50 mEq/day) and relatively

high urine pH (>5.5). Blood and urine chemistries for dRTA patients are presented in Table 2. Full details on blood and 24-h urine chemistries before and after potassium citrate therapy have been reported previously [5]. Hypokalemia $(3.4 \pm 0.8 \text{ mmol/l})$, hypophosphatemia, and low serum iPTH levels were observed at baseline. None of the patients had hypercalciuria. During alkaline therapy with potassium citrate, all dRTA patients could maintain their serum bicarbonate above 20 mmol/l. After treatment, serum potassium $(4.1 \pm 0.4 \text{ mmol/l})$, bicarbonate, phosphate, and iPTH levels rose significantly above the corresponding baseline values. There were no significant alterations in serum calcium, urine calcium, and urine phosphate after the treatment.

Bone mineral densities at baseline and the end of the study period are shown in Table 3. The basal BMD values of dRTA patients were lower than those of normal controls in all studied areas. After 1 year of alkaline therapy, there were significant elevations in the BMDs of total femur and trochanter of femur (P < 0.05). Bone histomorphometric data before and after the treatment are presented in Table 4. At baseline, there were significant elevations in the osteoid volume and surface (P < 0.05) compared to the corresponding parameters in normal controls. Osteoid thickness was slightly but insignificantly elevated. Osteoblastic and osteoclastic surfaces were decreased but the differences were not significant. Eroded surface was not different from controls. The reductions in the mineral apposition rate, mineralizing surface or osteoid surface, and adjusted apposition rate were accompanied by the prolongation of mineralization lag time (P < 0.05). Bone formation rate (BFR) per bone surface was suppressed at baseline (P < 0.05). While

Table 3
Bone mineral density (g/cm²) of dRTA patients

dRTA patients		Normal	
Baseline	After treatment		
1.05 ± 0.23	1.08 ± 0.17	1.15 ± 0.25	
0.89 ± 0.16	0.98 ± 0.17^{a}	1.05 ± 0.29	
0.85 ± 0.15	0.88 ± 0.18	1.00 ± 0.25	
0.68 ± 0.20	0.72 ± 0.17	0.89 ± 0.30	
0.67 ± 0.14	0.75 ± 0.13^{a}	0.81 ± 0.27	
	Baseline 1.05 ± 0.23 0.89 ± 0.16 0.85 ± 0.15 0.68 ± 0.20	Baseline After treatment 1.05 ± 0.23 1.08 ± 0.17 0.89 ± 0.16 0.98 ± 0.17^a 0.85 ± 0.15 0.88 ± 0.18 0.68 ± 0.20 0.72 ± 0.17	

 $^{^{}a}$ P < 0.05 compared to baseline BMD in dRTA patients.

^b Significant difference when compared to the corresponding baseline value (P < 0.05).

 $^{^{\}rm c}$ Significant difference when compared to the corresponding baseline value (P < 0.01).

Table 4
Bone histomorphometry of dRTA patients at baseline and after alkaline treatment

Histomorphometric parameters	dRTA		
	Baseline	After treatment	(range)
Bone volume (BV/TV), %	20.32 ± 3.54	24.91 ± 2.80	26.44 ± 7.21
	(15.63-25.56)	(20.64 - 28.00)	(12.72 - 36.88)
Osteoid volume (OV/TV), %	2.50 ± 1.65^{a}	1.83 ± 1.30	0.92 ± 1.05
	(0.18-4.53)	(0.42-4.2)	(0.2-3.06)
Osteoid surface (OS/BS), %	25.10 ± 21.4^{a}	24.02 ± 20.5^{a}	5.79 ± 4.39
	(3.27-39.8)	(7.12 - 32.16)	(0.30-15.86)
Osteoid thickness (O.th), µm	10.11 ± 3.2	10.16 ± 4.09	8.69 ± 2.14
	(5.29-14.34)	(6.12-17.5)	(5.53-15.87)
Osteoblastic surface (Ob.S/BS), %	1.05 ± 0.93	2.03 ± 1.92	2.6 ± 1.1
	(0-2.43)	(0.15-5.45)	(0.51 - 4.80)
Osteoclastic surface (Oc.S/BS), %	0.04 ± 0.33	0.06 ± 0.06	0.13 ± 0.23
	(0-0.08)	(0-0.16)	(0.01 - 0.59)
Osteoclast number (N.Oc/T.Ar), mm ²	0.14 ± 0.11	0.15 ± 0.14	0.24 ± 0.31
	(0-0.32)	(0-0.32)	(0.01 - 0.83)
Eroded surface (ES/BS), %	5.79 ± 3.02	4.32 ± 3.07	5.68 ± 2.32
	(1.78 - 9.71)	(1.69 - 7.94)	(2.08-10.06)
Mineral apposition rate (MAR), µm/day	0.74 ± 0.39^{a}	1.20 ± 0.42^{b}	1.32 ± 0.69
	(0.30-1.27)	(0.43-1.63)	(0.48-2.94)
Mineralizing surface/osteoid surface (MS/OS), %	20.59 ± 26.7^{a}	$39.83 \pm 31.33^{a,b}$	81.15 ± 23.66
	(3.51-71.82)	(8.41 - 89.79)	(36.84 - 97.79)
Adjusted apposition rate ^c (Aj.AR), μm/day	0.13 ± 0.17^{a}	0.52 ± 0.46^{6}	0.78 ± 0.59
	(0.03-0.49)	(0.04-1.24)	(0.35-1.93)
Mineralization lag time ^d (Mlt), days	240.93 ± 167.55^{a}	90.68 ± 172.67^{b}	15.42 ± 11.64
	(13.89 - 424.3)	(5.63 - 479.94)	(1.77 - 30.94)
Bone formation rate per bone surface ^e (BFR/BS), μm ³ /μm ² /year	5.97 ± 5.51^{a}	28.05 ± 15.96^{b}	29.83 ± 20.42
	(2.15-17.92)	(4.28-44.9)	(8.35 - 44.47)
Bone formation rate per osteoblast number (BFR/N.Ob), µm²/cell/day	55.57 ± 41.82	91.46 ± 30.98^{b}	88.64 ± 93.29
	(10.89 - 120.76)	(39.22 - 127.48)	(21.12 - 272.35)

^a Significant difference when compared to the corresponding normal value (P < 0.05).

bone formation rate per osteoblast number was lower than that of normal controls, the difference did not reach statistical significance. After potassium citrate therapy, bone volume and osteoblastic and osteoclastic surfaces were modestly increased, but the differences were not significant. A slight decrease in osteoid volume was observed. Osteoid surface and thickness were not significantly altered. Dynamic parameters showed significant improvement in the mineral apposition rate, mineralizing surface, and adjusted apposition rate compared to the baseline values (P < 0.05). Mineralization lag time also declined significantly (P <0.05). Bone formation rate per bone surface and bone formation rate per osteoblast number increased significantly after the treatment (P < 0.05). On regression analysis, a tendency toward negative correlation between the osteoid thickness and adjusted apposition rate was observed (r =-0.717, P = 0.07; Fig. 1). No positive staining for the aluminum was found in any of the bone specimens.

All the NCPs strongly stained the mineralized bone matrix compartment but variably stained osteoid and cellular components, including osteoblasts, osteoclasts, osteocytes, and lining cells (Fig. 2). Negative controls were devoid of staining. Each protein had a specific pattern of distribution, but an overlap in localization

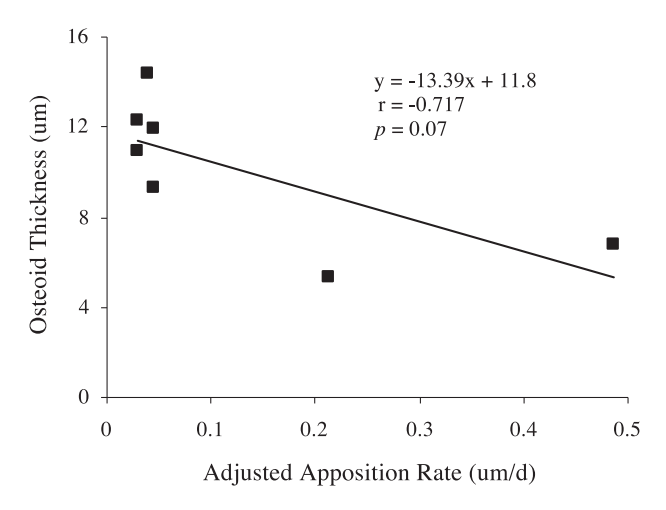


Fig. 1. Relationship between osteoid thickness (μm) and adjusted apposition rate ($\mu m/day$) of dRTA patients before treatment with alkaline.

^b Significant difference when compared to the corresponding baseline value (P < 0.05).

 $^{^{}c}$ Aj.AR was calculated from Aj.AR = [(MS/OS) \times MAR]/100.

^d Mlt was calculated from Mlt = O.th/Aj.AR.

^e BFR/BS was calculated from BFR/BS = $[(MS/BS) \times MAR]/100$, where MS/BS (mineralizing surface, %) was the extent of tetracycline labeled surface (double plus half single labeled surface) as a percentage of total trabecular bone surface.

^f BFR/N.Ob was calculated from BFR/N.Ob = MAR \times [osteoid perimeter (μ m)/number of osteoblasts].

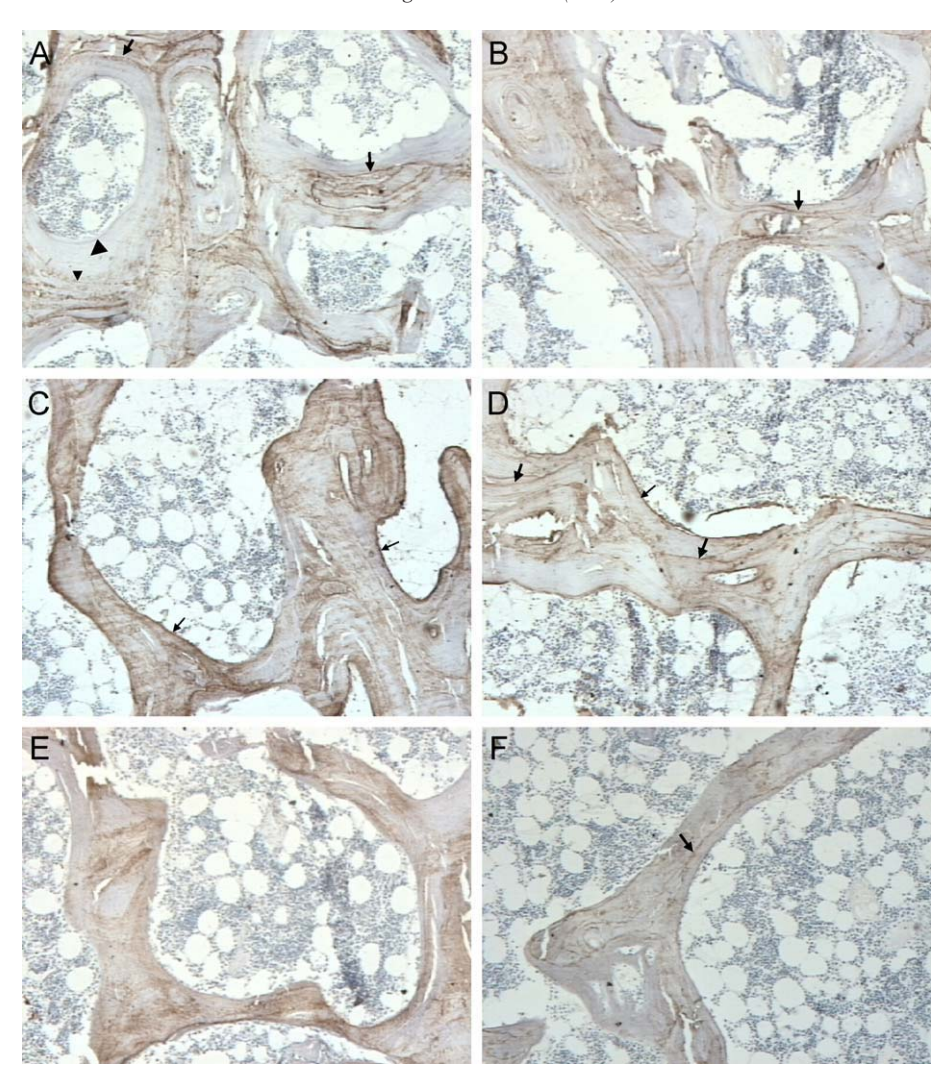


Fig. 2. Immunohistochemistry of NCPs in bone sections of patients with dRTA pre- and post-alkaline treatment. Each protein has specific pattern of distribution but an overlap in localization between the proteins was observed. (A) Osteocalcin pre-alkaline; (B) osteocalcin 1 year post-alkaline treatment. Osteocalcin was detected in the cement lines and more in the outer than the inner lamellae osteon. Note the increase in osteocalcin expression in the bone section after alkaline treatment. (C) Osteopontin pre-alkaline; (D) osteopontin post-alkaline. Osteopontin expressed more diffusely and most prominently in the area of the bone surface adjacent to the bone marrow (lamina limitans). Note the decrease in osteopontin expression in the bone section after alkaline treatment. (E) Osteonectin. Osteonectin diffusely expressed in the bone matrix but minimally in the cement lines. (F) Bone sialoprotein. Bone sialoprotein also diffusely stained the bone matrix and presented in the cement lines. Large arrowhead = inner lamellae osteon; small arrowhead = outer lamellae osteon; large arrow = cement lines; small arrow = lamina limitans. Original magnification, ×100.

between the proteins was observed. As shown in Fig. 2, osteocalcin (Figs. 2A and B) stained more intensely in the outer than inner lamellae osteon, while osteopontin stained diffusely and distinctively in the area of bone surface adjacent to the bone marrow (lamina limitans) (Figs. 2C and D). A significant increase in the area of osteocalcin staining from $16.65 \pm 9.25\%$ in bone biopsy at initial diagnosis to $22.26 \pm 8.16\%$ after alkaline treatment (P < 0.04) was observed (Fig. 3A). Six of seven patients showed decreased expression of osteopontin with an average of $28.91 \pm 10.4\%$ at initial biopsy to $22.3 \pm 3.76\%$ post-alkaline (P = 0.16) (Fig. 3B). Osteonectin and bone sialoprotein diffusely stained the bone matrix and cement lines (Figs. 2E and F). The area of staining of osteonectin ($19.46 \pm 10.92\%$ and $21.62 \pm 9.52\%$, P = 0.5) and bone

sialoprotein (11.94 \pm 4.37% and 12 \pm 3.76%, P = 0.98) was not significantly different post-alkaline therapy (Figs. 3C and D). After a careful examination of the sections obtained from initial biopsy and 1 year after alkaline treatment, there was no alteration in the distribution of any of the proteins.

Discussion

These seven patients have compatible characteristics of dRTA as described previously. Successful correction of metabolic acidosis with potassium citrate resulted in the increase in serum potassium, phosphate, and iPTH [4,5]. Earlier studies demonstrated that chronic metabolic acidosis

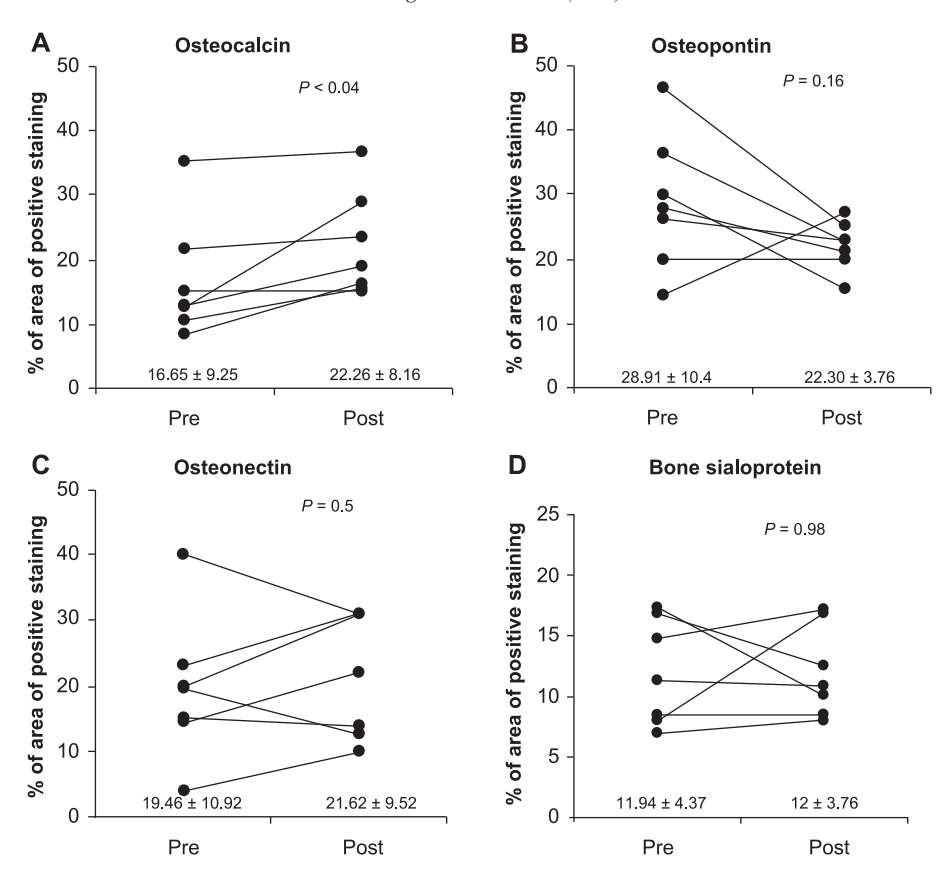


Fig. 3. Quantitation of NCPs expression using digital image analysis pre- and post-alkaline treatment. Data were expressed as percentage of area of positive staining or mineralized bone matrix area. (A) Osteocalcin, (B) osteopontin; (C) osteonectin; (D) bone sialoprotein. Osteocalcin expression significantly increased after alkaline treatment. Six of seven patients had decreased osteopontin expression.

induced by exogenous or endogenous acid loads resulted in physicochemical dissolution of the bone and enhanced osteoclastic bone resorption accompanied by marked elevation in the urinary calcium excretion [24-26]. In our patients, however, hypercalciuria was not observed. The difference in the urinary calcium excretion might be a result of the difference in the chronicity of the disease and the relatively low calcium intake in this group of Thai population. In a study by Lemann et al., all subjects had a rather short period of acidosis of less than a month when compared with our patients, who had suffered from metabolic acidosis for many years. Nevertheless, our findings were consistent with that of Coe and Firpo [27]. In Coe's study, chronic metabolic acidosis produced no hypercalciuria when dietary sodium intake was restricted. When sodium intake was increased, while maintaining the same acid load, hypercalciuria appeared [27]. The urinary sodium excretion in our patients was rather low and approximately half of the amount of urinary sodium excretion associated with hypercalciuria found in Coe's study. Therefore, the low urinary sodium excretion might contribute partly to the relatively low urinary calcium excretion. Another possible explanation is the histomorphometric finding of suppressed osteoclast population and activity, which suggests against a presence of significant process of bone resorption in our patients.

Metabolic acidosis has been known to result in renal phosphate wasting through the reduction in proximal tubular phosphate reabsorption [28,29]. In our patients, serum phosphate was low at baseline; however, the urinary phosphate excretion was unaltered compared to the healthy subjects. The prolonged negative phosphate balance and the chronically suppressed PTH levels might be responsible for the absence of phosphaturia. Correction of metabolic acidosis normalized the phosphate balance and serum phosphate.

The combination of negative calcium balance, phosphate depletion, and suppressed PTH during metabolic acidosis explains the findings of low bone density and the feature of low turnover bone disease, characterized by low bone volume, low osteoblast and osteoclast numbers, decreased mineralizing surface, and normal bone eroded surface, demonstrated by histomorphometry. In addition, the alteration in vitamin D metabolism might play a contributory role. Several studies reported inconsistent results on the levels of 1,25-(OH)₂ vitamin D during metabolic acidosis ranged from increased to unchanged to decreased [29–31]. In human, Krapf et al. [29] demonstrated an increase in 1,25-(OH)₂D level secondary to phosphate depletion in an experimental NH₄Cl-induced acidosis. The production rate of 1,25-(OH)₂ vitamin D was stimulated and PTH decreased

secondarily. We did not measure the 1,25-(OH)₂D levels in our patients; nevertheless, the finding of low PTH in our study is consistent with that of Krapf's. Correction of metabolic acidosis normalized the calcium balance, serum phosphorus, and PTH resulting in an increase in bone mass. The elevated osteoid surface and volume, the reduction in mineralizing surface, the falls in mineral apposition rate and adjusted apposition rate, and the prolonged mineralization lag time suggest toward a presence of mineralization defect in dRTA. Nevertheless, the degree of increased osteoid thickness, together with its negative correlation with the adjusted apposition rate, a cardinal feature of osteomalacia, was only borderline significant [32]. The explanation may be the high variability of the osteoid thickness among our patients, which in turn suggests the presence of heterogeneity of bone disease in dRTA. Previously, both osteomalacia and osteoporosis have been reported in association with metabolic acidosis [18,33]. Our findings also indicate that some patients have a histologic feature of osteomalacia associated with an increased osteoid thickness while others fall in a group of low bone turnover osteopenia accompanied by a normal to decreased osteoid thickness. The existence of diversity of bone disease in dRTA is further supported by the wide range of values reported on the mineralizing surface and mineralization lag time. The most likely causative factors for the defective mineralization in our patients were phosphate depletion and, perhaps, abnormal vitamin D metabolism. After successful correction of metabolic acidosis, the parameters associated with mineralization and bone formation improved considerably. In addition, alkaline therapy might also improve osteoblast function suggested by the increase in bone formation rate per osteoblast. While the negative calcium and phosphate balance and, perhaps, impaired osteoblast function contributed to the low bone mass, cell-mediated bone resorption did not seem to play a major role. Previous in vitro studies demonstrated enhanced osteoclastic bone resorption during metabolic acidosis [9,34]. Later on, Frick and Bushinsky [35] discovered that RANKL RNA expression was upregulated in mouse calvariae incubated in acidic media, suggesting that metabolic acidosis stimulates osteoclast differentiation. In addition to the proliferative effect on bone cells, PTH is also a potent stimulation for RANKL expression and osteoclast differentiation [36,37]. Thus, the absence of enhanced bone resorption in our patients could be explained by the presence of low PTH resulting in the reduction in osteoblast and osteoclast populations and the suppression of osteoclast differentiation. Substantial evidence suggested that growth hormone or insulin-like growth factor axis was suppressed during metabolic acidosis [38,39]. Therefore, in addition to the low PTH, the impaired growth hormone or insulin-like growth factor system, whose effect directly promotes cellular proliferation and differentiation, might also be responsible for the overall reduction in bone cell populations. After alkaline therapy, the parameters associated with bone resorption were unchanged. One would have expected the reduction in osteoclast number

and/or activity after correction of acidosis; however, such findings might have been prevented by the rise of the PTH.

Additional analysis on the bone matrix proteins demonstrated a significant increase in osteocalcin expression within the bone matrix after correction of metabolic acidosis. Osteocalcin, produced and secreted almost exclusively by cells of osteoblast origin, is well-known as a marker of osteoblast function and its serum level correlates with bone formation [11,40]. The increased osteocalcin expression. which might have occurred secondarily to the enhanced osteoblast function after correction of metabolic acidosis, corresponded to the improvement in bone formation and mineralization. In vitro studies using osteoblast culture model demonstrated the inhibition of osteoblast function by metabolic acidosis; for example, metabolic acidosis impaired osteoblastic collagen synthesis [8] and reversibly inhibited the expression of osteoblastic genes including type I collagen, matrix Gla protein, and osteopontin [41]. Our finding provides in vivo evidence on the inhibitory effect of metabolic acidosis on osteoblastic gene expression and its improvement after alkaline therapy. In support of our result, others have found an increase in serum osteocalcin after correction of metabolic acidosis corresponding to the improvement in bone mineral balance [42,43].

Osteonectin is another NCP that involves in the process of bone formation. Osteonectin-deficient mice have decreased bone formation and profound osteopenia [13]. Culture of bone marrow stromal cells and osteoblasts obtained from these animals revealed compromised osteoblast formation, maturation, and survival [44]. Previous in vitro study using osteoblast culture model in acidic medium found no alteration in the expression of osteonectin mRNA compared to control culture at neutral pH [41]. We also found no significant difference in the expression of osteonectin within the bone matrix before and after alkaline therapy, suggesting that the effect of metabolic acidosis on bone matrix protein expression might be selective.

Osteopontin and bone sialoprotein belong to the same family protein, which contains an RGD (Arg-Gly-Asp) cell attachment sequence, therefore play roles in the regulation of adhesion and the attachment and spreading of osteoclasts to the bone surface [45]. Osteopontin mRNA was found in both osteoblasts and osteoclasts [14] and especially highly expressed in the resorption lacunae and in the osteoclasts at immediate resorption surfaces [15]. In a study by Ihara et al. [36], PTH-induced increase in TRAP-positive cells was absent in osteopontin-deficient bones, emphasizing the role of osteopontin in osteoclast differentiation and bone resorption. In our study, six of seven patients had decreased osteopontin expression within the bone matrix after alkaline therapy. The expression of bone sialoprotein was not significantly altered. The discrepancy between our result and that of Frick and Bushinsky [41], who found decreased osteopontin mRNA in osteoblasts cultured in acidic media, could be because osteopontin production is almost undetectable in osteoblasts actively expressing osteocalcin [46]; therefore, the reduction in its expression might be secondary to the decreased production by osteoclasts rather than osteoblasts. Since RANKL is upregulated during metabolic acidosis; thus, the reduction in RANKL-stimulated osteoclast differentiation might be the reason for decreased osteopontin expression after alkaline therapy. PTH has been known to stimulate RANKL and osteopontin expression [37,47]; therefore, the increase in PTH levels after acidosis correction could overshadow the alterations in osteopontin expression and histomorphometric parameters related to bone resorption.

We found no significant alteration in the distribution of NCPs before and after alkaline therapy, suggesting minor roles of the distribution of the proteins in abnormal bone remodeling in patients with dRTA. The variability in the expression of NCPs among different patients might be due to sex and age differences in the composition of bone matrix [48]. This observation, however, will require further study in a larger number of patients.

Our study confirmed previous reports of preserved antigenicity within the mineralized compartment of the bone embedded in plastic [23,49]. The staining within the cellular components could be improved with embedding and polymerization performed at lower temperature $(-15 \text{ to } -20\,^{\circ}\text{C})$ [50]. The data on NCPs was limited by the semiquantitative nature of immunohistochemistry; however, the method we applied required measurements of at least 40 trabecular bone areas in multiple bone sections cut at different levels, which has been shown previously to be sufficient to obtain representative data with a small confidence intervals [23].

In summary, our data demonstrated abnormal bone remodeling in patients with dRTA characterized by low turnover bone disease with defective mineralization. Alteration of NCPs expression suggested the effect of metabolic acidosis on bone cells in vivo. Alkaline therapy improved bone formation through the restoration of bone mineral balance and, perhaps, enhanced osteoblast function. Further studies are required to elucidate the effect of chronic metabolic acidosis on bone resorption in vivo.

Acknowledgment

This work was supported by Thailand Research Fund.

References

- Caruana RJ, Buckalew Jr VM. The syndrome of distal (type 1) renal tubular acidosis. Clinical and laboratory findings in 58 cases. Medicine (Baltimore) 1988;67:84–99.
- [2] Wrong OM, Feest TG. The natural history of distal renal tubular acidosis. Contrib Nephrol 1980;21:137–44.
- [3] Richards P, Chamberlain MJ, Wrong OM. Treatment of osteomalacia of renal tubular acidosis by sodium bicarbonate alone. Lancet 1972;2: 994-7.
- [4] Domrongkitchaiporn S, Pongsakul C, Stitchantrakul W, Sirikulchaya-

- nonta V, Ongphiphadhanakul B, Radinahamed P, et al. Bone mineral density and histology in distal renal tubular acidosis. Kidney Int 2001;59:1086–93.
- [5] Domrongkitchaiporn S, Pongskul C, Sirikulchayanonta V, Stitchantrakul W, Leeprasert V, Ongphiphadhanakul B, et al. Bone histology and bone mineral density after correction of acidosis in distal renal tubular acidosis. Kidney Int 2002;62:2160-6.
- [6] Bushinsky DA, Krieger NS, Geisser DI, Grossman EB, Coe FL. Effects of pH on bone calcium and proton fluxes in vitro. Am J Physiol 1983;245:F204-9.
- [7] Bushinsky DA, Lechleider RJ. Mechanism of proton-induced bone calcium release: calcium carbonate-dissolution. Am J Physiol 1987; 253:F998-F1005.
- [8] Krieger NS, Sessler NE, Bushinsky DA. Acidosis inhibits osteoblastic and stimulates osteoclastic activity in vitro. Am J Physiol 1992; 262:F442-8.
- [9] Bushinsky DA. Stimulated osteoclastic and suppressed osteoblastic activity in metabolic but not respiratory acidosis. Am J Physiol 1995;268;C80-8.
- [10] Bushinsky DA. Metabolic alkalosis decreases bone calcium efflux by suppressing osteoclasts and stimulating osteoblasts. Am J Physiol 1996;271:F216-22.
- [11] Garcia-Carrasco M, Gruson M, de Vernejoul MC, Denne MA, Miravet L. Osteocalcin and bone morphometric parameters in adults without bone disease. Calcif Tissue Int 1988;42:13-7.
- [12] Gundberg CM, Lian JB, Gallop PM, Steinberg JJ. Urinary gammacarboxyglutamic acid and serum osteocalcin as bone markers: studies in osteoporosis and Paget's disease. J Clin Endocrinol Metab 1983;57: 1221–5
- [13] Delany AM, Amling M, Priemel M, Howe C, Baron R, Canalis E. Osteopenia and decreased bone formation in osteonectin-deficient mice. J Clin Invest 2000:105:915–23.
- [14] Merry K, Dodds R, Littlewood A, Gowen M. Expression of osteopontin mRNA by osteoclasts and osteoblasts in modelling adult human bone. J Cell Sci 1993;104(Pt. 4):1013–20.
- [15] Dodds RA, Connor JR, James IE, Rykaczewski EL, Appelbaum E, Dul E, et al. Human osteoclasts, not osteoblasts, deposit osteopontin onto resorption surfaces: an in vitro and ex vivo study of remodeling bone. J Bone Miner Res 1995;10:1666–80.
- [16] Yoshitake H, Rittling SR, Denhardt DT, Noda M. Osteopontin-deficient mice are resistant to ovariectomy-induced bone resorption. Proc Natl Acad Sci U S A 1999;96:8156–60.
- [17] Raynal C, Delmas PD, Chenu C. Bone sialoprotein stimulates in vitro bone resorption. Endocrinology 1996;137:2347–54.
- [18] Nilwarangkur S, Nimmannit S, Chaovakul V, Susaengrat W, Ong-aj-Yooth S, Vasuvattakul S, et al. Endemic primary distal renal tubular acidosis in Thailand. Q J Med 1990;74:289–301.
- [19] Mautalen C, Montoreano R, Labarrere C. Early skeletal effect of alkali therapy upon the osteomalacia of renal tubular acidosis. J Clin Endocrinol Metab 1976;42:875–81.
- [20] Henneman PH, Benedict PH, Forbes AP, Dudley HR. Idiopathic hypercaicuria. N Engl J Med 1958;259:802-7.
- [21] Parfitt AM, Drezner MK, Glorieux FH, Kanis JA, Malluche H, Meunier PJ, et al. Bone histomorphometry: standardization of nomenclature, symbols, and units. Report of the ASBMR Histomorphometry Nomenclature Committee. J Bone Miner Res 1987;2: 595-610.
- [22] Fisher LW, Stubbs III JT, Young MF. Antisera and cDNA probes to human and certain animal model bone matrix noncollagenous proteins. Acta Orthop Scand Suppl 1995;266:61–5.
- [23] Derkx P, Nigg AL, Bosman FT, Birkenhager-Frenkel DH, Houtsmuller AB, Pols HA, et al. Immunolocalization and quantification of noncollagenous bone matrix proteins in methylmethacrylate-embedded adult human bone in combination with histomorphometry. Bone 1998;22:367–73.
- [24] Bleich HL, Moore MJ, Lemann Jr J, Adams ND, Gray RW. Urinary calcium excretion in human beings. N Engl J Med 1979;301:535–41.

- [25] Lemann Jr J, Litzow JR, Lennon EJ. The effects of chronic acid loads in normal man: further evidence for the participation of bone mineral in the defense against chronic metabolic acidosis. J Clin Invest 1966:45:1608–14.
- [26] Kraut JA, Mishler DR, Singer FR, Goodman WG. The effects of metabolic acidosis on bone formation and bone resorption in the rat. Kidney Int. 1986;30:694-700.
- [27] Coe FL, Firpo Jr JJ. Evidence for mild reversible hyperparathyroidism in distal renal tubular acidosis. Arch. Intern. Med. 1975;135:1485–9.
- [28] Ambuhl PM, Zajicek HK, Wang H, Puttaparthi K, Levi M. Regulation of renal phosphate transport by acute and chronic metabolic acidosis in the rat. Kidney Int 1998;53:1288–98.
- [29] Krapf R, Vetsch R, Vetsch W, Hulter HN. Chronic metabolic acidosis increases the serum concentration of 1,25-dihydroxyvitamin D in humans by stimulating its production rate. Critical role of acidosisinduced renal hypophosphatemia. J Clin Invest 1992;90:2456–63.
- [30] Kraut JA, Gordon EM, Ransom JC, Horst R, Slatopolsky E, Coburn JW, et al. Effect of chronic metabolic acidosis on vitamin D metabolism in humans. Kidney Int 1983;24:644–8.
- [31] Reddy GS, Jones G, Kooh SW, Fraser D. Inhibition of 25-hydroxyvitamin D3-1-hydroxylase by chronic metabolic acidosis. Am J Physiol 1982;243:E265-71.
- [32] Parfitt AM. Osteomalacia and related disorders. In: Avioli LV, Krane SM, editors. Metabolic bone disease and clinically related disorders. San Diego: Academic Press; 1997. p. 327–86.
- [33] Weger W, Kotanko P, Weger M, Deutschmann H, Skrabal F. Prevalence and characterization of renal tubular acidosis in patients with osteopenia and osteoporosis and in non-porotic controls. Nephrol Dial Transplant 2000;15:975–80.
- [34] Meghji S, Morrison MS, Henderson B, Arnett TR. pH dependence of bone resorption: mouse calvarial osteoclasts are activated by acidosis. Am J Physiol Endocrinol Metab 2001;280:E112-9.
- [35] Frick KK, Bushinsky DA. Metabolic acidosis stimulates RANKL RNA expression in bone through a cyclo-oxygenase-dependent mechanism. J Bone Miner Res 2003;18:1317–25.
- [36] Ihara H, Denhardt DT, Furuya K, Yamashita T, Muguruma Y, Tsuji K, et al. Parathyroid hormone-induced bone resorption does not occur in the absence of osteopontin. J Biol Chem 2001;276:13065-71.
- [37] Huang JC, Sakata T, Pfleger LL, Bencsik M, Halloran BP, Bikle DD, et al. PTH differentially regulates expression of RANKL and OPG. J Bone Miner Res 2004;19:235–44.

- [38] Green J, Maor G. Effect of metabolic acidosis on the growth hormone/IGF-I endocrine axis in skeletal growth centers. Kidney Int 2000;57:2258-67.
- [39] Brungger M, Hulter HN, Krapf R. Effect of chronic metabolic acidosis on the growth hormone/IGF-1 endocrine axis: new cause of growth hormone insensitivity in humans. Kidney Int 1997;51:216-21.
- [40] Price PA. Gla-containing proteins of bone. Connect Tissue Res [discussion 57–60] 1989;21:51–7.
- [41] Frick KK, Bushinsky DA. Chronic metabolic acidosis reversibly inhibits extracellular matrix gene expression in mouse osteoblasts. Am J Physiol 1998;275:F840-7.
- [42] Lin YF, Shieh SD, Diang LK, Lin SH, Chyr SH, Li BL, et al. Influence of rapid correction of metabolic acidosis on serum osteocalcin level in chronic renal failure. ASAIO J 1994;40:M440-4.
- [43] Sebastian A, Harris ST, Ottaway JH, Todd KM, Morris Jr RC. Improved mineral balance and skeletal metabolism in postmenopausal women treated with potassium bicarbonate. N Engl J Med 1994;330: 1776–81
- [44] Delany AM, Kalajzic I, Bradshaw AD, Sage EH, Canalis E. Osteonectin-null mutation compromises osteoblast formation, maturation, and survival. Endocrinology 2003;144:2588–96.
- [45] Young MF. Bone matrix proteins: their function, regulation, and relationship to osteoporosis. Osteoporos Int 2003;14(Suppl. 3):S35-42.
- [46] Stein GS, Lian JB. Molecular mechanisms mediating proliferation/ differentiation interrelationships during progressive development of the osteoblast phenotype. Endocr Rev 1993;14:424–42.
- [47] Gopalakrishnan R, Ouyang H, Somerman MJ, McCauley LK, Franceschi RT. Matrix gamma-carboxyglutamic acid protein is a key regulator of PTH-mediated inhibition of mineralization in MC3T3-E1 osteoblast-like cells. Endocrinology 2001;142:4379–88.
- [48] Aerssens J, Boonen S, Joly J, Dequeker J. Variations in trabecular bone composition with anatomical site and age: potential implications for bone quality assessment. J Endocrinol 1997;155:411–21.
- [49] Ingram RT, Clarke BL, Fisher LW, Fitzpatrick LA. Distribution of noncollagenous proteins in the matrix of adult human bone: evidence of anatomic and functional heterogeneity. J Bone Miner Res 1993;8: 1019-29.
- [50] Erben RG. Embedding of bone samples in methylmethacrylate: an improved method suitable for bone histomorphometry, histochemistry, and immunohistochemistry. J Histochem Cytochem 1997;45: 307-13.